NOVEL SIMILARITY LEVEL CHARACTERIZATION METHODOLOGY INFORMED BY CFD FOR RCIC SYSTEM SCALING

A Dissertation

by

MOHAMMAD ABDEL MAJID MUSTAFA HAWILA

Submitted to the Office of Graduate and Professional Studies of
Texas A&M University
in partial fulfillment of the requirements for the degree of

DOCTOR OF PHILOSOPHY

Chair of Committee,	Karen Vierow Kirkland
Committee Members,	Yassin Hassan
	Pavel V. Tsvetkov
	Adolfo Delgado
Head of Department,	Yassin Hassan

December 2018

Major Subject: Nuclear Engineering

ABSTRACT

The Reactor Core Isolation Cooling (RCIC) System is a safety system that provides water to the reactor pressure vessel during off-normal Boiling Water Reactor (BWR) conditions, such as reactor isolation from the turbines or loss of AC power. Under loss of AC power conditions, the RCIC System is expected to fail due to battery depletion within 4 to 8 hours of operation for many units. However, the system did not fail until about 70 hours into the accident at Fukushima Dai-ichi Unit 2, which was well past the time of battery depletion. To investigate the full potential of the RCIC System, the Laboratory for Nuclear Heat Transfer Systems (NHTS) at Texas A&M University is modifying an existing experimental test facility to enable performance evaluation of BWR RCIC System components under nominal and beyond design basis event conditions. A careful scaling analysis is essential to ensure proper representation of the RCIC System's key components and phenomena in the experimental testing. This dissertation describes and applies a method to estimate the scaling Similarity Level of the RCIC system turbomachinery and Suppression Pool. The methodology is demonstrated with the Texas A&M University facility but can be applied to other RCIC system facilities.

With respect to any full-scale RCIC system, upon availability of data from a full-scale system of interest, the scaling Similarity Level values can be determined for the NHTS facility system. Those values will determine whether the NHTS facility is appropriate for studying that particular full-scale system's behavior. Additionally, the scaling Similarity Level values can decide what modifications would need to be done to

the NHTS facility to make it appropriate for a particular system, as well estimating the testing operating conditions. Scaling will justify the use of the NHTS facility as is or with modifications to understand the full-scale system behavior and investigate ways to expand operation for longer time, which is of great interest to the U.S nuclear industry.

This study is the first of its kind to employ Computational Fluid Dynamics (CFD) to obtain necessary input for the scaling analysis and Similarity Level estimation. Output from CFD analysis with the STAR-CCM+ code were used to obtain characteristic time ratio input parameters for Similarity Level estimation of the RCIC System's Terry Turbine.

Original contributions of this study are the derivation of Similarity Level equations for the RCIC System turbomachinery and BWR Suppression Pool, the development of CFD models for the Terry Turbine, the validation of one of the CFD models against experimental data and application of the CFD simulation results to provide input for Similarity Level estimations. Using the information provided by the CFD analyses, the Similarity Level between the GS-1 and ZS-1 Terry Turbines were computed, and showed that a high level of similarity exists between the actual turbines. Furthermore, the characteristic time ratios of the Suppression Pool were calculated for the NHTS facility to provide reference data for Similarity Level calculations.

DEDICATION

For my mother. God bless her soul.

ACKNOWLEDGEMENTS

Alhamdulillah for everything. I owe many thanks to Dr. Karen Kirkland who has helped me in the success of this research and the achievements I made. She guided, encouraged, supported, and provided me with all resources to conduct this research. Also I would like to thank my research committee members and colleagues for the great help and advice they provided to me. In addition, thank you to Dr. Tsvetkov for help and great discussions about this research.

Thank you to my friends, NUEN professors, staff, and everyone for making my time at Texas A&M great. Finally, thanks to my family and loved ones for the continuous encouragement, prayers, and love.

CONTRIBUTORS AND FUNDING SOURCES

This work was supervised by a dissertation committee consisting of Professor Karen Vierow Kirkland (Advisor), Professor Yassin Hassan and Professor Pavel Tsvetkov of the Department of Nuclear Engineering and Professor Adolfo Delgado of the Department of Mechanical Engineering. The data analyzed in Chapter 7 about the NHTS RCIC system testing was provided by Professor Karen Vierow Kirkland. The NHTS RCIC system turbine tests were performed by Nicholas Gerard Luthman Jr. The NHTS RCIC system Suppression Pool tests were performed by Matthew Alan Solom.

This research study was prepared under award # 707K722 from the Board of Regents of the University of Wisconsin System. The prime sponsor is the Office of Nuclear Regulatory Research, Nuclear Regulatory Commission. The statements, findings, conclusions, and recommendations are those of the author(s) and do not necessarily reflect the view of the Office of Nuclear Regulatory Research or the US Nuclear Regulatory Commission.

TABLE OF CONTENTS

Page

LIST OF FIGURES

Page

LIST OF TABLES

Page

1. INTRODUCTION

The Reactor Core Isolation Cooling (RCIC) system is a safety system that is found in many Boiling Water Reactors (BWR) with a Mark I containment design. In the event of an accident scenario, such as a station blackout (the loss of offsite power in conjunction with loss of onsite emergency AC power systems (General Electric , 2018)) or Loss Of Coolant Accident (LOCA), the main steam line is isolated from the plant turbine-generator, and steam is directed to the RCIC, system which consists of a Terry turbine, centrifugal pump, and suppression chamber. The Terry turbine converts the energy of steam into shaft work which drives its connected pump, and the pump sends water from a primary or secondary source back to the Reactor Pressure Vessel (RPV) to maintain core cooling (General Electric, 2011).

Under loss of AC power conditions, the RCIC System is expected to fail due to battery depletion, within 4 to 8 hours of operation for many units. However, the system ran for nearly 70 hours during the accident at Fukushima Dai-ichi Unit 2, which was well past the time of battery depletion. This developed an interest of the performance of the RCIC system under extended station blackout conditions. The RCIC System's potential for increasing response time during Diverse and Flexible Coping Strategies (FLEX) procedures. Also, it provides more-than-credited-for core cooling renders investigation of the RCIC System's capabilities for long-term operation under station blackout conditions of high importance.

An experimental test facility was designed and constructed in the Laboratory for Nuclear Heat Transfer Systems (NHTS) at Texas A&M University in order to investigate thermal stratification in the Suppression Chamber during long-term operation of the RCIC System ((Solom & Kirkland, 2016), (Solom, 2016)). Steam and water were injected into a water pool, simulating RCIC turbine exhaust into the Suppression Pool. The experimental objectives at the NHTS facility have been expanded from separate component studies to investigations of the long-term operation of the RCIC System. This creates the need to perform a scaling analysis to ensure proper representation of all of the RCIC System key components and phenomena during long-term operation, including steam/water supply to the RCIC turbine, Suppression Chamber, water return to the Reactor Pressure Vessel, turbine oil heat up, etc.

This research started with Zuber's H2TS (Hierarchal Two-Tiered Scaling) methodology (Zuber , 1991) to show the required level of detail for scaling. The key importance of the scaling, if correctly implemented provides assurance that the experimental system accurately represents the prototypical system for the main and important processes under the conditions of interest, or that the model components can be modified to achieve similarity. Most scaling techniques have common steps to derive the characteristic time ratios. In this dissertation, estimation of the required level of details for scaling assisted with the development of a scaling methodology for complex systems, which is called scaling Similarity Level (SL) estimation analysis. The scaling Similarity Level approach consolidates some steps and provides a direct derivation of the

characteristic time ratios. This methodology is applicable for the RCIC system complex scaling for steady/quasi-steady and transient system behavior.

Scaling produces unit-less equations that are used to estimate the level of similarity or distortion between the test facility and the prototype for a steady/unsteady state case. Estimation of the scaling Similarity Level value requires collection of input parameters, with many of which are not readily available. The input parameter sources therefore include experimental measurements, numerical calculations, and Computational Fluids Dynamics (CFD) analysis. As an outcome of this research, complex, full-scale RCIC system behaviors can be predicted with reference to the experimental NHTS RCIC system based on Similarity Level analysis estimation.

CFD models are developed for the NHTS facility Terry turbines based on a BWR RCIC system GS-1 turbine Computer Aided Drafting (CAD) model and used as a tool to estimate some input parameters for the Similarity Level value estimation. For the CFD code, STAR-CCM+ has been chosen because of its capabilities, portability and availability. As an example of using CFD to inform the scaling analysis, one of the main input parameters for scaling Similarity Level is the jet velocity through the turbine steam inlet nozzle. This parameter is investigated with STAR-CCM+ using the models developed for the RCIC system Terry turbine.

1.1 Dissertation Objectives

The RCIC System scaling Similarity Level analysis now being performed is to support the design modifications of the NHTS facility to include these additional components and phenomena, and to demonstrate the applicability, or lack thereof, of the

new design to the full-scale reactor system. Another objective of the scaling Similarity Level analysis is to identify the data needs for development/verification/validation of computational models with varying degree of complexities. Proper scaling will ensure that the NHTS facility is applicable for testing and studying a full-size facility under Design Basis Accident (DBA) conditions. Furthermore, it will help addressing the Beyond Design Basis Accident (BDBA) testing conditions in the future regarding studying the RCIC system long operation behavior.

1.2 Significance of Work

This dissertation assists in development of a new set of unique, unit-less equations for demonstration and use in complex RCIC Systems scaling under steady state and transient conditions within the realm of Design Basis Accident conditions. Furthermore, conducting a detailed assessment of the steam injection into BWR RCIC System establishes an equation that estimates the jet velocity as a function of the steam inlet nozzle inlet/outlet pressure ratio. The combination of the findings from the experimental data, geometry records and CFD analysis enables more accurate scaling for the RCIC system and provides the ability to modify existing system component to have higher similarity. Additionally, the Similarity Level values help identify the most appropriate operating conditions and procedures at the NHTS facility for future testing and studying the behavior of the full-scale system. Importantly, the developed scaling Similarity Level model of the RCIC Suppression Pool is unique and can be used with any referenced Suppression Pool if the characteristic time ratio input parameter data are accessible.

The U.S nuclear industry and other nuclear parties are interested in studying the full-scale RCIC system behavior to understand the possible ways to expand the current RCIC systems operations for longer durations (Sandia National Laboratory, 2017). In addition, they showed interest in the scaling Similarity Level analysis presented in this dissertation as it serves their objective of estimating the confidence level in using the NHTS facility in its current configuration to test various aspects of a full-scale RCIC system. Also, to specify what kind of modification (if any) would be needed to have a higher confidence level. Currently, there is no facility that can test a full scale RCIC system. Therefore, this scaling research would help justify the use of small-scale work properly to predict full-scale system behavior, which is important for U.S nuclear industry.

The expectation is that the work will promote deeper investigation of severe accidents under beyond design basis conditions (if identified) in order to draw conclusions about a full-size RCIC system behavior. The benefits of this research extend for many Light Water Reactor (LWR) systems that have similar components of the RCIC system, such as turbines and pools. In addition, the CFD simulation provides a source of data for characteristic time ratio input parameters. The data provides insight into the Similarity Level values for full-scale system components.

The technical contributions of this dissertation are:

- Scaling model development and formulation of dimensionless (unit-less) equations that are used to estimate the scaling Similarity Level between the test and prototype RCIC Systems.

- Identification of the data requirements for development / verification / validation of computational models with varying degree of complexities based on scaling Similarity Level analysis.
- Development of a CAD model that represents the NHTS Terry turbine with the steam inlet nozzle inside the turbine casing and application with a CFD code (STAR-CCM+) to investigate flow parameters (such as the jet velocity) through the turbine.
- Collection of available input parameters and estimation of Similarity Levels of the RCIC system main components between the NHTS and full-scale equipment. The data sources for the scaling Similarity Level input parameters are (1) NHTS RCIC system's geometry descriptions, experimental data records, lab notebook data, and CFD analyses (2) Prototype RCIC system's available geometrical data and GS-1 Terry turbine model CFD analysis.
- Development of a scaling Similarity Level model that is applicable for the NHTS RCIC system Suppression Pool. This model will be used to estimate the Similarity Level of the Suppression Pool with reference to a prototype pool upon availability of the prototype one geometrical and operation data.

A byproduct of this research is an experimentally-validated CFD benchmark of the steady-state Terry turbine thermal hydraulics.

1.3 Technical Approach

This dissertation aims to develop a Similarity Level estimation methodology that uses unit-less equations based on a scaling normalization process. This makes the unit-less equations applicable for Similarity Level estimation between the NHTS RCIC system component and any prototype system. The equations developed can examine the similarity or distortion between the turbo-pump and Suppression Pool of the model and prototype facility systems. Also, the credibility of the NHTS RCIC system component allows it to be used for addressing plant safety issues because the facility can be used for long-term performance testing.

The data for the NHTS RCIC component unit-less equations are based on a wide range of experimental tests that were performed at the facility on the turbo-pump and Suppression Pool components. The CFD modeling and testing of the NHTS RCIC system turbine provided some input parameter data, while the data for the prototype systems are based on the available open source information.

The data available from testing at the NHTS facility is used for validation of the CFD testing model of the NHTS RCIC system turbine. Single phase flow simulations of dry steam were developed and implemented in STAR-CCM+ to investigate the torque, steam jet velocity injection, and other parameters that are used in the Similarity Level unit-less equations. These models that were used in the STAR-CCM+ code representing the full turbine geometry (ZS-1 and GS-1 types) and the converging-diverging nozzle type.

Finally, the achievements of this research can be summarized as following:

- Provided a detailed description of the full scale and small-scale RCIC system component and determined the phenomena.
- Developed RCIC system scaling approach and estimated the main input parameters that describe and govern the operational behavior of the RCIC system major component.
- Developed RCIC system components control volume as well as estimating the proper governing equations for various operating conditions.
- Derived a unique characteristic time ratios that describe the operation of the RCIC system component and are used in estimating the Similarity Level values.
- Assembled data necessary for calculating the Similarity Level values for the RCIC system major component.
- Developed a CFD models that describe and simulate the operation of the RCIC system ZS-1 and GS-S turbines, which provided data for Similarity Level estimation.
- Validated the ZS-1 model against experimental data of tests performed at the NHTS facility.
- Developed a CFD model that describes and simulate the converging-diverging turbine nozzle.
- Provided a reference model and data that describe the Suppression Pool operation and calculated the pool characteristic time ratios.

2. RCIC SYSTEM OVERVIEW

The RCIC System is a safety–related system designed to provide core cooling under reactor isolation conditions including the isolation of the main steam lines and feed water unavailability. The RCIC system employs a steam impulse turbine that exhausts to the Suppression Pool and powers a pump to deliver water to the reactor pressure vessel. The RCIC System starts providing coolant inventory to the reactor pressure vessel 15 minutes after shutdown. The RCIC System is configured such that it can be initiated despite a complete loss of AC power. A diagram of the RCIC System component in a Mark I containment is shown in Figure 1 (General Electric , 2018).

The RCIC System pump delivers water to the reactor pressure vessel through the main feed water line. The pump can take supply water from two sources: the Condensate Storage Tank (CST), which is the normal suction source of the RCIC system or the Suppression Pool as an alternate source of water for the RCIC pump. The system is designed to deliver a full load within 30 seconds of actuation and automatically regulate the reactor pressure vessel water level between upper and lower levels (General Electric, 2011).

The pump is located at an elevation lower than both suction sources to ensure that the required Net Positive Suction Head (NPSH) is available. Existence of NPSH allows the pump to operate without cavitation. If the pressure at the pump inlet drops below the local saturation pressure, cavitation could occur at the pump inlet, creating bubbles that can collapse inside the pump and lead to eventual destruction to the pump. Pump failure

would terminate RCIC system operation. The system keeps operating until it receives a shutdown signal either automatically or manually. Detailed description of the RCIC system component will be discussed in the next subsections.

During station blackout, power from station batteries is required for the RCIC System turbine governor to control the turbine speed and governor valve open fraction. Therefore, power availability is a limitation of the RCIC System for long-term operation. The RCIC System in US reactors is assumed to fail upon battery depletion, typically within 4 and 8 hours. In contrast, the Unit 2 RCIC system of Fukushima Dai-ichi ran for nearly 70 hours, long after the batteries depleted or went offline (Institute of Nuclear Power Operators , 2011).

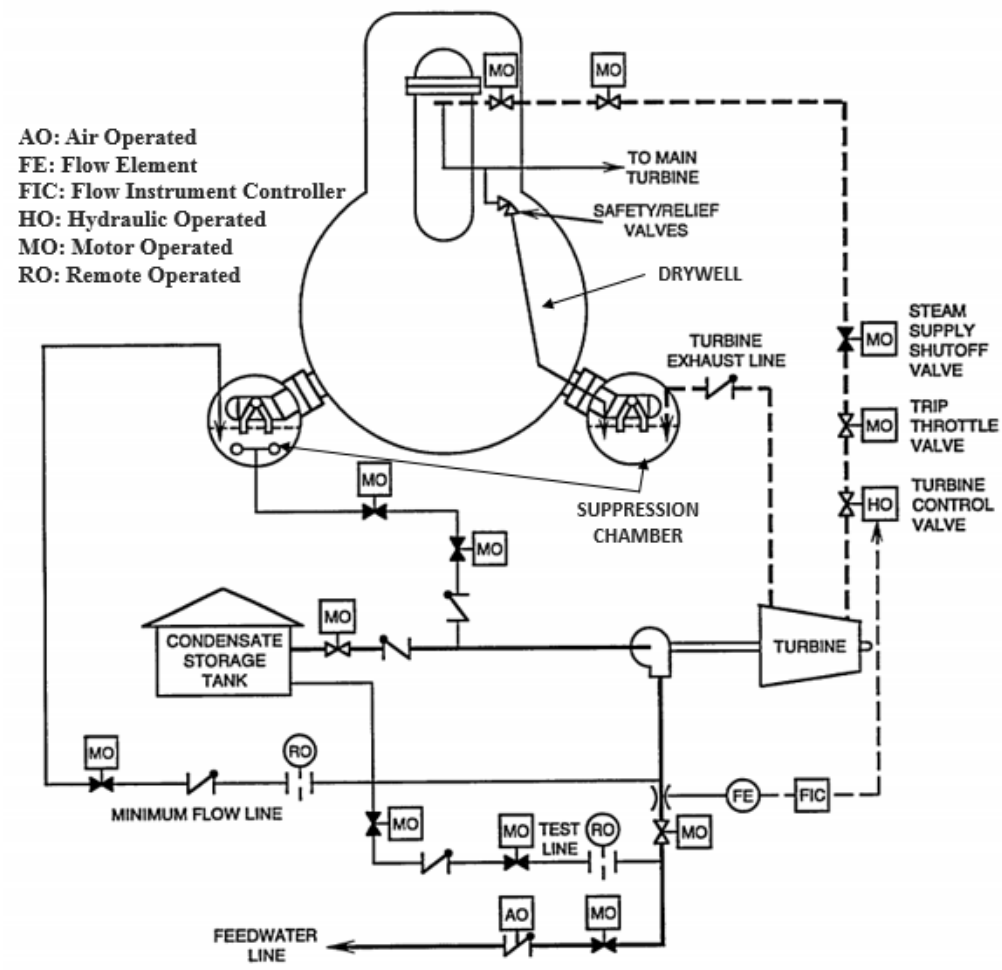

Figure 1 RCIC system component layout (General Electric , 2018).

2.1 RCIC System Geometrical Configuration

2.1.1 RCIC system Terry turbine

The source of power for the RCIC system is steam that is injected into a turbine connected to the RCIC pump by a shaft. The turbine design belongs to Terry Steam Turbine Company and was invented in the early 20th century. The design model is based on the turbine wheel diameter and number of nozzles, such as the large standard sizes of the GS-1 and GS-2 models of the RCIC turbine system and the smaller size and less

number of nozzles as in the ZS-1 model. However, all sizes of Terry turbine could be classified as a Pelton impulse type turbine with multi-stages velocity (Moyer, 1917).

In this dissertation, the Peach Bottom Unit 2 RCIC System was chosen as a reference system for the turbine part scaling Similarity Level analysis. The reason is being, this reactor is very similar in design to Fukushima Dai-ichi Unit 2. Further, being the most studied reactor for BDBA conditions, more data is readily available for this reactor than for other reactors.

The Terry turbine has a solid interior wheel with buckets milled into the face. Steam is injected through nozzles where it exits and hits the u-shaped buckets of the wheel, which forces it to rotate. The nozzles can be located along one half of the wheel or uniformly distributed around the entire wheel. Figure 2 shows a drawing of the turbine body, wheel, and nozzle. Reversing chambers are installed at the exit of the nozzle, so the steam is able provide enough energy to rotate the wheel even at low steam pressure. Figure 3 shows the GS-2 turbine wheel with the buckets, and a set of reversing chambers distributed in the interior of the upper part of the turbine body. Figure 4 shows the steam flow path as it is exiting the nozzle.

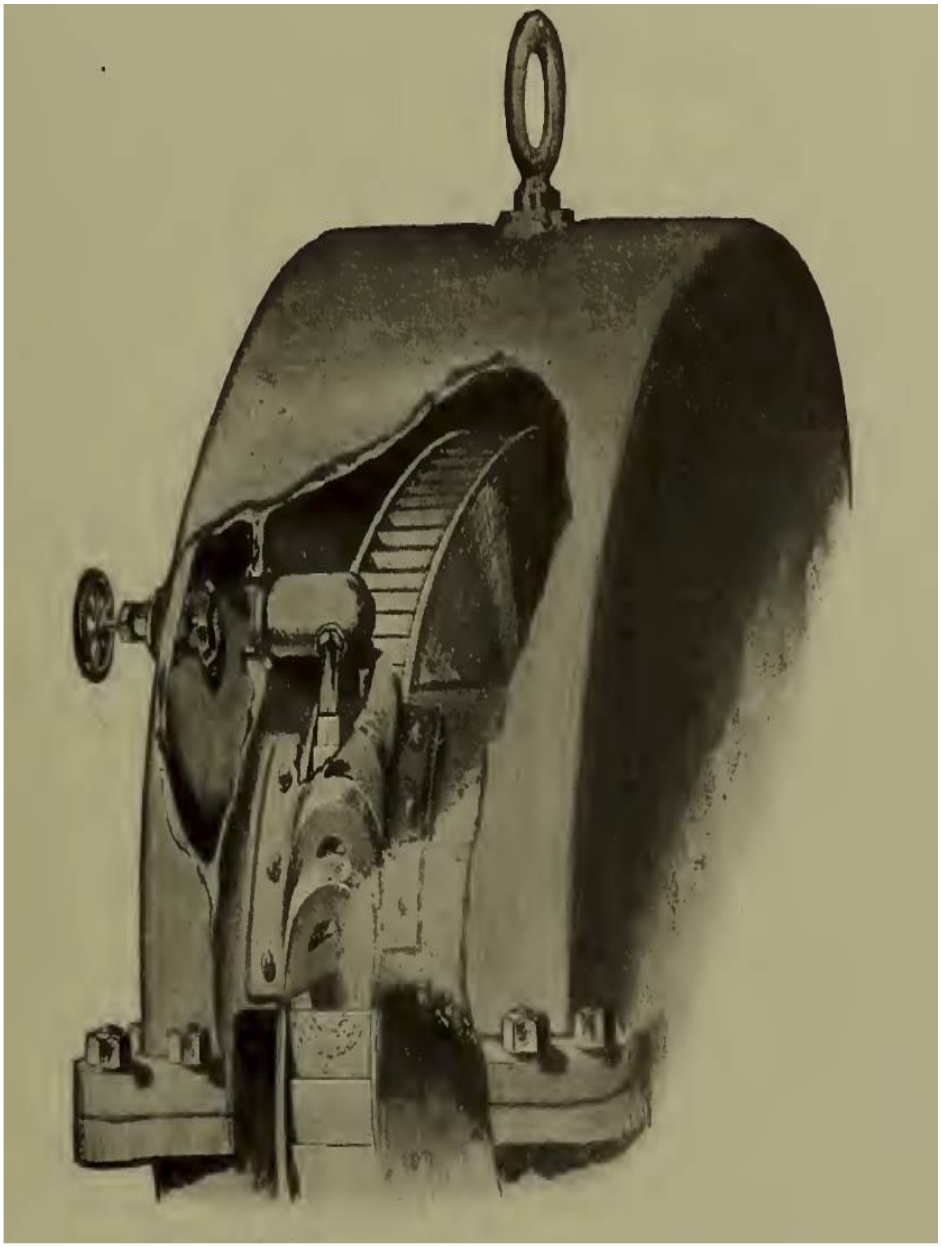

Figure 2 Terry turbine layout with injection nozzle and reversing chambers (Leland, 1917).

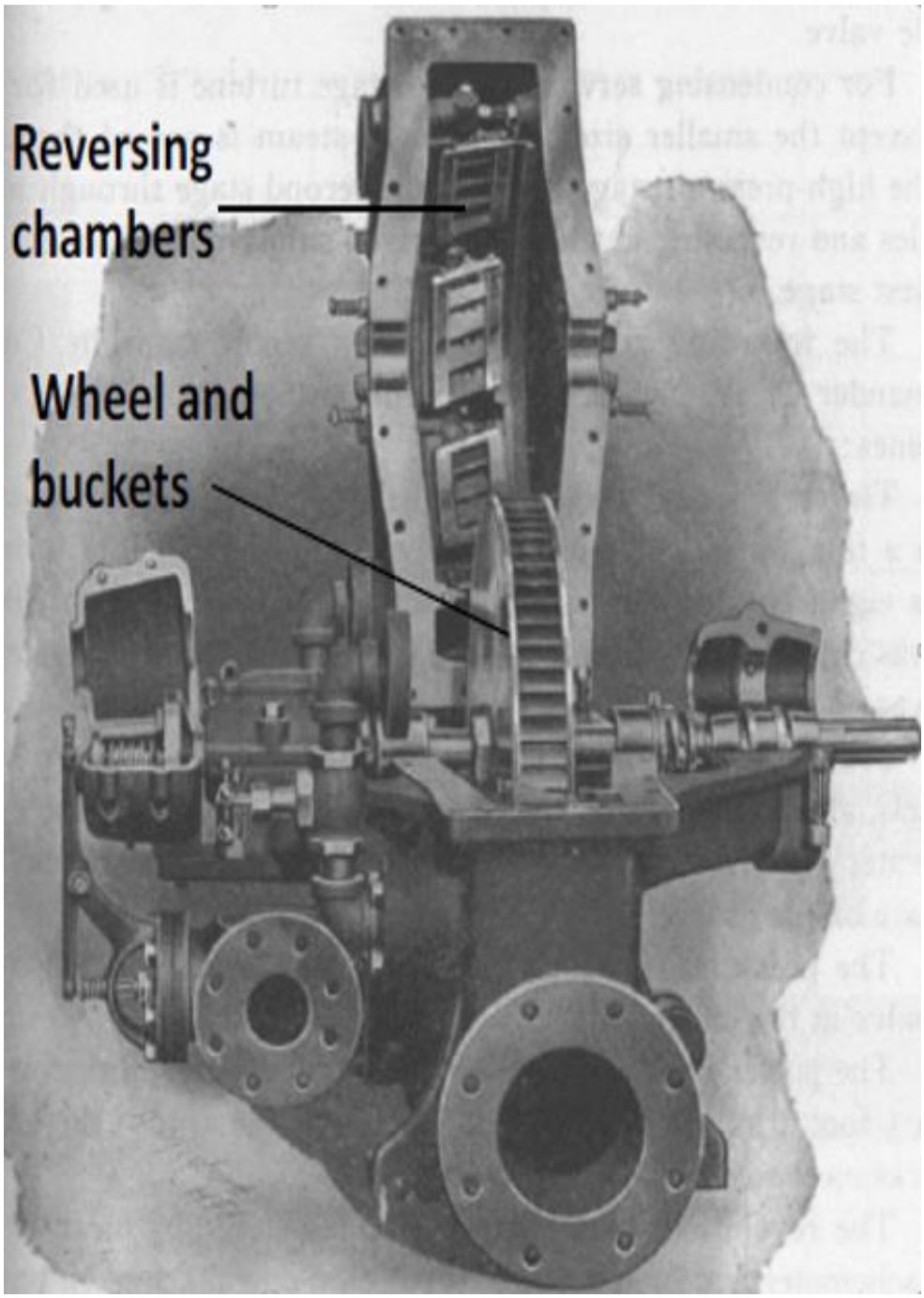

Figure 3 Terry turbine wheel along with buckets and set of reversing chambers (Terry Steam Turbine Company , 1953).

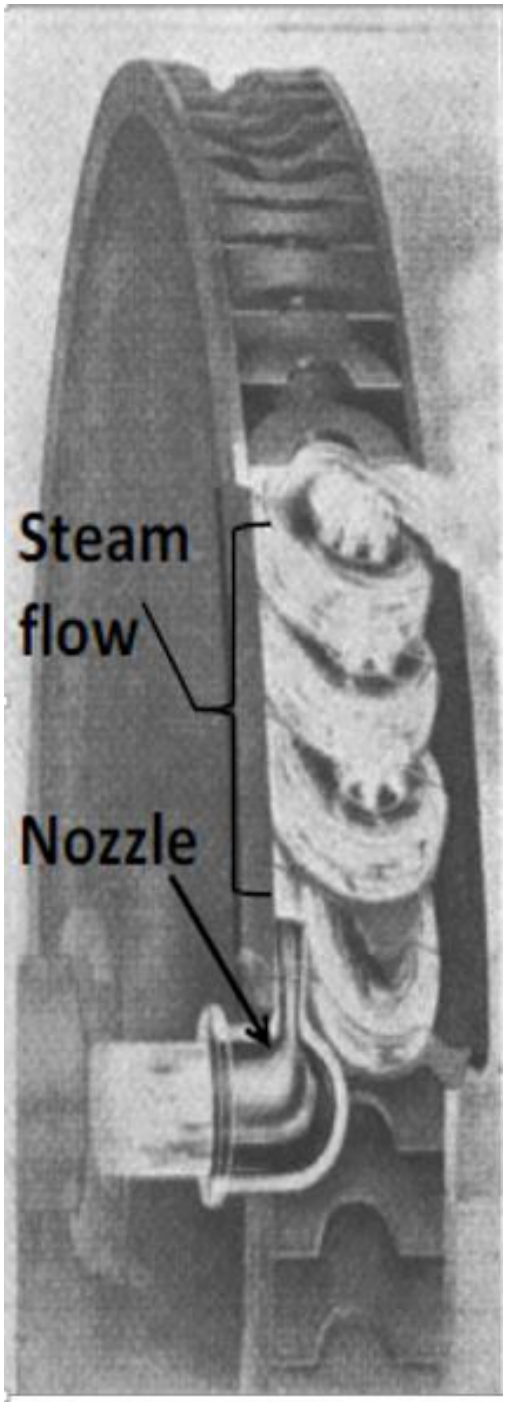

Figure 4 Terry turbine steam flow path as exiting the nozzle (Terry Steam Turbine Company , 1953).

To have a better illustration of the connection between the Terry turbine and the pump, Figure 5 shows an old drawing from the Terry turbine Steam Company of the turbine coupled to a multi-stages pump by a shaft.

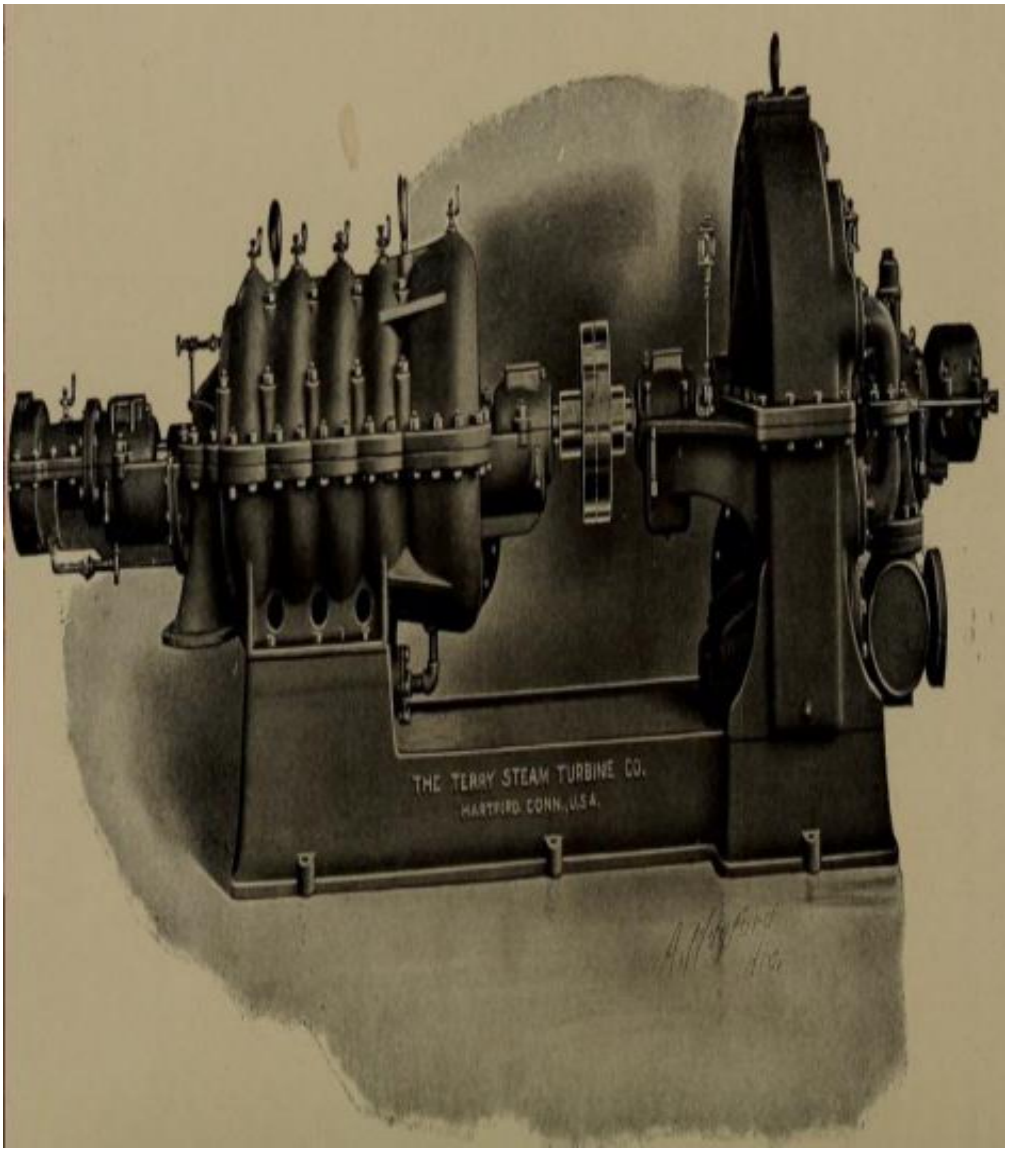

Figure 5 Terry turbine connected to a multi-stages pump by shaft (Terry Steam Turbine Company , 1953)

2.1.1.1 RCIC system Terry turbine valves

The RCIC system turbine has important components that are vital to controlling its operation. One of these vital components for control are valves. The valve collections are: isolation valves, steam to turbine valves, turbine trip and throttle valves, and turbine governor valve. Two isolation valves are lined up to the turbine and will open if there is a RCIC initiation signal to maintain the steam path to the turbine. Meanwhile, the steam to turbine valve is normally kept closed to isolate steam to the RCIC turbine in the standby condition (General Electric, 2011).

The turbine trip and throttle valve is located upstream to the governor valve and provides a rapid turbine tripping after receiving a trip signal based on various conditions. Normally, the valve is open and can throttle steam flow to the RCIC turbine if the governor valve fails to open. A turbine trip can happen after receiving an electrical trip signal, in which the turbine releases a latch on the traveling nut with the closing of the spring forcing the valve stem down into the closed position. On the other hand, a mechanical trip (such as over speeding) releases the same latch and causes tripping (General Electric, 2011).

Important to the RCIC turbine, the governor valve opens by a spring force and is controlled by an electro-hydraulic system. The valve can be closed by controlling the oil pressure, which is opposed by the spring force (General Electric, 2011).

2.1.1.2 RCIC system Terry turbine auxiliaries

The auxiliary systems at the RCIC turbine includes: the oil system, barometric condenser system, and line fill system. The oil system is a lubricating oil that supplies the

turbine, pump bearings, and governor valve. Oil pressure varies with the turbine speed and is maintained by the governor valve that limits the turbine minimum speed to 1000 rpm.

The barometric condenser system prevent steam leakage from the shaft seals and casing drain. This system consists of a barometric condenser, vacuum pump, and a condensate pump. At the RCIC line fill system, water is taken from the CST suction line and discharged into the RCIC line. This minimizes the RCIC injection time and prevents piping voids, which could result in a water hammer by keeping the pipes full (General Electric, 2011).

2.1.1.3 RCIC system Terry turbine velocity limits and over speeding

The Terry turbine is a velocity working machine that can work at a range of velocities between 1000 rpm to almost 4500 rpm. This rotational speed is a result of the force generated by the steam that flows in the direction of the bucket motion. The wheel diameter creates torque on the turbine shaft that provides pumping power. Above the operational top speed up to 125%, the turbine trip signal is designed to be initiated in order to protect the integrity of the RCIC system. The turbine trip signal will be actuated and cause an automatic electrical trip at a level of 110% at top operation speed. Other trip signals could be caused by (General Electric, 2011):

- Low pump suction pressure (15'' Hg vacuum).
- High turbine exhaust pressure (50 psig).
- Any isolation signal.
- Manual operation.

If a trip does not happen for any reason, the RCIC system integrity will be lost as a result of turbine damage. Figure 6 and Figure **7** show severe damage that happened to a GS-1 Terry turbine as a result of over-speeding.

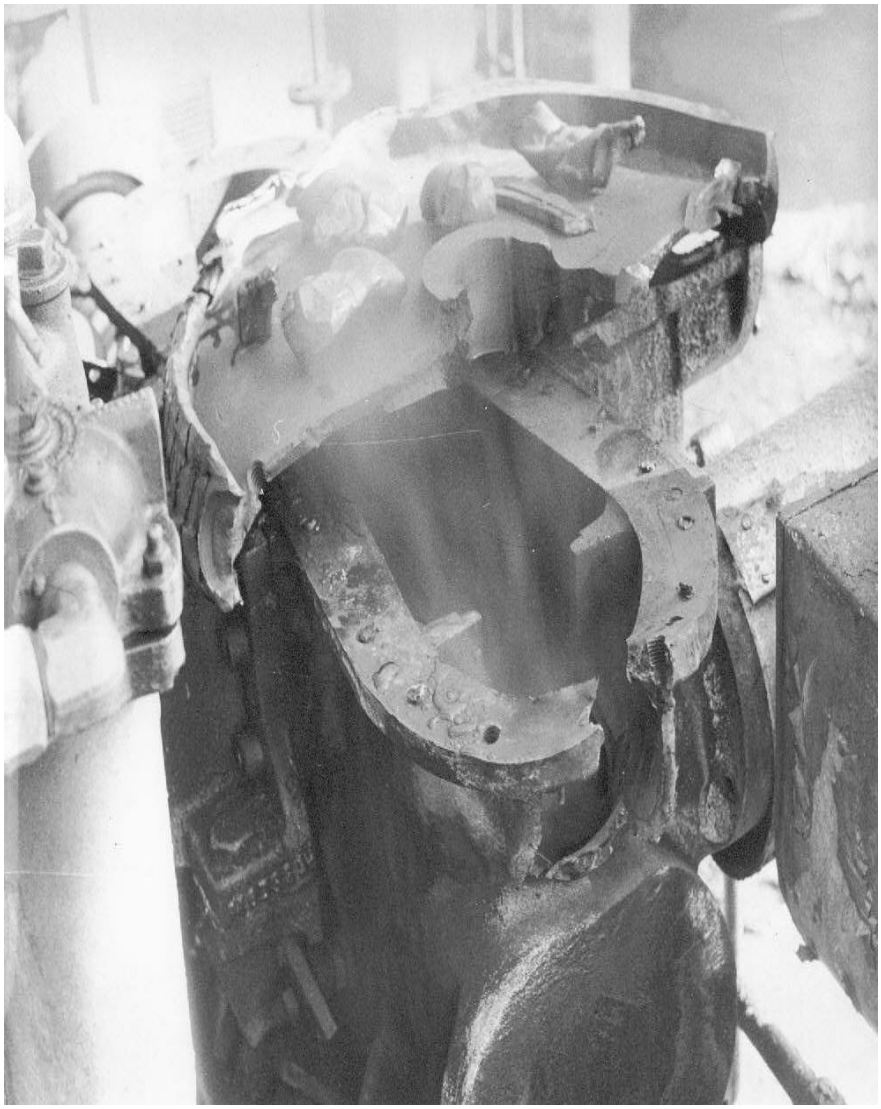

Figure 6 Terry turbine wheel and lower case damaged severely (Kirkland, 2018).

Figure 7 Terry turbine upper case damaged severely (Kirkland, 2018).

2.1.1.4 Peach Bottom RCIC system Terry turbine characteristics

The Peach Bottom RCIC System turbine is classified as a GS-1 turbine. The solid cylindrical turbine wheel has several semi-circular "buckets" that are machined into the body of the wheel (General Electric, 2011). The Terry turbine wheel diameter is 0.61 m (2 ft.). The five steam inlet nozzles each have a width of 0.01 m (0.4 inch) and four reversing chambers per nozzle, with a nozzle inlet/outlet angle of 0.79 rad (45° degree).

The GS-1 RCIC System turbines only have steam nozzles in the lower half of the steam ring with a nozzle diameter of 1.5 cm (0.584 inch). Meanwhile, the GS-2 turbines have nozzles in the upper half of the steam ring in addition to the ones in the lower half. The GS-1 turbine has 84 buckets on wheel as adopted from a CAD model of (Ross , et al., 2015).

The GS-1 turbine is designed in order for a steam inlet pressure of 6.8 to 10.2 atm (100 to 150 psig) to supply sufficient pump power with a rated speed of approximately 419-492 rad/s (4000-4700 rpm). An inlet pressure of up to 78.3 atm (1150 psig) to the turbine, makes it capable of supplying several times the rated horsepower (Electric Power Research Institute , 2002).

2.1.1.5 NHTS RCIC system Terry turbine characteristics

The NHTS facility employs a 157-kW steam generator to electrically provide the steam to power a RCIC turbine analog. The modified facility will have an actual turbine in place of the current turbine analog. The turbine will exhaust steam to another pressure vessel that represents the Suppression Chamber. The turbine will be connected by a shaft to a RCIC pump and will power the pump to return Suppression Chamber water to the reactor pressure vessel, represented by the steam generator. The Suppression Chamber has two lines that can vent steam below the water surface, one representing the RCIC turbine exhaust line and the other representing a Safety/Relieve Valve (SRV) line. A water injection line tees into the steam line upstream of the turbine, to enable two-phase steam/water injection to the turbine.

The NHTS RCIC System turbine is classified as a ZS-1, with a wheel diameter of 0.46 m (1.51 ft.). One steam inlet nozzle with three reversing chambers is mounted on the turbine, with a throat diameter of a 1 cm (0.38 inch). Initially, the turbine had three nozzles, but was modified to have just one nozzle. The location of the nozzle and the reversing chambers is near the bottom of the turbine wheel with a measured nozzle inlet/outlet angle of 0.52 rad (30° degree).

The maximum pressure measured on the inlet and exhaust ends is up to 5.1 atm (75 psia), while the exhaust pressure typically reaches only 1 or 1.1 atm (15 or 16 psia). The turbine speed ranges from 157 to 314 rad/s (1500 to 3000 rpm). The turbine exhaust line in the suppression pool is 0.61 m (2 ft.) from the rearmost tank position. The turbine exhaust line outlet is at half-elevation of the pool water (0.4 m or 1.3 ft.) and the Safety Relief Valve (SRV) discharge is at 0.2 m (7 in) from the tank bottom. Figure 8 shows the NHTS ZS-1 Terry turbine assembled on a platform. Figure 9 shows the NHTS Terry turbine lower case after being modified with one nozzle installed. While a closer view of the NHTS ZS-1 turbine nozzle and reversing chambers are shown in Figure 10.

Figure 8 The NHTS ZS-1 Terry turbine on a platform assembled with its instrumentation.

Figure 9 The NHTS ZS-1 Terry turbine lower casing with one nozzle installed.

Figure 10 NHTS ZS-1 terry turbine nozzle and reversing chambers.

The scaling factor for the turbine wheel diameter between the GS-1 and the NHTS ZS-1 models is 1:1.33. The five nozzles in the GS-1 turbine provide higher rotational speed than one nozzle in the ZS-1 turbine to work at low pressure (below 10.2 atm) of inlet steam. Similarity will be verified in this dissertation using the scaling Similarity Level analysis, which will tell the Similarity Level value between scaled systems.

2.1.2 RCIC system pump

2.1.2.1 Prototype RCIC system pump

The RCIC System pump is a multi-stage horizontal pump designed to deliver a flow rate of water equal to the boil off rate of the reactor inventory. The pump suction is from the CST until the water level reaches a low prescribed level, after which the Suppression Chamber serves as the alternate water source. The pump can deliver up to 0.05 m^3/s (800 gpm) of water to the reactor pressure vessel based on the plant design (General Electric, 2011). The Peach Bottom RCIC System pump is typical to the general design of the Peach Bottom RCIC System pump with a volumetric flow rate of 0.0268 m^3/s (425 gpm).

The relative locations of the turbine and SRV exhaust lines to the RCIC System pump suction for Peach Bottom Unit 2 are not available in public literature. If the pump suction happens to draw water at a temperature close to saturation, either from a localized hot spot in the pool or an overheated pool, this would lead to pump cavitation. The Peach Bottom RCIC System pump suction piping is 0.154 m (0.51 ft.) internal diameter. The pump's nominal volume flow rate is 0.0268 m3/s (425 gpm). In a pipe of similar diameter and volumetric flow rate, the corresponding velocity is 1.44 m/s (Ross , et al., 2015). The turbine governor valve is the main regulator of the pump flow. If the turbine reaches an over-speed threshold, a mechanical turbine trip is actuated. The pump is located at an elevation lower than both suction sources to ensure that the required NPSH is available (Electric Power Research Institute , 2002).

2.1.2.2 NHTS RCIC system pump

In the NHTS test facility, the RCIC System pump is a 5-stage, horizontal centrifugal pump. The pump suction is at the very bottom of the Suppression Pool (cylindrical tank), at the opposite end of the tank from the turbine and SRV exhaust lines. The suction location is important because it determines the temperature of the ingested water. The turbine exhaust line is 0.61 m (2 ft.) from the rearmost tank position, while the pump suction is 2.65 m (8.7 ft.) from that end (0.45 m or 1.5 ft. from the front most part of the vessel) – a separation of 2.04 m (6.7 ft.). The pump inlet and outlet pipes dimension are 1.9 cm (¾-inch) pipe size.

The NHTS facility pump is a Dayton model 5UXF5 with a 0.55 kW (0.75 HP) electric motor running off 115 VAC and producing up to 6.3 atm (93 psig) of boost pressure. The motor speed nominally is 361 rad/s (3450 rpm), with a maximum capacity of 0.0013 m3/s (20 gpm). The NHTS pump flow is derived from its relation with the total head based on the manufacturer's published head vs flow data (Dayton Pump Manual) . The NHTS Dayton 5UXF5 pump curve is shown in Figure 11 and it is designed for 90 ^{o}C (194 ^{o}F) maximum liquid temperature. During the tests on the NHTS facility, no cavitation was identified at the RCIC System pump (Solom, 2016) .

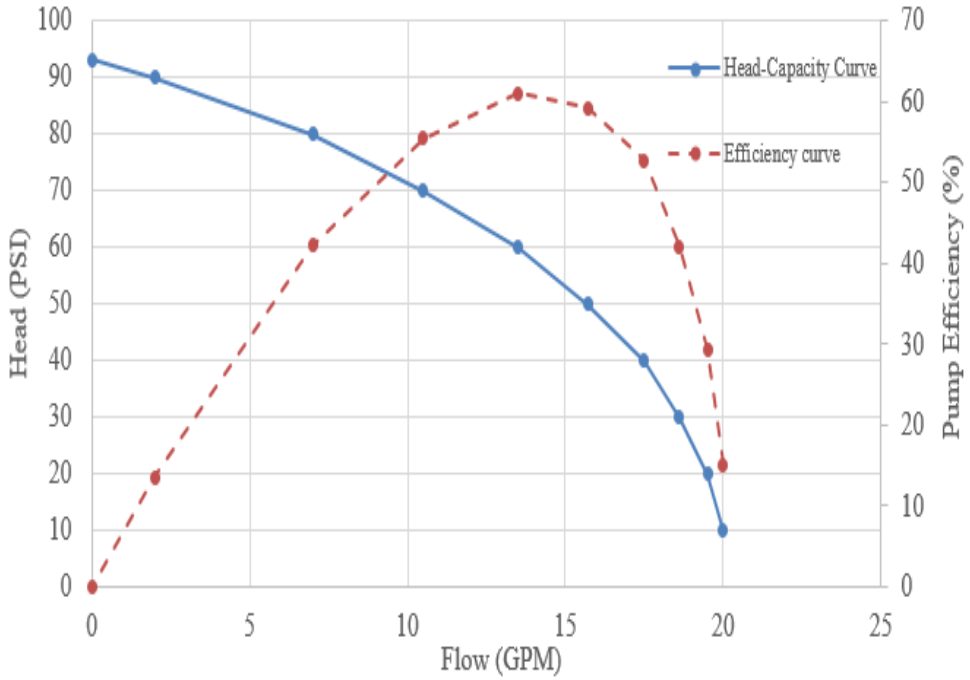

Figure 11 NHTS RCIC System Dayton 5UXF5 pump performance curve.

Different water sources in the NHTS facility create challenges for scaling and testing process, which are the following:

- NHTS facility has no CST.
- Switchover from the CST to the Suppression Pool is not modeled.
- NHTS Suppression Pool shape is not toroidal in shape.

In the NHTS facility, the source of the water is the Suppression Pool tank only, since there is no CST. The RCIC pump volumetric scaling factor between the NHTS and Peach Bottom facilities is 1:21.25. The scaling factor for the pump suction internal diameter is 1:8.1.

2.1.3 RCIC system suppression chamber

The empty space in the toroidal shape of the pool along with the water volume is called the Suppression Chamber (wetwell). The Suppression Chamber of a Mark I containment is a steel pressure vessel of toroidal shape, located below and surrounding the drywell as shown in Figure 12. The Suppression Pool is used to remove the heat that is released if an accident occurs. During RCIC System operation, heat is delivered to the Suppression Pool mainly as steam exhaust from the RCIC System turbine. The steam is condensed in the Suppression Pool water, which also provides a source of water to be injected to the core by the RCIC System pump (USNRC, 1994). Normally, the water level is at the mid height of the suppression chamber as shown in Figure 12, which also shows the pipe that carries the water from the Emergency Core Cooling System (ECCS).

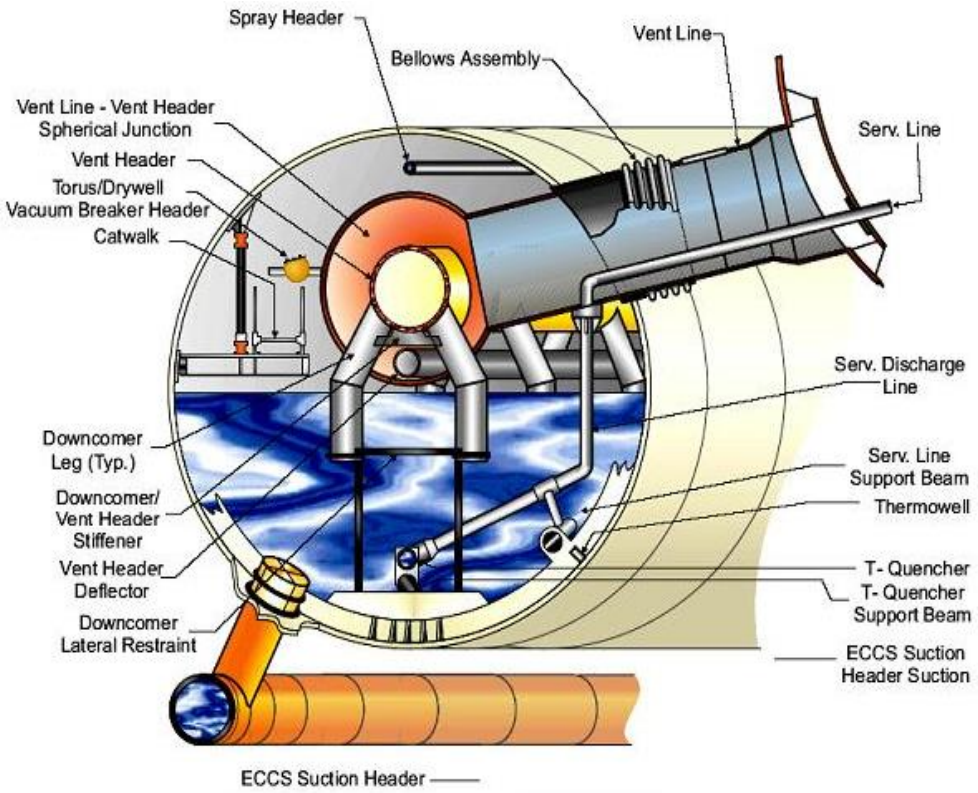

Figure 12 Side view of the BWR Mark I containment Suppression Chamber (Lochbaum, 2016).

2.1.3.1 Peach Bottom RCIC system suppression chamber

The Suppression Pool works as the plant's heat sink during accident conditions. In addition to this function, it provides a secondary cooling water source for the main RPV after the primary plant CST is depleted. For Peach Bottom Unit 2, the Suppression Chamber has a torus shape with a centerline-to-centerline diameter about 33.8 m (110.9 ft.) and the cross sectional diameter is 9.5 m (31 ft.). The torus water level is nominally near the axial midpoint. This gives an average Suppression Chamber free gas volume of about 3695 m^3 (130,000 ft^3) with an average water volume of 3556 m^3 (125,100 ft^3). Figure 13 shows the Mark I containment suppression Chamber.

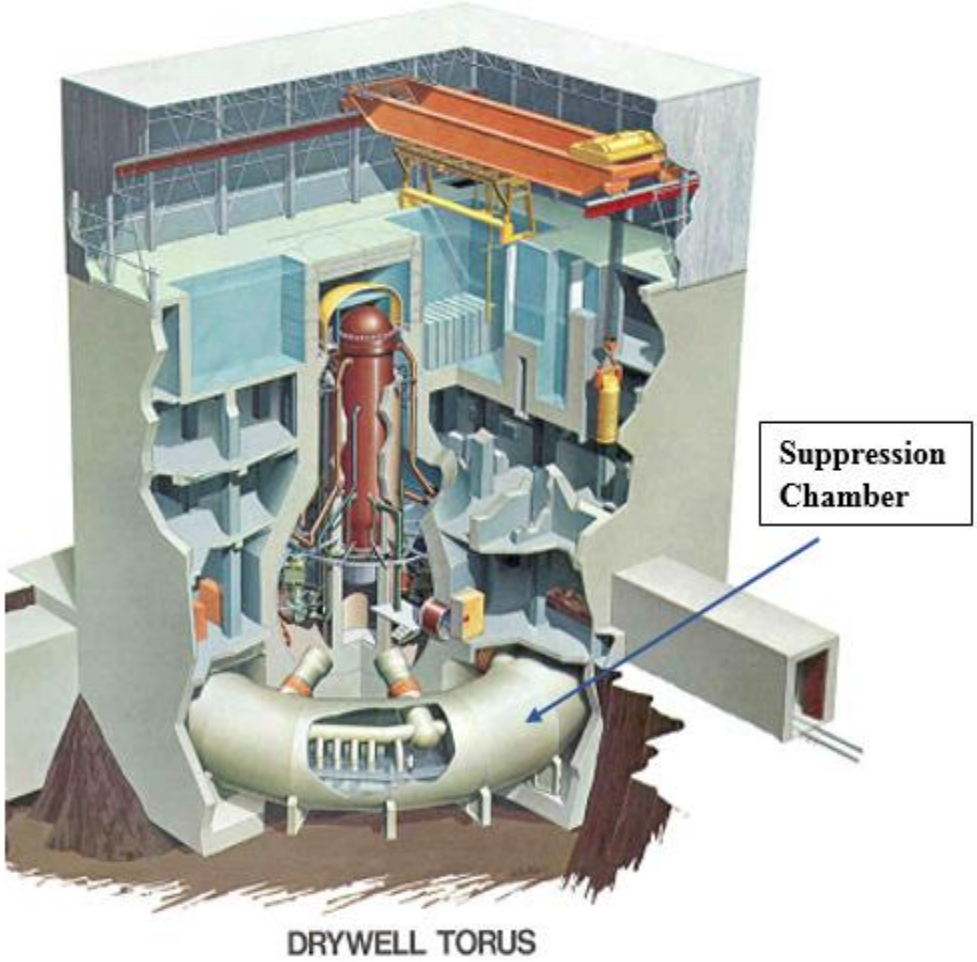

Figure 13 BWR Mark I containment Suppression Chamber (General Electric, 2011).

The operating conditions of the Suppression Pool, such as water surface temperature and thermal stratification can affect the containment pressure response since it determines the vapor partial pressure (Gamble, et al., 2001). Thermal stratification and mixing within the pool can change the pool surface temperature and therefore affect the peak containment pressure as well as the available net positive suction head for the RCIC pump. Also, it will degrade the performance of the RCIC system after actuation once it switches to the Suppression Pool as a secondary water source.

2.1.3.2 Monticello RCIC system suppression chamber

The Monticello reactor has a Mark I containment with a toroidal Suppression Chamber. The cylindrical shape still allows for a pump suction which is located at the bottom of the Suppression Chamber. This suction location is important because it determines the temperature of the water ingested by the reactor pressure vessel.

The Monticello plant configuration is shown in (Figure 1-4) of (Asai, et al., 1979). The torus elevation from the ground base is almost 912 ft., with a torus centerline to centerline distance of 98 ft. The Suppression chamber cylindrical diameter is 27 ft., 8 in., and it has a Safety Relief Valve (SRF) T-Quencher, which discharges near the bottom of the suppression pool. The T-Quencher layout and location of suction and discharge piping of Monticello Suppression Chamber are shown in (Fig .1-1 and Fig .1-6) of (Patterson, 1979) respectively.

The Suppression Chamber has a total of 8 T-Quencher and 4 Residual Heat Removal (RHR) suctions with a diameter of 20 in (Patterson, 1979). The Suppression Chamber water temperature is from 50 to 55 ^{o}F, with a water volume ranging from 68,000 to 70,000 ft^3. The normal height of the water inside the Suppression Chamber is 131.4 in.

The steam flows through the T-quencher into the Suppression Pool when the SRV is opened. The steam energy and momentum result in circulation of the pool water and creates thermal currents. These thermal currents would be contained within the discharge location if there is no bulk circulation around the torus. If there is a bulk circulation of the pool water, the thermal current will have a pattern based on the flow velocity. Low velocity

results in thermal currents patters in the direction of the flow, and high velocity results in a turbulent mixing that breaks up the created patterns (Patterson, 1979).

To examine the Monticello pool mixing, tests were conducted on the pool without modifying the T-quencher design and RHR lines. It was found that without having the RHR system in operation, the steam flow through the T-quencher resulted in high vertical thermal stratification with a temperature difference vertically of 52 ^{o}F. When the RHR was under operation, no thermal stratification was present (Asai, et al., 1979) .

2.1.3.3 NHTS RCIC system suppression tank

The Suppression Chamber tank in the NHTS facility is a horizontally-mounted stainless steel cylindrical pressure vessel with an inner diameter of 1.51m (5ft). The cylindrical shape of the NHTS Suppression Chamber was chosen based on the availability of reasonably large-sized pressure vessels and manufacturing costs. The volume is about 5.3 m^3 (1,400 gallons). With the tank half full, the water volume is about 2.8 m^3 (750 gallons). The cylindrical body has a head welded on both ends, with a tank cylindrical length of 2.7 m (8.9 ft.) and a head center-to-head center length of 3.1 m (10.2 ft.).

The water level at the NHTS facility is slightly above the axial mid-plane of the tank at about 0.77 m (2.5 ft.), since the nominal water level at the actual plant Suppression Chamber is roughly at the axial mid-plane of the torus. Figure 14 shows the NHTS facility Suppression Chamber tank with associated pipes and lines. Based on the mentioned diameters and capacities of the NHTS and Peach Bottom Suppression Pools, the resulting volumetric scaling factor is about 1:1,368 while the diameter scaling factor is 1: 6.3. Later in this study, the Similarity Level scaling analysis will be considered as the main scaling

process and a replacement for linear scaling (scaling factors) because of the complexity of the system.

At the NHTS facility, steam is injected into the tank through pipes called Spargers. This suction location is important because it determines the temperature of the water ingested by the reactor pressure vessel.

By comparing the NHTS and Monticello water capacities, the resulting water volume scaling factor is about 1:688-708 while the diameter scaling factor is 1: 5.6. In addition, the flow injection pipe diameter scaling factor is 1:12.4 and the level of water scaling factor is 1:4.33. The cylindrical shape of the NHTS Suppression tank is comparable in shape to a representative portion of the Monticello torus. Indeed, the centerline of the NHTS tank is straight, while the Monticello one is curved (Patterson, 1979).

Figure 14 NHTS facility Suppression Chamber tank.

2.2 RCIC System Reliability

The depletion of onsite DC power is a limitation of the RCIC system operation. Though, failure of the RCIC system is not limited to DC depletion and could be because of other limitations to the turbine that may not be instantly apparent such as (Solom, 2016):

- Lubrication oil system failure due to insufficient cooling.
- Bearings and seals failure due to lubrication system failure.
- Pump overheat and inside cavitation.
- Valves misalignments.

Hence, the turbine system is may not operate at off-normal conditions due to failure of its constituents, which is consider a robust system. Indeed, the turbine system may fail to operate in normal conditions. In the late 1980s examination study of the RCIC system turbine in BWR plants showed that the system had significant probability of failure on demand due to constituent's failure. The majority of the failures were because of the governor failure with a 70% (Houghton & Hamzehee, 2000).

Additionally, operational conditions could be a potential failure cause including operator incorrect signal reading and hostile turbo-pump conditions presence (Solom, 2016). Alteration of the RCIC system water source signal may be a reason of failure as a system initiation failure along with operator failure to manually launch a switchover. Moreover, water slugs can degrade the functionality of the governor valve and cause failure to compensate for the turbine rapid speed changes and eventually causing a turbine trip (Solom, 2016).

2.3 Fukushima Dai-Ichi RCIC System Performance

The RCIC system at Unit 2 of Fukushima power plant started performing its duty after the accident and stopped based on a water level signals. After the tsunami hit, it caused flood in the building and resulting in loss of off-site and on-site power supply. The operator had successfully restarted the RCIC system manually, which continued operating until its failure. The switchover between the CST and the Suppression Pool happened successfully after several hours. The RCIC system worked for nearly 70 hours without available DC power or operator intervention before it eventually failed perhaps due to Suppression Pool saturation (Institute of Nuclear Power Operators , 2011).

The RCIC system in Unit 3 behaved similar to the one at Unit 2 at the beginning of the accident by starting and stopping due to water level signals. After the tsunami hit, the offsite power was lost, while the onsite DC power was partially lost (Unit 3 had battery power still available for). Similar to Unit 2, the operator restarted the RCIC system manually and it kept running for 19.5 hours (Institute of Nuclear Power Operators , 2011). Yet, there is no clear explanations for the operation behavior of the RCIC systems at Fukushima Daii-Chi power plants. For this reason, experimental test facilities were constructed and built to study the long-term performance of the RCIC system such as the NHTS testing facility.

3. COMPLEX SYSTEMS SCALING METHODS AND PRINCIPLE

Scaling analysis is required to ensure well representation of the system key components and phenomena. The phenomenon for this dissertation are the phenomena peculiar to long-term operation of the RCIC System during Extended Loss of AC Power (ELAP). Many scaling laws are used for the design of testing facilities such as linear scaling and volume scaling. Moreover, creating scaling models helps predicting and studying the full-scale system behavior at operating and accident conditions. Additionally, applying a correct scaling might show the level of similarity between the scaled systems or distortion at certain areas of the system.

In this dissertation, scaling methodology is developed to be applicable for the RCIC system complex scaling and is called the scaling Similarity Level estimation analysis for steady/quasi-steady and transient system behavior as will be shown in the coming sections. Scaling has a mathematical foundation in which the governing quantities of the dimensional equations are non-dimensionalized to identify parameters that must be conserved between model and prototype. So, estimating the Similarity Level is vital for complex systems scaling analysis, where in this research it is dependent on the control volume governing equations and normalization process.

The linear scaling method, based on length ratios, are not used in this study. However, scaling factors are mentioned to provide an idea about the dimensions difference between scaled systems. Many of the physical processes in nuclear safety systems are not proportional to the physical dimensions of the components and therefore the fluid's

momentum and energy transfer will be distorted if this method is applied. Moreover, as the scaling factor becomes extremely small, some of the processes of interest (those sensitive to length scale) either disappear or behave differently. In addition, this would create difficulty in implementing some energy transfer processes in the scale model if its component are physically very small compared to the prototype (Bestion, D'Auria, Lien , & Nakamura, 2016).

One of the main pillars for complex nuclear systems scaling analysis is the (Bestion, D'Auria, Lien , & Nakamura, 2016). This report is a state of art in scaling of thermal hydraulics systems in nuclear complex systems. It describes scaling techniques and methods that governs many phenomena in nuclear systems. Another important reference in scaling is the analysis methods book of (Krantz, 2007). This book describes the systematic scaling analysis in fluid dynamics, heat transfer, mass transfer, and reaction processes with no specific discipline. It also explains the basic scaling steps and considers many complex problems involved in transport phenomena. A brief description about previous scaling methods that has been in used in nuclear systems is coming in the next subsection.

3.1 Prior Scaling Methods and Phenomena

In order to design, built, and understand collected testing data, scaling processes started. This section provides a brief overview of scaling processes applied in nuclear systems for specific phenomena. Where experiments conducted in scaled down facilities due to difficulties of conducting tests in full scale ones. Generally, for a certain phenomenon the scaling parameters are derived by applying the dimensional or

dimensionless approaches (Bestion, D'Auria, Lien , & Nakamura, 2016). The next subsections describe some of the prior methods applied into nuclear systems scaling.

3.1.1 Volume scaling method

When governing equations are known, dimensionless scaling can be used. For systems where the time scale, velocity, heat flux, and gravity force is need to be conserve, the volume scaling method is appropriate. The volume scaling was introduced by (Nahavandi, Castellana, & Moradkhanian, 1979). This method can be applied to produce time-reducing or time-preserving scaling laws. While preserving the length between scaled systems, it reduces the area and volume. This method was widely used and to design nuclear testing facilities for LOCA accident. The study provided scaling laws for modeling of nuclear systems by using the volume conservation laws. The mass, momentum, and energy equations were used in 1-D analysis to persevere property transient in nuclear systems. Regardless of the volume scaling method benefits, if applies into a small area scale; phenomena such as heat loss and pressure drop can be distorted significantly and that makes it inadequate method of scaling (Bestion, D'Auria, Lien , & Nakamura, 2016).

3.1.2 Linear and modified linear scaling methods

Linear scaling laws based on system governing equations were derived at (Cudnik & Carbiener , 1969). Linear scaling methodology was modified and applied to the analysis of direct ECCS bypass in the reactor down-comer area (Yun, Cho, Euh, Song , & Park , 2004). The method was based on two-dimensional governing equations of a fluid model at (Ishii, 1975). The scaling method reduced the velocity and time scale and preserved the gravity one. The “modified linear scaling methodology” was validated by using

experimental data from different scaled facilities and concluded as an appropriate for designing of small scale testing for studying the ECCS bypass phenomena.

The linear scaling method is not used for the Complex RCIC system scaling. Many of the physical processes in nuclear safety systems are not proportional to the physical dimensions of the components and therefore the fluid's momentum and energy transfer will be distorted if this method is applied. Moreover, as the scaling factor becomes extremely small, some of the processes of interest (those sensitive to length scale) either disappear or behave differently. In addition, this would create difficulty in implementing some energy transfer processes in the scale model if its component are physically very small compared to the prototype (Bestion, D'Auria, Lien , & Nakamura, 2016).

3.1.3 Three-level scaling method

This method was derived to cover the natural circulation under single and two-phase flow conditions phenomena by (Ishii & Kataoka, 1983). The method helped designing integral test facilities (Bestion, D'Auria, Lien , & Nakamura, 2016). Geometrical and operational similarity groups were obtained to study the phenomena in a prototype model. The derived scaling laws were applied to the Loss of Fluid Test (LOFT) to simulate natural circulation. The analysis resulted in usable time scale simulation for single phase flow and distortion for the two-phase flow cases. The distortion in some scale component resulted from different time and velocity scales between the model and prototype systems of interest.

3.1.4 H2TS scaling method

The H2TS scaling method was developed by the NRC for the purpose of estimating similarity criteria, which in this dissertation is called Similarity Level values. The method is fully described in Appendix D of NUREG/Cr-5809 (Zuber , 1991). The method divides the system into a hierarchy of subsystems and further subdivisions of the subsystems. The subdivisions includes geometrical configuration, conservation equations for each component of the systems.

This method was successfully adopted in designing the APEX facility and other applications. More details about the APEX facility scaling is introduced in subsection 3.2. Figure 2.1 of (Reyes, 2001) shows an example of a hierarchal levels developed for the APEX-CE test facility. Generally, the scaling hierarchy includes: (1) the process to be scaled, which covers the phenomena that being studied and (2) the constituent part element of the H2TS method that requires performing "Top-down" system scaling analysis. This level expressed the effects on the system caused by complex interaction between the system components and lead to the similarity criteria estimation as will be shown in the scaling analysis of NHTS facility section in this dissertation.

3.1.5 Buckingham Pi theorem

The Buckingham scaling principle is a used to estimate expected phenomena depending on dimensional analysis (empirical approach), which starts by listing all dimensional variables. It used a concept called the method of repeating variable, which is based on dimensions of variables and constants to obtain a complete set of dimensionless groups (Buckingham, 1914). This method can be performed without estimating the

phenomena of interest nor the governing equations. Buckingham formulated a theorem to study the scaling properties of any system based on its constituents. Actually, The Russian scientist Dimitri Riabou-chinsky first published this method in 1911. The method requires listing the main parameters of the governing equations and set a reduction parameter called *j* as a guess. The reduction parameter *j* is guessed by setting its value to the number of primary dimensions represented in the problem. Guessing a wrong value of *j* lead to a wrong number of Pi quantities and not accurate solutions. As a summary of the method, the following are the steps of the Buckingham Pi theorem of non-dimensionlizing system governing equations:

- Define the problem, list its parameters and count the total number as *n*.
- List the dimensions for each *n* parameters.
- Set *j* as the primary dimension number.
- Calculate the expected number of unit-less quantities as $k= n-j$.
- Choose *j* repeating variables that will be used for constructing unit-less equations.
- Generate the unit-less equations and manipulate as necessary.
- Check the dimensionless of the generated quantities and write functional relationship between the dimensionless quantities.

The main benefits of the Buckingham Pi method if well implemented are summarized as follows:

- Generating unit-less parameters that helps design s specific experiments.
- Predict the prototype system performance based on scaling laws.

- To predict trends between the system parameters.

However, the method has inherent difficulties which makes it sometimes hard to implement such as identification of the phenomena of interest. Also, the difficulty of choosing the right set of dimensional variables, which results in inadequate dimensional parameters that produces wrong number of dimensionless groups that complicates the process.

3.2 APEX-test facility scaling

One of the good references for testing facility design and scaling analysis is the scaling of the High Temperature Test Facility (HTTF) at Oregon State University (OSU) (Woods, Jackson, & Nelson, 2009). This analysis examined the thermal hydraulic system behavior for design basis and beyond design basis transients. The scaling analysis was based on the H2TS method and was used to validate analytical tools and methods that were proposed for the HTTF. Based on general scaling analysis the design parameters and operating conditions for the test facility were estimated.

The HTTF scaling analysis addressed specific phenomena of interest that serve analysis ultimate goal and initial and boundary conditions for the considered mode of operation. The analysis presented specifically the Depressurization Conduction Cooldown (DCC) scenario, where it was divided into three modes of operation of the VHTR (Woods, Jackson, & Nelson, 2009):

- Very rapid reactor vessel depressurization.
- Onset of primary side natural circulation.
- Extended period of air ingress and molecular diffusion.

The original reference of the HTTF analysis was scaling analysis performed for the Oregon state university Advanced Plant Experiment (APEX) in the early 2000s (Reyes, 2001). The test facility was to obtain data to support the Pressurized thermal Shock (PTS) rule of the NRC (10 CFR 50.61) report. The APEX scaling report (Reyes, 2001) describes the scaling basis for the test facility. The reference nuclear plant for the APEX scaling was the Palisades Nuclear Plant. Most importantly, the scaling analysis was used as a guide to modify the APEX facility. The analyst used the H2TS method to estimate the Similarity Levels between the scaled facilities for the following modes of operation phenomena:

- Primary loop natural circulation.
- Cold leg and down-comer fluid mixing.
- Reactor coolant system depressurization.
- Steam generator depressurization/ RCS cooldown.

The different modes of operation lead to obtaining different sets of similarity criteria depending on the geometrical configuration of the systems components. The GSM steps that were applied for the APEX facility can be summarized as followed:

- Determining of the phenomena control volume.
- Writing the control volume balance equations.
- Reformation of the balance equation into dimensionless form.
- Estimating the characteristics time ratios (dimensionless groups).
- Calculating numerical estimates for the characteristics time ratio for the model and prototype for the hierarchical level of interest.

- Evaluations of the scaling criteria to check if the scaled system would introduce any scaling distortion.

4. RCIC SYSTEM SIMILARITY LEVEL SCALING METHODOLOGY AND PRINCIPLES

For this dissertation, Similarity Level scaling analysis methodology were developed providing state of art RCIC system scaling Similarity Level equations. Zuber's H2TS methodology (Zuber , 1991) was started with in this research to show the required level of details for scaling. Other scaling methodologies were avoided because of the significance distortion level that produced when applied to complex nuclear systems. The RCIC system Similarity Level analysis uses the dimensionless approach in deriving the unit-less equations that are used in estimating the Similarity Level value of the NHTS RCIC system with respect to a prototype one.

A Similarity Level is the ratio of values for the prototype and model of a unit-less characteristic time ratio (Π) parameter that is used to characterize the system. These unique characteristic time ratios (Π) are derived for the system under consideration by normalization of the system's governing equations and terms. This dissertations describes the development and derivations of unique characteristic time ratios for the turbomachinery and Suppression Pool in the NHTS RCIC system facility. These characteristic time ratios are used as the basis for estimating the Similarity Level between the scaled systems. The scaling methodology for the NHTS facility RCIC system is shown in Figure 15.

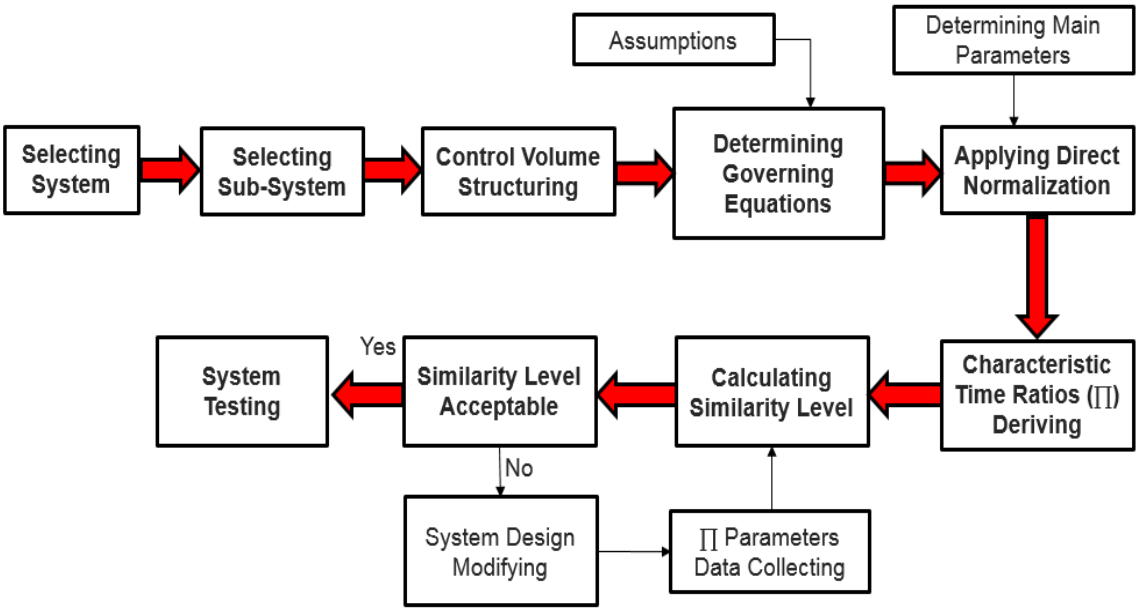

Figure 15 NHTS facility RCIC system scaling level methodology

4.1 Similarity Level Characteristic Time Ratio Derivation

The characteristic time ratios are derived by normalizing each term of the governing equations. Working on a control volume basis, the conservation equations are formulated as in Equation (1). This method leads to derivation of characteristic time ratios that cover the transfer process of interest for a specific constituent "M".

$$\frac{d\,V_M \Psi_M}{dt} = \Delta C_M \pm P_{MN} + F_M \tag{1}$$

where M represents the control volume constituent, V is the control volume, Ψ_M is the conserved quantity in the control volume (mass, momentum, or energy), C is the convection term of the quantity in the control volume, P is the process of transport from M to N, and F is any distributed source or force inside the control volume. The next step

is normalization, which is done by dividing each term by its nominal quasi-steady value, denoted by the superscript “o”, as shown in Equation(2).

$$C_M^{+} = \frac{C_M}{C_M^{o}} \tag{2}$$

The result of normalizing the governing equations for a quantity in the control volume is one or more unit-less $\prod$ groups that govern the quantity’s transfer and are composed of a process frequency part (fr : the process transfer rate) multiplied by a time scale part (τ : the time available for the process to transfer). It is possible to solve for the reference time scale by solving for the exact similarity condition, where the $\prod$ value for the prototype equals the $\prod$ value for the model. A transfer frequency which is very small ($\prod << 1$) means that the specific process is not important in the transient process when comparing between the scaled systems. A $\prod$ value greater than one means the process transfer occurs at a high rate, and the process is important in the transient process when comparing between the scaled systems.

Once the $\prod$ parameters are derived, the numerical values for the model and prototype systems are used to estimate the Similarity Level by Equation (3), thereby revealing how well the transported quantities are conserved between the model and prototype systems.

$$\mathrm{SL} = \frac{\prod_M}{\prod_P} = (\prod)_R \tag{3}$$

If the numerical values of the Similarity Level between the model and prototype systems are approximately equal to or near 1.0, then similarity exists between the scaled

systems. If the Similarity Level is much smaller or much greater than one, then either the process is not well conserved or it is of limited importance in the transient since only a small amount of the quantity is transported (Krantz, 2007). In the case of a low Similarity Level, modification of the model system for improved scaling may be possible by adjusting the physical geometry, fluid properties, operational conditions, and/or boundary conditions of the model. Identification of the need for model modifications is an important outcome of the scaling analysis.

The dimensionless process reduces the number of variables in the problem to the number of fundamental units. The normalizing term has a value corresponding to a nominal condition. This is equivalent to considering every scaled quantity to be a primary quantity. Furthermore, reaching a unique minimum parametric representation permits assessment of the relative magnitude of the various terms in the governing equations.

In this dissertation, the governing equations of the control volume are determined and used for RCIC turbopump and Suppression Pool scaling Similarity Level analysis to derive unique characteristic time ratios. The authors report herein the derivation of new characteristic time ratios related to the RCIC component, which are used in later sections to estimate the Similarity Level values.

The RCIC system has many other components and details. Some components of the RCIC system other than the turbine and pump, such as pipes and connections, can be scaled more simply by calculating linear scaling factors and matching Reynold and Nusselt numbers for the flow properties. Equipment which require a more involved scaling

analysis to investigate the long-term RCIC System performance in a full-scale facility include:

- RCIC System turbine;
- RCIC System pump;
- RCIC System water source(s); and
- Suppression Chamber (BWR containment).

Modification of the model system for improved scaling may be possible by adjusting the physical geometry, fluid properties, operational conditions and/or boundary conditions of the model. Identification of the need for model modifications is an important outcome of the scaling analysis.

To conclude, the scaling analysis procedure applied in this dissertation can be summarized in the following steps:

- Determine the problem phenomena (the case or accident scenario);
- Obtain the balance equations (conservation of mass, momentum and energy) in dimensional form;
- Formulate and simplify the governing equations as appropriate to the RCIC System ELAP scenarios;
- Change the dimensional quantities to non-dimensional quantities using the initial and boundary conditions;
- Define unique characteristic time ratios; and
- Determine numerical values of the scaling characteristic time ratios and estimate Similarity Level value between the model and prototype.

The authors report in this dissertation the derivation of scaling equations related to the RCIC System turbo-pump and Suppression Pool. The RCIC System governing equations and derivations of the system's time ratios are presented in Chapter 6. The equipment which must be properly scaled in the NHTS facility to investigate the long-term RCIC System performance in a full-scale facility is:

- RCIC System water source;
- RCIC System Terry turbine; and
- RCIC System Pump.

4.2 Scaling Challenges

Many challenges were encountered during the RCIC system scaling analysis with respect to a prototype facility systems. These challenges include:

- Incomplete Peach Bottom RCIC System geometrical data and description, including:
  - Size and number of the RCIC turbine steam inlet nozzles consistent with the performance information of the Peach Bottom RCIC System.
  - Component parameters such as the angle between the steam inlet nozzles and the turbine wheel buckets and other geometrical dimensions for the RCIC turbine.
- Lack of the Peach Bottom and Monticello RCIC System operational records and archived history.
- Limited performance data from the NHTS equipment based on previous tests that had a different configuration and different research objectives.

- Variations in operating procedures and boundary conditions between the Peach Bottom unit and the NHTS facility.

To estimate some of the missing information about the Peach Bottom RCIC system, a Sandia National Laboratories (SNL) report that describes models of the Peach Bottom RCIC system to the best of their knowledge (Ross , et al., 2015) has been referenced. This report includes estimations of RCIC turbine parameters based on CFD results and other analyses. Moreover, steam tests were performed at the NHTS facility that covered the range of operating conditions and provided experimental data for scaling purposes. These separate-effects tests on the ZS-1 turbine were part of an earlier program (Luthman, 2017) and the data have proven to be useful also for the current scaling analysis.

As for differences in boundary conditions between Peach Bottom and the NHTS experimental facility, the NHTS facility will be able to cover the entire pressure range of the containment for Design Basis Accidents (DBA), because the Suppression Chamber pressure vessel is rated for up to 80 psig, which is above the design pressure of Mark I Suppression Chambers. Some of the other boundary and inlet conditions such as the steam flow rate will be scaled down to correspond to the expected the RCIC System start time. Also, a range of operating conditions has similarly been applied in the earlier configuration of the NHTS RCIC system to study the sensitivity of the Similarity Levels to various operating parameters, as shown in Chapter 7.

5. COMPUTATIONAL FLUID DYNAMICS CODE AND RCIC SYSTEM TURBINE MODEL DEVELOPMENT

The CFD analyses in this dissertation are performed for turbine models of the ZS-1 and GS-1 designs using STAR-CCM+ commercial code. The purpose of the analyses were to investigate and collect some features parameters of the Terry turbine under normal operating conditions that can be used in scaling Similarity Level analysis. Furthermore, to prepare and validate a testing model of the ZS-1 Terry turbine and nozzle that represent the turbine at the NHTS facility. A detailed description of the CFD analyses in this dissertation is presented in this chapter.

5.1 STAR-CCM+ CFD Code

STAR-CCM+ is a computer code developed and maintained by CD-ADAPCO as a multidisciplinary platform of simulations by developing models and predicting its performance. The STAR-CCM+ code has been chosen for this dissertation as a CFD code because of the following reasons:

- Availability
- Capability
- Portability
- Convenience

The code is capable of handling large models very quickly and efficiently and it became recently the first commercial CFD package to mesh and solve a billion- level number of cells. The components of the code include (STAR-CCM+ User guide, 2018):

- 3D-CAD modular
- CAD embedding
- Surface preparation tools
- Automatic meshing technology
- Physics and turbulence modeling
- Post processing

The 3D-CAD modular is a feature built in the code that allows building geometries from scratch and storing them as 3D-CAD models. Also, it allows the user to modify the model from outside the 3D- CAD. It basically allows to change and modify the size of the geometry components and run the case in a quick manner. In this dissertation the GS-1 turbine geometry was imported to the STAR-CC+ and the 3D-CAD was used to modify the GS-1 geometry to represent the ZS-1 turbine one.

The surface preparation in the STAR-CCM+ has powerful tools that increase the efficiency of simulation and reduce surface cleanup time by applying automated surface wrapper. The surface wrapper close holes in the geometry and provide a manifold surface that generate a powerful computational mesh automatically in short time.

STAR-CCM+ allows for automatic meshing that generates polyhedral, tetrahedral, or hexahedral control volumes that allows simulations to operate at high speed and accuracy. The meshing tool provide automatic high quality layer mesh on the walls in the domain and allows for controlling of the size, cell layers, and growth-rate. The automated mesh option is used herein for the turbine geometries. On the other hand, the STAR-CCM+ has a variety of physics models that built in to the solver. Some of the physics

models that are used in this dissertation for the RCIC system turbine and nozzle geometries include:

- Coupled flow and coupled energy
- Steady state time model.
- RANS (Reynolds Averaged Navier Stokes) turbulence model
    - K- Epsilon turbulence
    - Realizable K-Epsilon two –layer
    - Exact wall distance (using projection method)
- Ideal gas compressibility model
- Moving Reference Frame (MRF)

Coupled flow model provides converged results for simulations that has a compressible steam in a supersonic and hypersonic flow as in the turbine nozzle. The model solves in a coupled manner the momentum and mass equations implicitly in pseudo-time approach. Higher pseudo-time step in this model relatively lead to fast convergence. The coupled flow model is used also because it yields more robust and accurate solution for the steam compressible flow, especially in the presence of shocks. Velocity is obtained from the momentum equation, while pressure from the equation of state. The STAR-CCM+ coupled flow model governing equations in integral form for a volume V and differential surface area "*d*a" is represented in Equation (4) and the vectors are defined in Equation (5)

$$\frac{\partial}{\partial t}\int_V \mathrm{W}\, dV + \oint [F - G].da = \int_V \mathrm{H}\, dV \tag{4}$$

$$\mathrm{W} = \begin{bmatrix} \rho \\ \rho v \\ \rho E \end{bmatrix}, F = \begin{bmatrix} \rho v \\ \rho v v + p\mathrm{I} \\ \rho v H + \rho v \end{bmatrix}, G = \begin{bmatrix} 0 \\ \mathrm{T} \\ \mathrm{T}.v + q^{''} \end{bmatrix} \tag{5}$$

Where ρ is the density of the fluid, v is the velocity of the fluid, E is the total energy per unit mass, p is the pressure, $q^{''}$ is the heat flux vector, and H is the vector of body forces (CD-ADAPCO, 2018).

The steady state time model was applied since it simulates the steady long–term operation of the RCIC turbomachinery system Suppression Pool mixing. RANS models solves the Reynolds-Averaged Navier-Stokes equations to solve the transport parameters of the main turbulent flow. While the K-Epsilon turbulence model is a two equation model that solves transport equation and calculates the turbulence kinetic energy as well as its dissipation rate to determine the flow viscosity. Two- layer realizable K-Epsilon model was applied as two layers of computations that provides better results than the standard K-Epsilon model. The steam turbulence kinetic energy transport solved by STAR-CCM+ using Equation (6) (CD-ADAPCO, 2018).

$$\begin{aligned} &\frac{\partial}{\partial t}\int_V \rho_{steam}\, k\, dV + \oint_A \rho_{steam}\, k\left(\left(\vec{u} - \vec{u}_{grid}\right) * d\vec{A}\right) = \oint_A \left(\mu_{steam} + \frac{\mu_t}{\sigma_k}\right)\left(\nabla \vec{k} * d\vec{A}\right) \\ &+ \int_V \left(f_c\, G_k + G_b - \rho_{steam}\left(\left(\in - \in_o\right) + y_M\right) + S_k\right) dV \end{aligned} \tag{6}$$

Where ρ_{steam} is the steam density (kg/m^3), k is the turbulent kinetic energy (J/kg), $\vec{u}_{grid}$ is the velocity of the grid (m/s), μ_t is the turbulent viscosity (Pa.s), σ_k is the turbulent Prandtl number, G_b is the Buoyancy production source term for k, G_k is the production

source term for k, f_c is the curvature factor, $\in$ is the turbulence dissipation rate (J/kg.s), $\in_o$ is the ambient turbulence value, Y_M is the dilation dissipation, and the S_k is the miscellaneous source term for k.

MRF is a reference frame that can rotate and translate with respect to the laboratory reference frame. The MRF assumes that the angular velocity of the body is constant and the mesh is rigid. It was applied to turbine body regions to generate a constant grid flux. The inner part of the turbine geometry was modeled as rotating with reference to the outer turbine geometry. In the Navier-Stokes equations, the extra terms of compressible flow receives no contribution from the motion of the reference frame. This Lead to dealing with incompressible Navier-Stokes Equations in the laboratory reference frame. Considering a moving reference frame *W* and rotating with angular velocity ω_W in the laboratory frame **0**, Equation (7) describes how the rotating body velocity u_W related to the moving reference frame is related to the absolute velocity u_0 (CD-ADAPCO, 2018).

$$u_0 = u_W + \omega_W \times r \tag{7}$$

In addition, STAR-CCM+ has a suite of post-processing tools, the ones used in the turbine simulation including scalar and vector scenes, animation, plotting, data tables, and numerical reporting.

5.1.1 Code process and workflow

The STAR-CCM+ object tree describes the simulation detailed component such as the physics models, continua, parts, regions, meshing, conditions, and etc. The parts of the code represent the model geometry and regions, and can be used as inputs to other

objects in STAC-CCM+. The continua are objects that applied to one or more regions and contain selections of physics or meshing models. The physics continua allows the selection of the simulation physics models. The continua can be renamed, deleted, or copied between continuums. The copying feature can be used within the simulation or between different ones.

The models in the object tree represent the active models that has been selected for the simulation and can be found in the meshing or physics continua. The meshing models enables construction of surface or volumes meshes, while the physics models define the physics of the materials in the simulation (CD-ADAPCO, 2018). The regions in the code are volume domains or areas that are surrounded by user defined boundaries. Whereas, the boundaries are surfaces that surround a defined region and can be created by volume or surface mesh import, or interface creation. The interface itself provides a connection between boundaries during simulation setup.

Solvers are important in the STAR-CCM+ since they control the solution and they are different form the models. The solver can be activated in the fluid continuum to control the flow process, while if activated in the solid continuum would be to control the energy flow. Finally, after completing the simulation setup, scenes are important to visualize the geometry, mesh, and solution. Usually, scenes are used with derived parts to obtain specific simulation data.

STAR-CCM+ applies the models into the selected materials to govern their behavior under certain conditions. The general workflow of the STAR-CCM+ is illustrated in the following Figure 16.

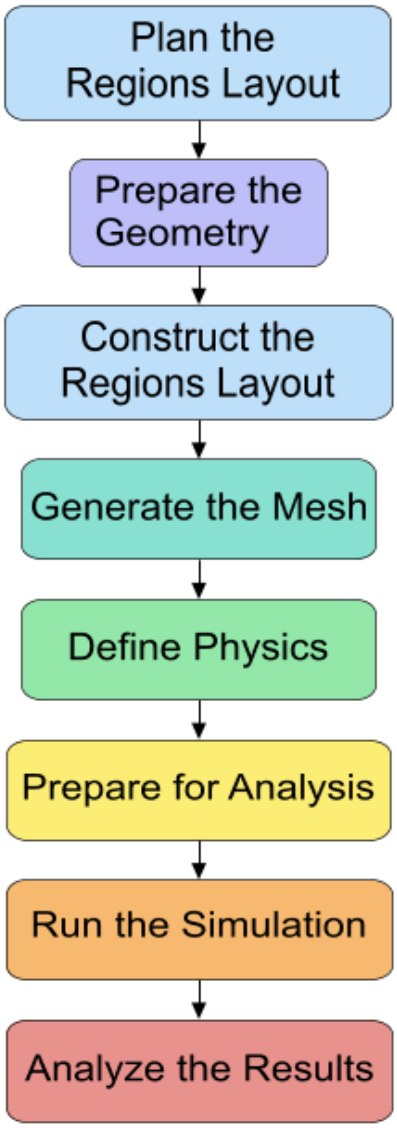

Figure 16 General sequence of operations in STAR-CCM+ analysis (CD-ADAPCO, 2018).

5.1.2 Meshing

Generating a mesh is the discretization of the geometry volume or surface where the physics solver provides a numerical solution. STAR-CCM+ has multi meshing tools

and types that can generate mesh for various kinds of geometries. The main supported meshers that were used for the RCIC turbine can be summarize as: surface wrapper, polyhedral mesher, and prism layer mesh under the automated meshing option that created specific number of cells. Where, the cell is methodical collection of faces that makes a closed volume in space.

Prerequisite to meshing is a surface repair to make sure the surface is ready for meshing. This done through the surface repair tools or geometry repair tools that provides checks for assessing the validity of various geometry parts for meshing. The surface repair tools provides repairs for the surface and fix leaks to generate surface mesh successfully. Repairs can be done to surface faces or edges. In the STAR-CCM+ the surface repair tools operates on the discretized surface and are chosen based on the quality of the geometry such as (CD-ADAPCO, 2018):

- Surface wrapper: provides manifold non intersecting surface when starting from poor quality CAD data. It also has leak detection tool that is useful for determining if any leaks are existed in the wrapped surfaces, specifically the ones created from imported surfaces. This tools was used in this dissertation manually to check leaks and to provide surface wrapping that helps prepared the turbine geometry for surface meshing.
- Surface remesher: used to create high quality triangulated surfaces as a prerequisite for volume mesh. Figure 17 shows the RCIC turbine exterior body CAD geometry before surface meshing. Figure 18 shows the results of applying surface remeshing that created triangulation with a dense dark

cluster of triangles in place that provides better representation for volume mesh models. A closer view of the triangulation is shown in Figure 19 in a 2D surface remesh view of the turbine exhaust.

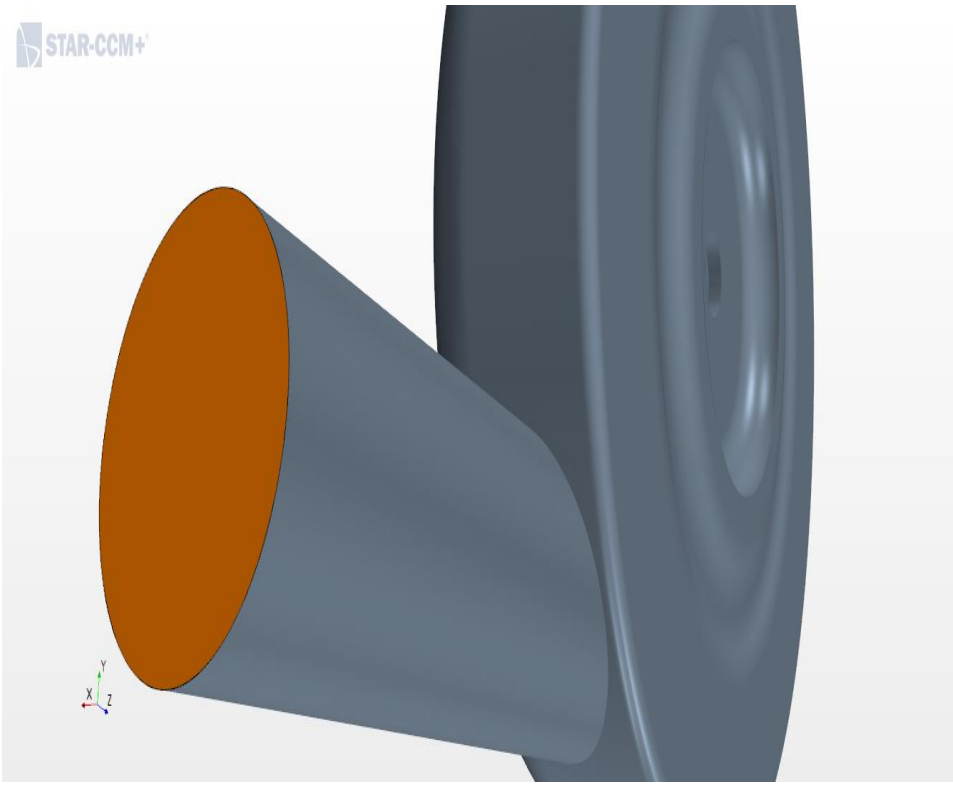

Figure 17 RCIC system turbine exterior geometry without mesh triangulation.

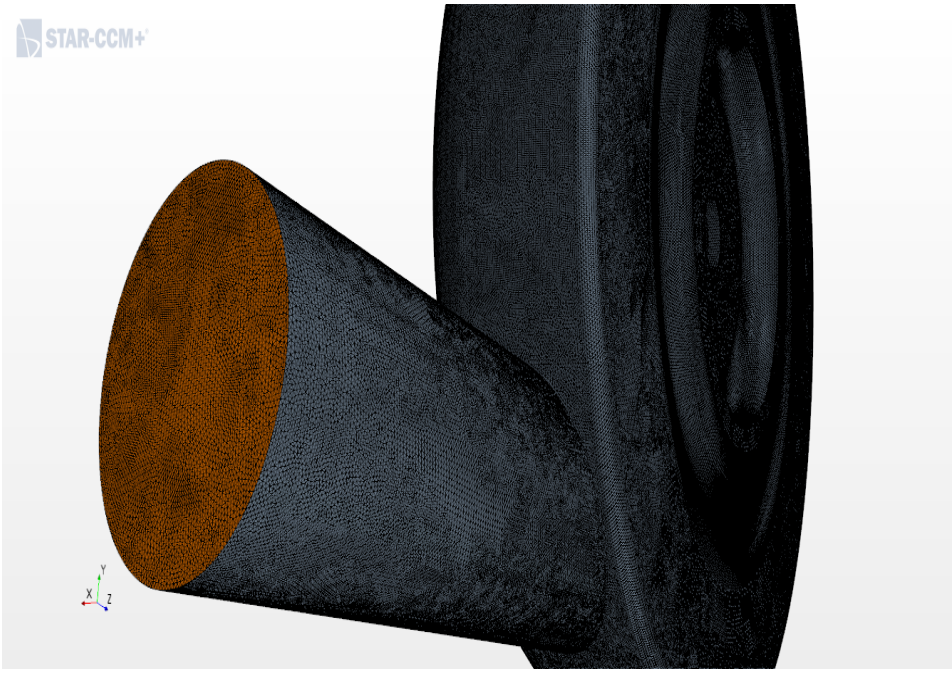

Figure 18 RCIC system turbine with surface mesh triangulation.

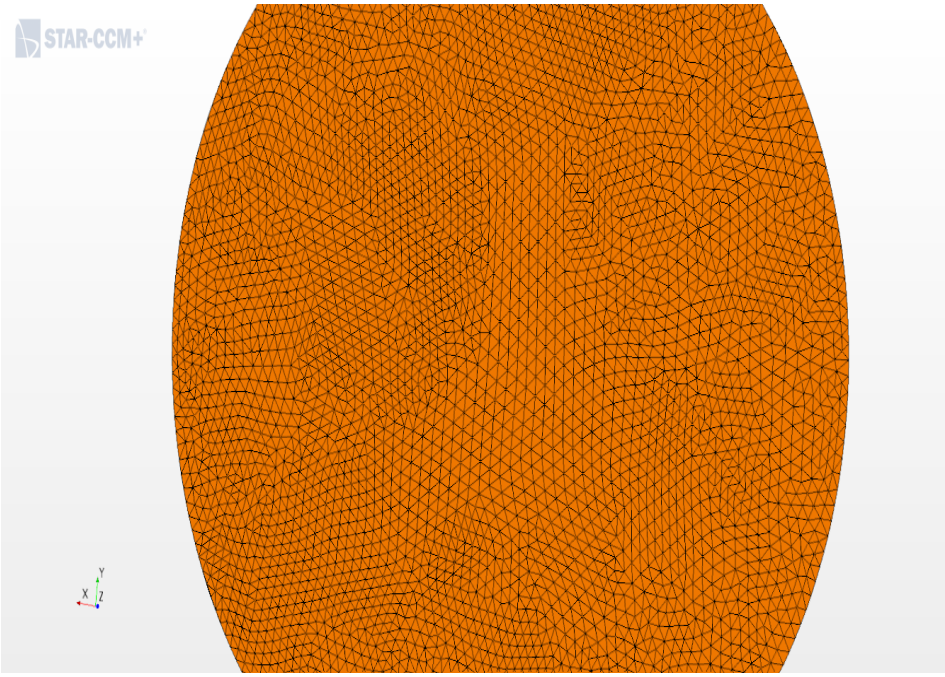

Figure 19 RCIC turbine exhaust surface triangulation.

- Automatic surface repair: this tool provides an automatic repair for a range of geometric problems that exist once the surface remeshing is complete. It was widely used in this dissertation on the turbine geometry, which helped providing clean surface and removed the geometry surface problems. The tool also connects small disconnected parts of the surface mesh.

Efficient refinement of the meshing process was achieved for the RCIC turbine meshing by activating the wake refinement option that reduced the cell size of the mesh in the area of interest for more accurate numerical solution values, which in this dissertation was at the interface regions of the interior and exterior turbine body. Figure 20 shows mesh refinement at the interface region, with a larger mesh size at the exterior turbine body. The advantage of using the wake refinement is that the user define the zone of interest. The wake refinement shape takes the shape of the boundary surface the user defines. Also the user can define the wake refinement mesh size at the refined zone, which can be absolute or relative to the base size (CD-ADAPCO, 2018). Model grid independent was tested on the GS-1 and ZS-1 turbine models with mesh base size starting at 0.015m since this is a reasonable size based on the computational cost to test the meshing sensitivity as the mesh becomes finer. Finer mesh size applied to make sure the grid independent condition is met, which was achieved at 0.001 m. The results showed a steady state values at mesh size of 0.001 m, which means the results were independent of the grid size. More details about grid independent testing is provided in STAR-CCM+ results section.

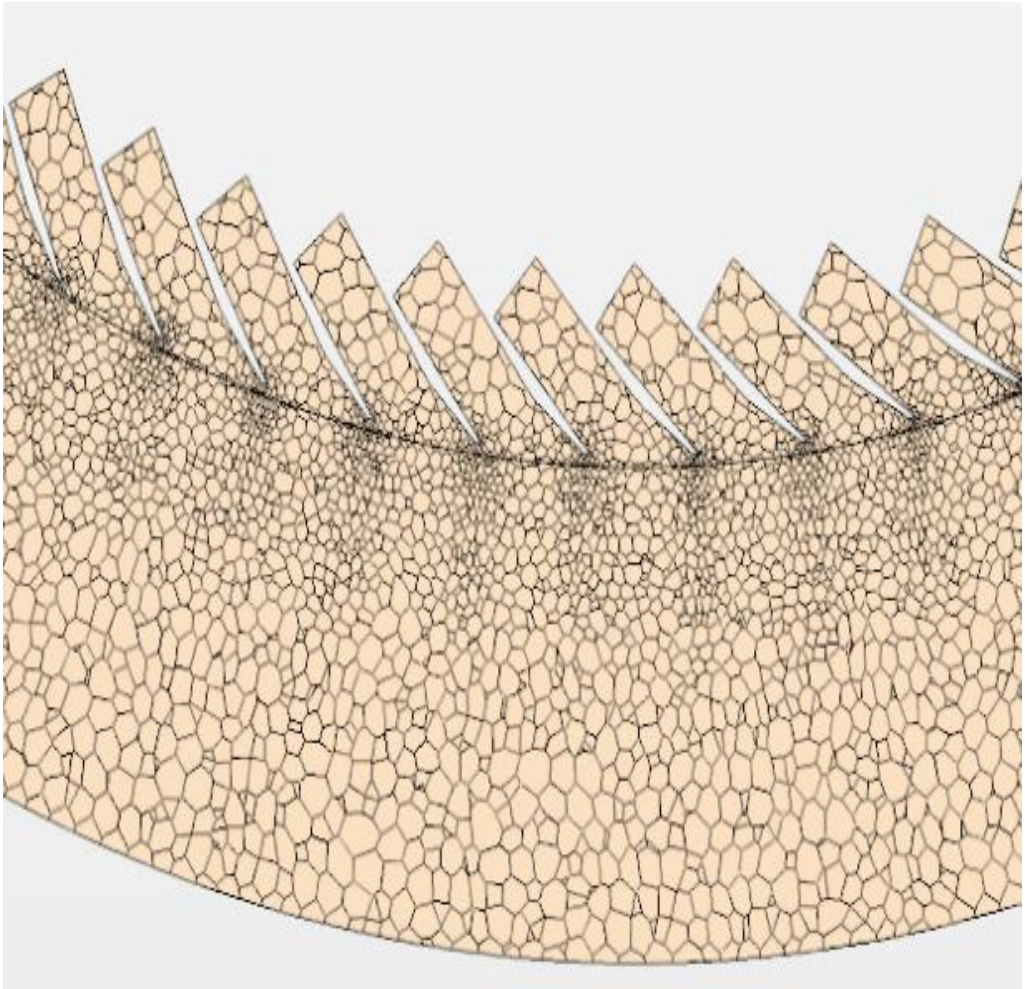

Figure 20 2D mesh refinement view at the interface of the turbine wheel and body.

5.2 New RCIC System Terry Turbine CAD Models

Fukushima accident is a motivation for studying the severe accidents that could happen to a Nuclear Power Plant (NPP) systems. Many research institutions such as SNL and Idaho National Laboratories (INL) are studying the RCIC system performance at normal and beyond design basis operations. SNL has studied the RCIC system response to beyond design bases operation by developing a GS-1 Terry turbine model that is suitable for simulation testing (Ross , et al., 2015). SNL used a CFD computational code

(FLUENT) to support the system-level modeling of the RCIC system and the developed a GS-1 Terry turbine CAD model testing.

Moreover, INL developed a Terry turbine RELAP-7 model based on SNL original work to test and simulate the normal operation condition of the RCIC system (Zhao, Zou, Zhang, & Edward, 2016). The INL introduced a model to calculate the nozzle velocity and other parameters at different operating conditions. Sandia turbine model were modified and implemented into the RELAP-7 by INL team for normal operation conditions. The INL model predicts the mass flow rate of the steam to the Terry turbine bucket entrance as well as the steam supersonic velocity (Zhao, Zou, Zhang, & Edward, 2016).

In this dissertation, NHTS Terry turbine model was developed by modifying the SNL CAD model and use it in the STAR-CCM+ code. The author prepared simulations investigated the steam jet velocity outside the turbine nozzle as it enters the turbine wheel buckets. In addition, scaling analysis was informed by input parameter estimated by simulating the NHTS ZS-1 Terry turbine model as well as the GS-1 Terry turbine one. Furthermore, a STAR-CCM+ test nozzle model is developed and used to measure the jet velocity of the steam flow at a range of steam inlet pressures to provide a correlation that calculates the jet velocity based on inlet/outlet pressure ratio.

5.2.1 Full-scale RCIC system GS-1 Terry turbine CAD model

The GS-1 Terry turbine is a representation of the full-scale RCIC system Terry turbine, which is existed in most of the BWR RCIC systems. It is consisted of a solid cylindrical wheel with a diameter of 0.61m and has several semi-circular “buckets” that are machined into the body of the wheel. The GS-1 Terry turbine has 5 nozzles each with

4 reversing chambers. In this dissertation, the full-scale GS-1 turbine model description is adopted as described by SNL (Ross , et al., 2015), where nozzles and the reversing chambers are distributed around the turbine wheel.

The nozzle width is 0.01m and its length is 1.7cm with a circular throat diameter of 0.56cm (General Electric, 2011). SNL has collected information through the available blueprints and other resources with respect to the Peach Bottom RCIC system turbine. Also, SNL team has prepared a CAD model that reflects the design of the GS-1 Terry turbine with a nozzle inlet/outlet angle of 45^0 and a wheel width of 7cm (Ross , et al., 2015). The CAD model was prepared with 84 bucket on wheel and designed such that an inlet pressure steam of 100 to 150 psig can supply sufficient pump power with a rated speed of 4000-47000 rpm (Ross , et al., 2015). The SNL CAD model is adopted in this study to represent a full-scale (Ex: Peach Bottom RCIC system turbine) and is modified and simulated in STAR-CCM+ CFD code to provide scaling Similarity Level required input parameters and data.

A solid 3D geometry representation of the GS-1 CAD model with five nozzles (purple colored inlet pipes) penetrating the exterior turbine body is shown in Figure 21. The orange circle in Figure 21 represents the turbine exhaust pipe exit. Figure 22 shows a front transparent view of the GS-1 turbine model. It's clear in the figure, the five purple nozzles each with 4 reversing chambers, distributed around a yellow turbine wheel. Figure 23 shows a transparent side view of the turbine geometry with arrows that represent the direction of the flow (inlet through the nozzles and exit through the exhaust pipe). The steam flowing at the nozzle exit hits the wheel buckets creating a momentum that causing

the wheel to rotate. As the flow pass through the turbine it loses sensible (pure steam) and latent (two-phase flow) heat and exit through the turbine exhausts, into the Suppression Pool of the RCIC system.

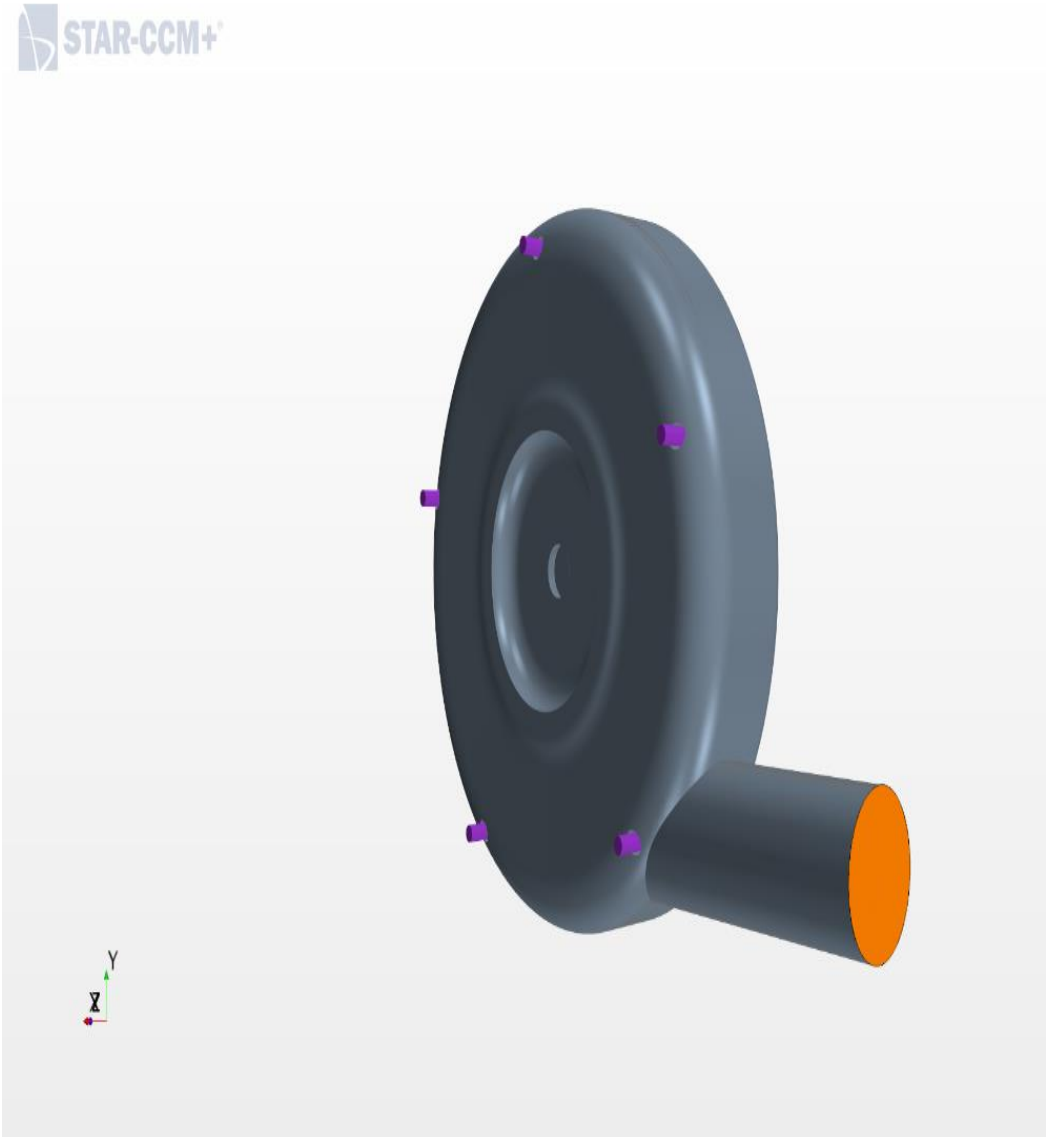

Figure 21 GS-1 Terry turbine CAD model with 5 nozzles distributed around the exterior body.

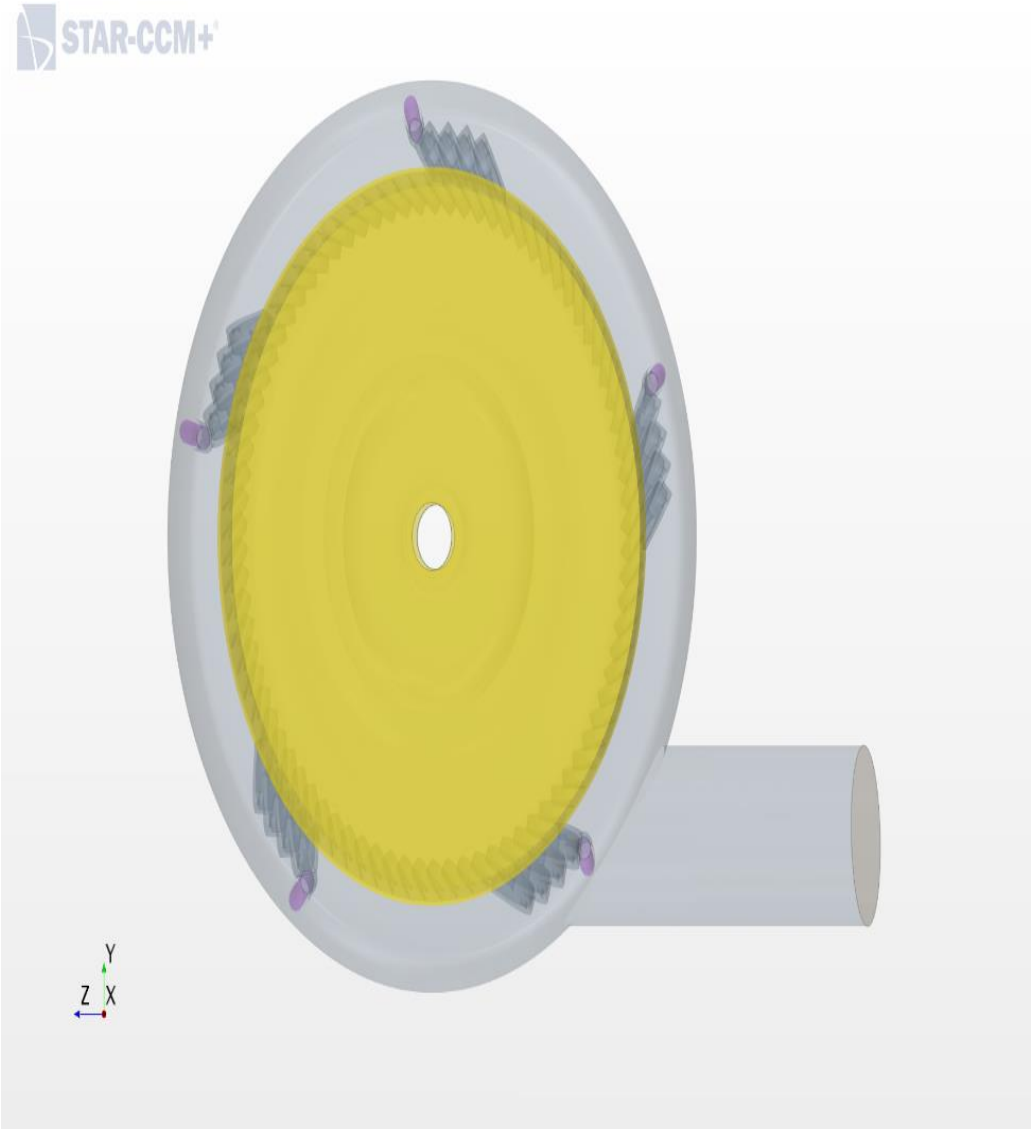

Figure 22 Transparent front view of the GS-1 CAD model with the interior wheel, nozzles and reversing chambers.

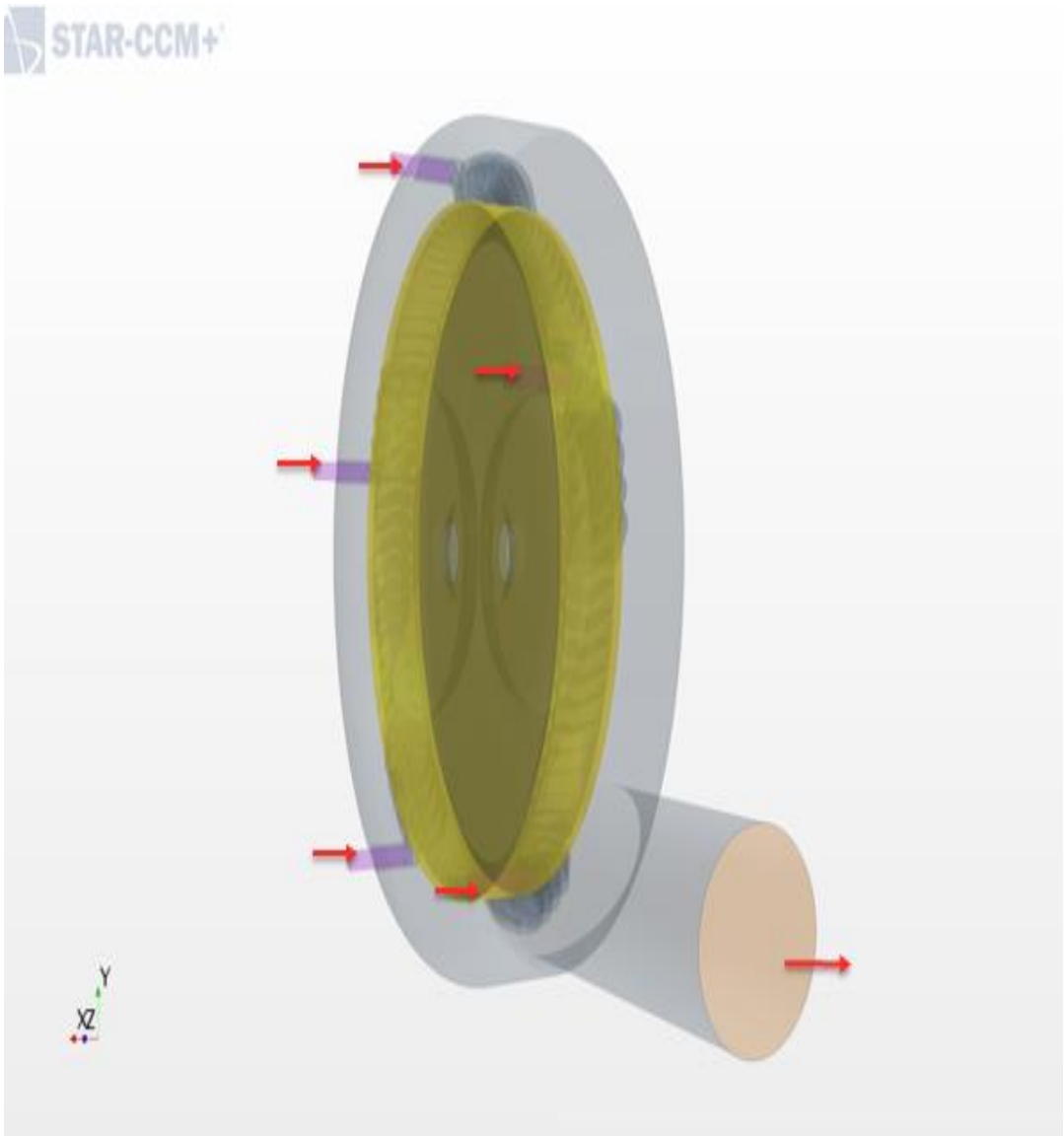

Figure 23 Side transparent view of the GS-1 CAD model along with flow direction arrows.

The details of the RCIC system turbine wheel CAD is shown in Figure 24 with the buckets inlet/outlet flow direction as well as the rotation axis. The buckets shape are similar and the distance separates buckets is constant.

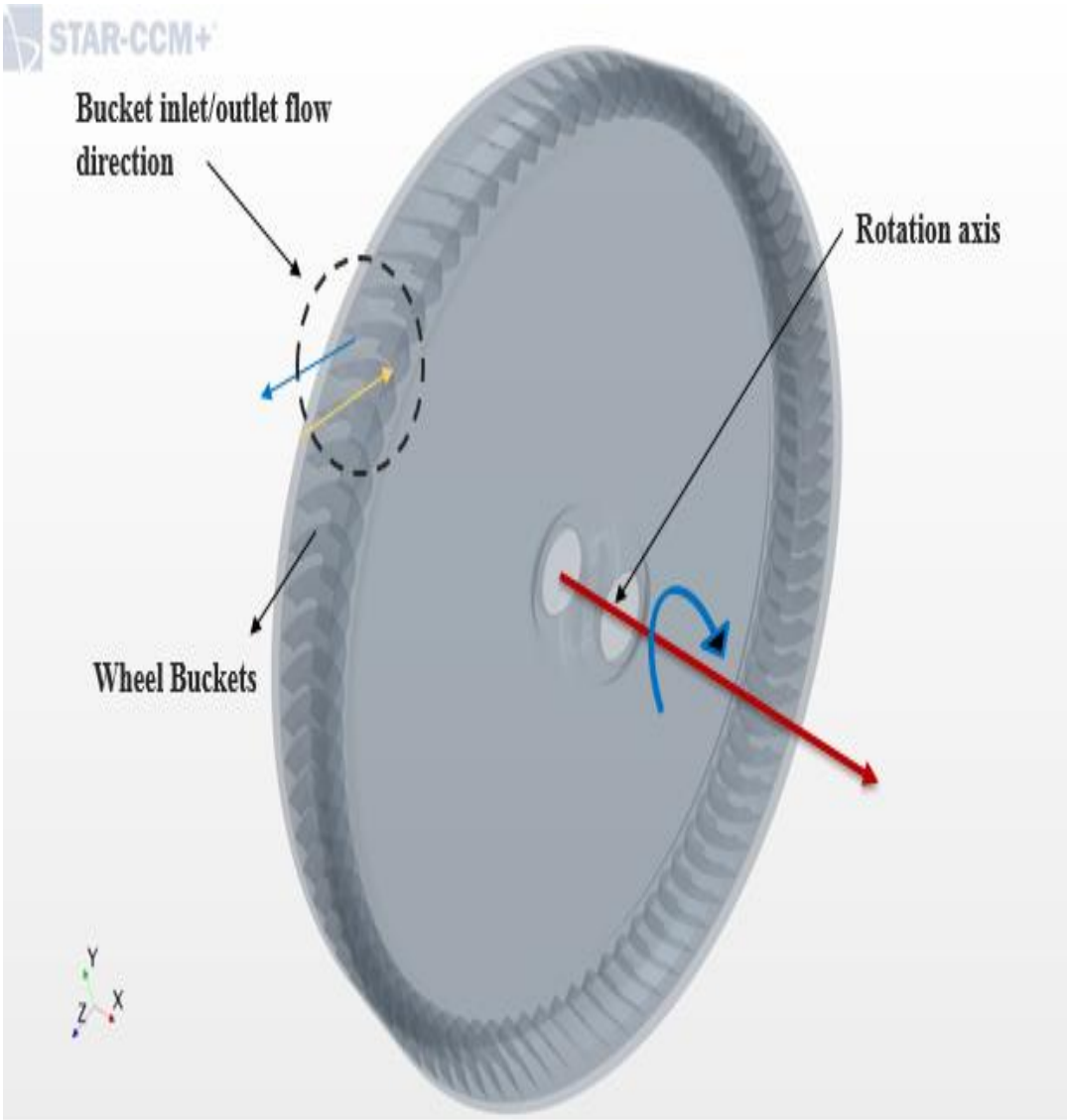

Figure 24 The RCIC turbine interior wheel CAD model along with its buckets distributed around.

Simulations are prepared to study the steam jet velocity as it flows outside the nozzle to the buckets using CFD code (STAR-CCM+). A polyhedral volume mesh is chosen for the whole geometry with a total number of cells around 12 million, which is considered a high number of cells that is computationally expensive. The turbine geometry presents a high complexity with almost 23 million interior faces.

The resulted mesh was accepted based on the mesh report that was generated using the STAR-CCM+ diagnostics window after applying wake mesh refinement with 8 optimization cycles and quality threshold of 1.0 to maximize the meshing quality. The outer body of the turbine is used as lab reference frame for the inner wheel of the turbine. This allows for applying a constant grid flux to the governing equations of fluid motion and helps getting a time-averaged steady state solution for the turbine flow involving a rotational motion of the wheel which is inherently unsteady. The rotating reference frame is created automatically for user defined rotation motion to regions to generate constant grid flux and was applied to the turbine body.

To achieve successively more accurate solutions and mesh size independency, mesh sensitivity analysis (wake refinement and mesh size) was applied into the selected mesher type (Polyhedral with a maximum skewness angle of 75 degree). The chosen parts for wake refinement were: turbine inlet, outer body, and interior wheel. Figure 25 shows the turbine interior and exterior parts meshing scalar section plane with a base mesh size of 0.001m.

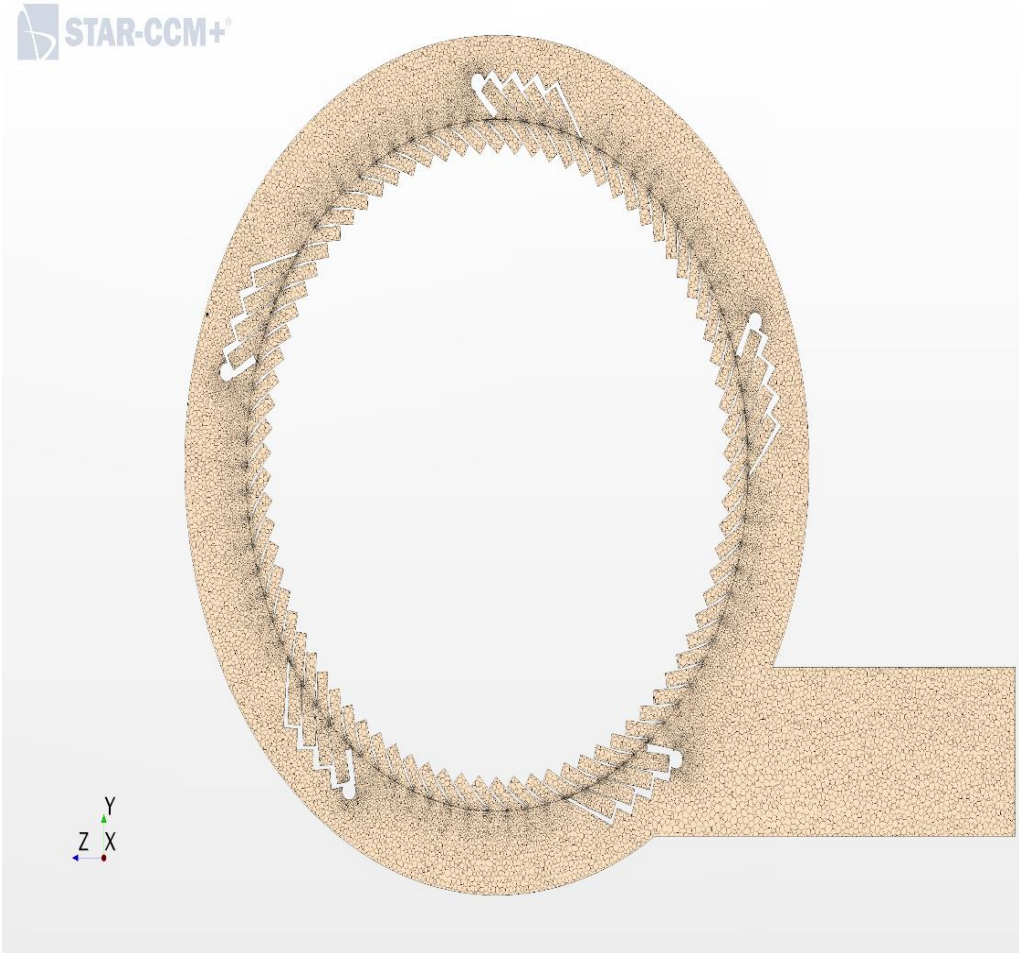

Figure 25 2D section view of the GS-1 turbine meshing.

The GS-1 CAD model is used in simulations that are prepared to measure the velocity of the steam at the buckets of the nozzle output. The jet velocity of the flow is one of the major input parameters for scaling Similarity Level estimation as will be shown in Chapter 6 of this dissertation. In the simulations the steam injected into the turbine through the five nozzles at a high pressure of a range 750 psi and higher and exiting from the outlet of the turbine at a low pressure of a range 29 psi and lower. Coupled flow is

chosen as it's effective in handling complex geometries and reasonable computational cost.

5.2.2 NHTS RCIC system ZS-1 turbine CAD model

The NHTS RCIC turbine is a ZS-1, with a rotor diameter of 0.46m installed with a one converging – diverging nozzle along with 3 reversing chambers. The nozzle throat diameter is almost 1cm. The location of the nozzle and its reversing chambers is near the bottom of the turbine wheel. In addition, the nozzle- reversing chamber inlet/outlet angle is 30^0 as measured. The maximum pressure measured on the inlet and exhaust ends is up to 75 psia, while normally exhaust pressure only reaches 15 or 16 psia. Moreover, the turbine measured testing speed ranges from 1500 to 3000 RPM. Also, the turbine exhaust line outlet is at half-elevation of the pool water (15.5 in., or 0.4 m) and the SRV discharge is at 7 in. (0.2 m) from the tank bottom.

The SNL GS-1 CAD model was modified to represent the ZS-1 turbine with the characteristics mentioned in the previous paragraph. The goal is to have a standalone ZS-1 model that is subjected for validation against the tests that were performed at the NHTS testing facility. Figure 26 shows the NHTS RCIC system turbine model that developed and used in this dissertation for scaling purposes with arrows that shows the flow direction. The ZS-1 turbine model has one nozzle at the bottom of the wheel with three reversing chambers, which match the ZS-1 turbine configuration. Figure 27 shows a transparent view of the ZS-1 turbine geometry, where the interior wheel is installed with one nozzle and three reversing chambers.

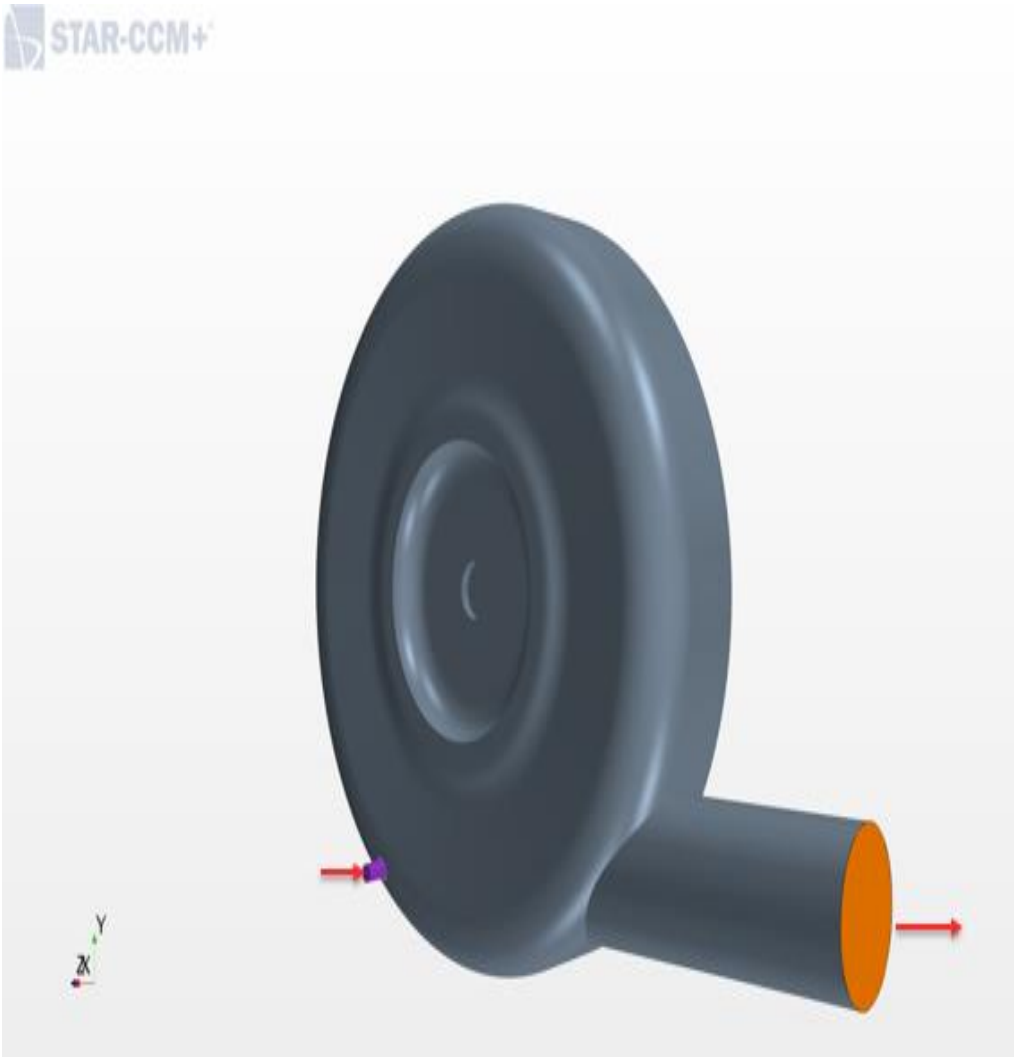

Figure 26 3D NHTS ZS-1 Turbine CAD model with one nozzle.

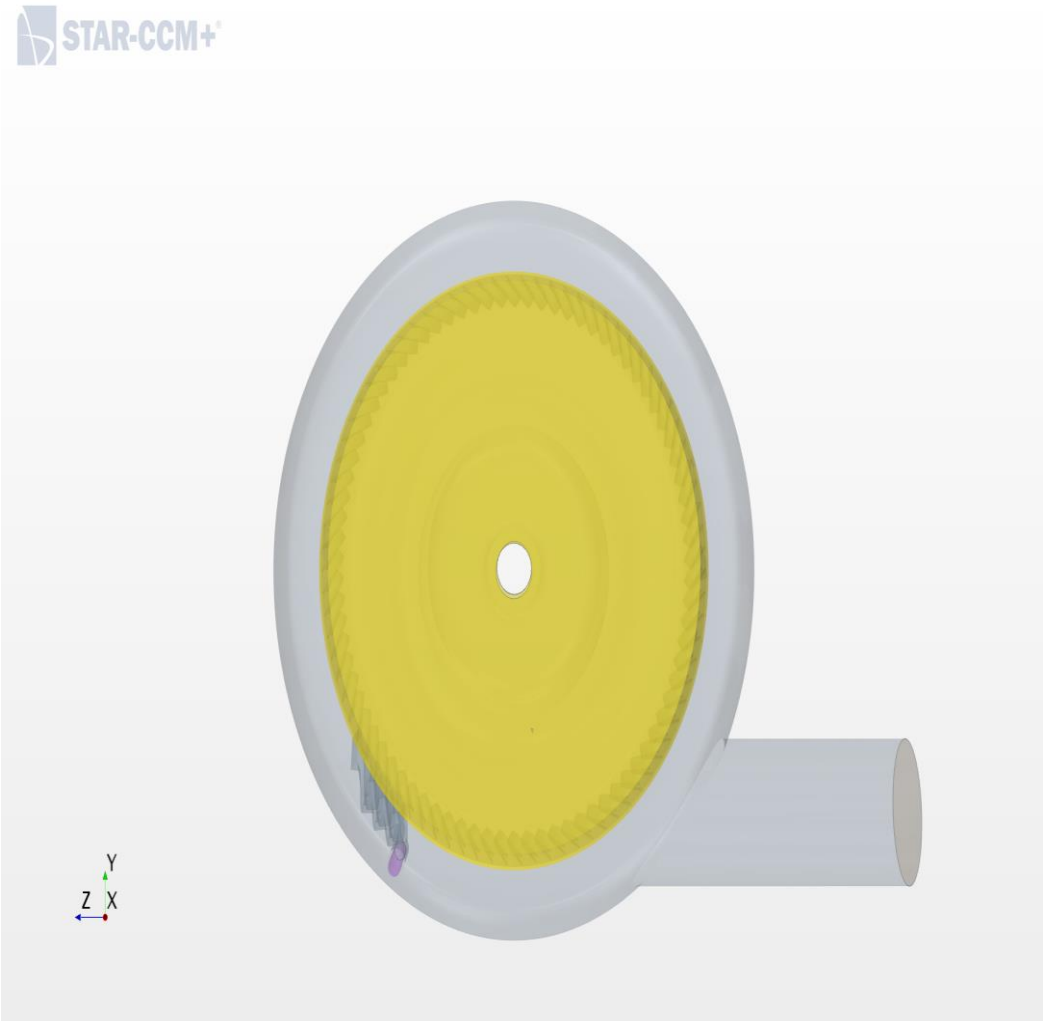

Figure 27 Transparent front view of the ZS-1 turbine CAD model with its components.

Similar to the GS-1 CAD model, simulations are prepared using the ZS-1 CAD model to measure the nozzle jet velocity hitting the buckets at NHTS RCIC system operating conditions with a polyhedral mesh. Steam injected into the turbine wheel through one inlet nozzle at a pressure of 55 psi (Operating pressure of most of the tests that is done in the NHTS facility) and exiting at a pressure of 15 psi of the turbine exit pipe. In the simulations, coupled flow is chosen similar to the full size GS-1 turbine model

simulations with a compressible flow and a turbulence density of 1%. A reference frame is selected to allow for the wheel rotation with a rotation rate relative to the outside turbine body of a 3000 rpm. Mesh sensitivity analysis was applied with wake mesh refinement, 8 optimization cycles, and 79° as the best achieved skewness angle. Also, simulations were applied with range of mesh sizes to make sure the results are accurate and independent on the mesh size as will be shown in the results chapter of this dissertation.

5.2.3 NHTS RCIC system Terry turbine nozzle CAD model

As a part of the turbine component, the nozzle represent the main path of flow toward the wheel buckets. A CAD model of the nozzle developed to help simulating the flow conditions into the turbine. The nozzle simulated individually and as a prat of the turbine to study the jet velocity of the flow. The nozzle CAD model total length is 3.8cm with throat diameter of 0.56cm. The nozzle CAD model geometry is shown in Figure 28. The left side of the figure is a bottom view of the nozzle geometry that shows the total length of the lower part including the throat structure. While, the right side of the figure represents a side view of the nozzle pipe and exist throat. Figure 29 shows a 3D representation of the nozzle CAD model with arrows that shows the fluid flow direction.

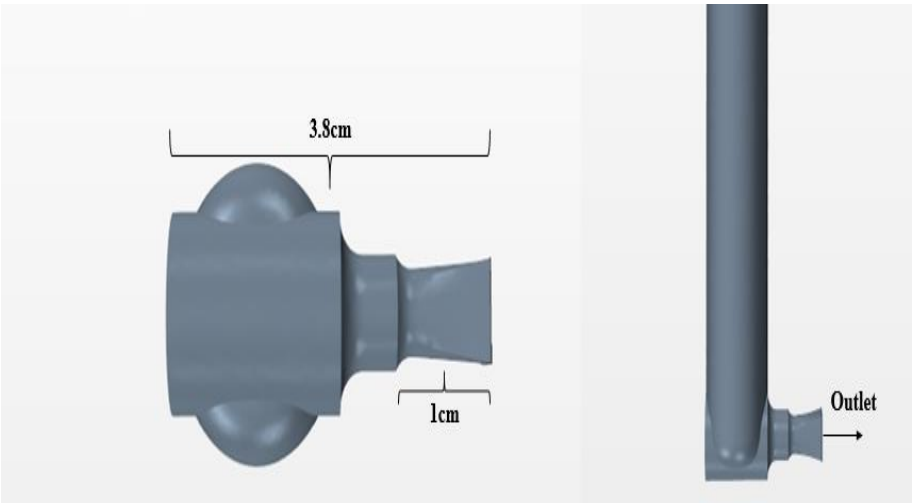

Figure 28 RCIC system turbine nozzle CAD model.

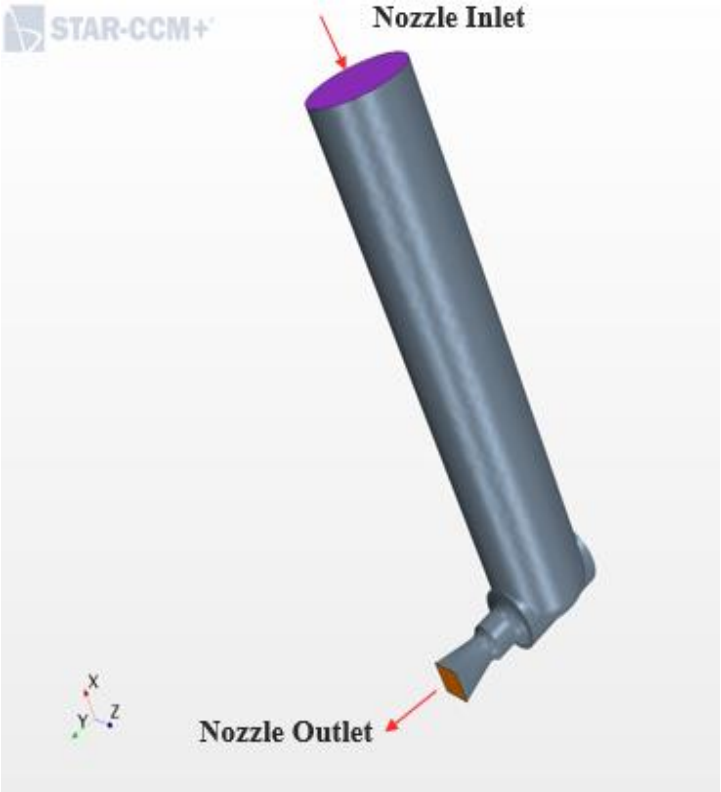

Figure 29 3D view of the turbine nozzle with arrows representing flow direction.

Simulations with conditions similar to the GS-1 Terry turbine simulation conditions were prepared and run for the individual nozzle CAD model. The nozzle geometry is chosen so that is comparable to the real one used in the NHTS RCIC system ZS-1 turbine as appears in Figure 10. The steam supersonic jet velocity at the nozzle exit depends on the inlet/exit pressure value. In this dissertation, the steam nozzle model is tested at a range of pressure values to provide analytical solution that can predict the jet velocity at if the pressure ratio (inlet/exit) is known.

5.3 New RCIC System Suppression Pool Model

Efforts has been made to study the RCIC system Suppression Pool thermal stratification and its effects on the long-term operation of the overall system. Pools have been built and tested at several operating conditions to study indicate the thermal stratification and mixing such as the POOLEX experiment (Li & Kudinov, 2009). The POOLEX facility has cylindrical stainless steel tank similar to the NHTS Suppression Tank with different dimensions and capacity. CFD code was used to simulate the experimental data including the heating rate and heat loss through the pool surface, sides, and walls. The heat flux and average temperature in the pool are of interest for scaling Similarity Level along with other parameters. This makes modeling of the Suppression Pool of interest in the future to study the long-operation post-accident scenario.

INL used STAR-CCM+ and made a geometry similar to the POOLEX and simulated the heat up experiment thermal stratification and compared the results with other code results (Zhao, Zou, & Zhang, 2012). In the simulation, the heat source were simulated uniformly distributed along the blowdown pipe. K-ε turbulence model along with implicit

unsteady state method were used. The total time required for convergence was 14000s and three time steps were used of 20s, 10s, and 5s. Figure 5 of (Zhao, Zou, & Zhang, 2012) shows the 2D mesh of the geometry, while figure 6 in the same report shows the STAR-CCM+ temperature distribution in the pool using the developed CFD simulation. In the figure, at the depth between the 0.25 m-1 m the temperature is almost constant. From such model the average temperature value in the pool depth of 0.25 m-1 m can be considered as a quasi-steady state input parameter for the scaling Similarity Level estimation.

In order to estimate the scaling Similarity Level between the NHTS Suppression Tank and any full-scale Suppression Pool, a CFD model representing the full-scale model should be developed to provide the required scaling input parameter. This model should able to be modified to represent the NHTS Tank and benchmarked with experimental testing that are conducted at the NHTS pool. However, developing a similar CFD model is beyond this dissertation objectives and is part of the future tasks that will provide more data for scaling purposes. While in this dissertation, the Suppression Pool scaling Similarity Level provides a reference model for the NHTS pool as shown in chapter 7.

6. RCIC SYSTEM SCALING SIMILARITY LEVEL DERIVATION AND ANALYSIS

Scaling Similarity Level principle includes the development of dimensionless time ratios for the Similarity Level estimation. The time ratios calculation is to quantify the degree of similarity between the scaled systems such as: the RCIC System constituents of the NHTS test facility and a prototype full-size facility system. The turbine, pump, and Suppression Pool are focused on herein because the greatest modeling challenges are with the long-term operation of these components. The Texas A&M experiments are providing data for analytical models of the turbomachinery, where the applicability of the data must be evaluated. Similarly, the test facility provided many tests data at different operating conditions related to the Suppression Pool and turbomachinery. These tests data are the basis for Similarity Level estimation as well as system models validations.

Equations related to transient/ steady processes in the RCIC System control volume processes can be used for scaling and to simplify modeling of the integral system behavior. They can also be used for optimization, in which the similarity between the model and prototype systems are improved. The equations used for scaling Similarity Level include conservation of mass, momentum, and energy, as these quantities must be conserved. Herein, for the RCIC System components (turbomachinery and pool), a formulation with a control volume that surrounds the RCIC subsystem (such as turbine wheel and buckets) is studied and the conservation equations for mass, momentum, and energy are developed. Similarly, a control volume developed for the Suppression Pool and

studied. The dimensionless time ratios resulting from scaling Similarity Level analysis is used estimate scaling Similarity Level value. This formulation is convenient because most of the related input parameters are available or could be modeled. Some of the dimensionless time ratios are not used to estimate the Similarity Level at present, because the input parameters for the related equations will be obtained as part of the future work. This approach is valid because estimation of the RCIC System component similarity can be achieved using any dimensionless time ratios of the three conserved control volume equations (mass, momentum, and energy). Control volume conservation equations and the derivation of the dimensionless time ratios for the RCIC system component are shown in details in the next subsections.

6.1 RCIC System Turbopump Governing Equations and Analysis

The control volume of the RCIC system turbopump is cylindrical in shape and includes the turbine wheel and buckets as shown in Figure 30. The RCIC System pump is connected to the RCIC System turbine by a common shaft and creates a resistance equal to the turbine acceleration. Under the assumption of an adiabatic turbine, the angular momentum for the control volume containing the turbine is described in Equation (8). The approach and the derivations of turbopump governing equations are described by (Ross , et al., 2015).

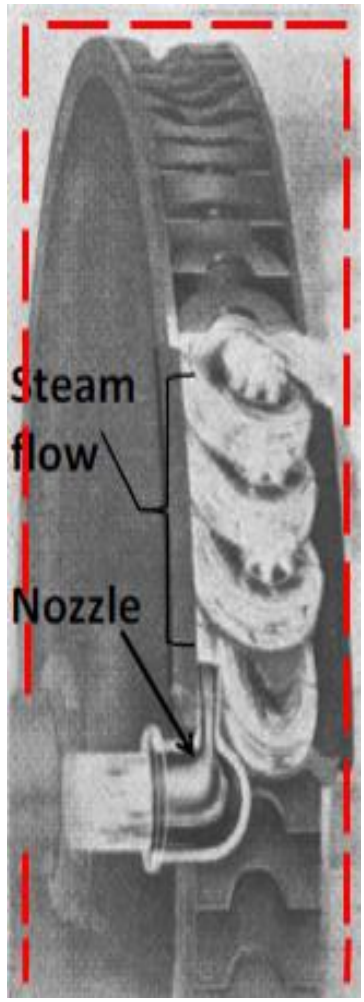

Figure 30 RCIC system turbopump control volume.

Equations (8)-(10) are used herein as the first step of the dimensionless analysis for the scaling.

$$\oiint r\,T_\theta\,dA + \iiint r\,B_\theta\,dV = \oiint r\,u_\theta\,(\rho\,\boldsymbol{u}.dA) + \frac{\partial}{\partial t}\iiint r\,u_\theta\,\rho\,dV \tag{8}$$

Where, r is the radius of the turbine wheel (m), T_θ is a force function over the surface of the control volume, B_θ is a body force, u is the velocity vector, u_θ is the tangential

component of the outlet velocity of fluid leaving the bucket, and ρ is the fluid density (kg/m^3).

Minor losses are assumed negligible (with flow loss about of 0.66 psi per 100 ft), and the shaft torque, i.e. the pump torque, is the only torque that penetrates the control volume. The pump torque is represented by the first term in Equation (8) based on Newton's third law, since the pump torque is equal and opposite to the torque developed by the turbine. The first term expressed in Equation (8) is therefore:

$$\oiint r\, T_{\theta}\, dA = -T_{shaft} = -T_{pump} \tag{9}$$

Where, T_{pump} is the pump torque that is generally a function of other variables including time. The quasi steady-state scheme is adopted under the assumption that the accident and transient scenarios for LWRs are slowly evolving with respect to time, as was the accident at Fukushima Dai-Ichi Unit 2. Under this quasi–steady state assumption, the torque equation of the pump for a single phase flow can be expressed as in Equation (10) . This equation can be extended to include the two-phase flow process.

$$T_{pump} = 2\, r\, \dot{m} V_j \cos\beta - r^2\, \dot{m}\, \omega (1 + \cos\beta) \tag{10}$$

Where, $\dot{m}$ is the mass flow rate to the turbine (kg/s), V_j is the fluid jet velocity as coming through the nozzle outlet (m/s), β is the inlet/exit angle between the fluid velocity vector and the horizontal/tangential direction of the turbine motion (rad), and ω is the turbine speed (rad/s). Equation (10) is used to produce unit-less time ratios in the normalization process for Similarity Level estimation.

Other unit-less numbers and parameters that should be conserved in the transient processes include: the Reynolds Number, Nusselt Number, and Pump Specific Speed Ns. As an example: The flow at the NHTS pump suction piping is calculated as turbulent with Reynolds number greater than 20,000, while for the Peach Bottom pump suction piping is turbulent flow with Reynolds number value of 9E+5. This is because the flow rate, flow velocity, and flow density in the NHTS pump are different than for Peach Bottom. Furthermore, the characteristic pump pipe length and flow thermal conductivity are different than the Peach Bottom pump characteristics. The non-conserved Reynolds and Nusselt numbers as pump parameters are current distortions between the two system pumps. Pump specific speed formulated as in Equation (11) (Lobanoff & Ross, 2013) is a useful parameter to evaluate the pump curve and to support the pump distortion finding and resolve it, as will be shown in the results section of this study. The pump specific speed also helps select the most economical and efficient pump operating conditions. The specific pump speed is as follows.

$$N_S = \frac{N\,Q^{0.5}}{H^{0.75}} \tag{11}$$

Where N is the pump rotational speed (rpm), Q is the volumetric flow rate (gpm) at the point of best efficiency and H is the total head in (ft.) per stage at the point of best efficiency. The pump specific speed is unit-less and in this dissertation it is considered as a characteristic time ratio ($\prod_{Ns}$) because it will be used later to estimate the pump Similarity Level. The centrifugal pump head is related to the fluid pressure at the inlet and

outlet of the pump and outlet velocity using Bernoulli's principle as shown in Equation (12).

$$H = \frac{(P_2 - P_1)}{\rho g} + \frac{V_2^2}{2g} \tag{12}$$

Where P is the pressure at the inlet/outlet (N/m^2), V_2 is the outlet fluid velocity (m/s), and g is the gravity acceleration (9.8 m/s^2). The resultant H in (m), is then converted to (ft.).

6.1.1 RCIC system turbine momentum characteristic time ratios derivation

For the quasi- steady state operation case of the turbopump, the derived unit-less numbers $\prod$ can be still called characteristic time ratios. This because the individual parameters of the $\prod$ can be solved to estimate the scaling reference time of the system control volume by solving for the full similarity condition ($\prod$ =1). The main goal is to produce unit-less time ratios to be used in estimating the scaling Similarity Level values for the RCIC turbine. In this section, the torque from the angular momentum equation of the RCIC System turbine in Equation (10) is reformulated by applying direct scaling similarity analysis normalization principle. Applying the first step of dimensional analysis is to normalize terms in the equations. Equations (13) through (18) represent normalization of Equation (10) parameters.

$$T_{pump}^{+} = \frac{T_{pump}}{T_{pump}^{o}} \tag{13}$$

$$r^{+} = \frac{r}{r^{O}} \tag{14}$$

$$\dot{m}^{+} = \frac{\dot{m}}{\dot{m}^{o}} \tag{15}$$

$$(\cos\beta)^{+} = \frac{\cos\beta}{(\cos\beta)} \tag{16}$$

$$V_j^{+} = \frac{V_j}{V_j^{o}} \tag{17}$$

$$\omega^{+} = \frac{\omega}{\omega^{o}} \tag{18}$$

Substituting Equations (13) through (18) into Equation (10) yields Equation (19) as follows.

$$\begin{aligned} T_{pump}^{+}\, T_{pump}^{o} &= 2\, r^{+}\, r^{o}\, \dot{m}^{+} \dot{m}^{o}\, V_j^{+}\, V_j^{o}\, (\cos\beta)^{+}\, (\cos\beta)^{o} - \\ & r^{+2}\, r^{o2}\, \dot{m}^{+} \dot{m}^{o}\, \omega^{+}\ \omega^{o}\, (1+\cos\beta)^{+}\, (1+\cos\beta)^{o} \end{aligned} \tag{19}$$

Dividing both sides of Equation (19) by ($r^{o}\, \dot{m}^{o}\, V_j^{o}\, (\cos\beta)^{o}$) yields Equation (20)

$$\begin{aligned} \frac{T_{pump}^{+}\ T_{pump}^{o}}{r^{o}\, \dot{m}^{o}\, V_j^{o}\, (\cos\beta)^{o}} &= 2\, r^{+}\, \dot{m}^{+}\, V_j^{+}\, (\cos\beta)^{+} - \\ & \frac{r^{+2}\, r^{o}\, \dot{m}^{+}\, \omega^{+}\ \omega^{o} (1+\cos\beta)^{+}\, (1+\cos\beta)^{o}}{V_j^{o}\, (\cos\beta)^{o}} \end{aligned} \tag{20}$$

Two unit-less time ratios ($\prod$) yielded from Equation (20) are shown in Equations (21) and (22). The unique derived unit-less characteristic time ratios contain the parameters that govern the RCIC turbine flow properties, which qualifies them to be tested and used for Similarity Level estimation. The time ratios are given subscripts (I & II) for easier identification.

$$\prod_{I} = \frac{T_{pump}^{o}}{r^{o}\, \dot{m}^{o}\, V_j^{o}\, (\cos\beta)^{o}} \tag{21}$$

$$\prod_{II} = \frac{r^{o}\, \omega^{o}\ (1+\cos\beta)^{o}}{V_j^{o}\, (\cos\beta)^{o}} \tag{22}$$

Substituting Equations (21) and (22) into Equation (20) yields Equation (23).

$$T^{+}_{pump} \prod_{I} = 2 r^{+} \dot{m}^{+} V^{+}_{j} (\cos\beta)^{+} - \prod_{II} r^{+2} \dot{m}^{+} \omega^{+} (1+\cos\beta)^{+} \tag{23}$$

Based on the characteristic time ratios ($\prod$) analysis, the scaling Similarity Level between the model and prototype turbine systems can be demonstrated by collecting and inserting the numerical values of the parameters of Equations (21) and (22) as well as other derived characteristic time ratios (if any) for the model and prototype systems. Then, computing the Similarity Level value using Equation (3) .

6.1.2 RCIC system turbine mass and energy characteristic time ratios derivation

Mass and energy equations are used to complete the RCIC turbine scaling Similarity Level analysis as a part of the governing equations of the systems. Actually, the mass and energy equations are used to estimate the integral similarity of the thermodynamic state for each component of the RCIC System. The mass and energy equations for the turbine system can be applied for steady state /transient cases to represent the long term operation phenomena.

The resulting dimensionless mass equation under the steady state condition, assuming the pump inlet and outlet mass flow rates are equal, and is shown in Equation (24) in the normalized format. While, the unsteady state mass conservation equation is expressed at Equation (25). Normalizing Equation (25) and substitute to Equation (24) yields one unit-less time ratio as expressed in Equation (26)

$$\sum \dot{m}^{+}_{in} = \sum \dot{m}^{+}_{out} \tag{24}$$

$$\frac{dM}{dt} + \sum \dot{m}_{in} = \sum \dot{m}_{out} \tag{25}$$

$$\prod_{III} = \frac{\rho^o \, \mathrm{V}}{\dot{m}^o \, t^o} \tag{26}$$

Where, V is the volume of the system control volume, and the (t^o) is time reference, which can be called the scaling reference time for the scaled system (τ). As an example, for a full similarity condition, the $\prod$ = 1, solving for the scaling reference time under this condition for Equation (26) yields Equation (27). Where τ_{III} is the reference time scale based on the fifth derived characteristic time ratio.

$$\tau_{III} = \frac{\rho^o \, \mathrm{V}}{\dot{m}^o} \tag{27}$$

The total energy inside the control volume of the RCIC System turbine (see Figure 30) component can be expressed by Equation (28) under the steady state condition (neglecting the change in potential energy).

$$q - w + \sum \dot{m}_{in} \, i_{in} - \sum \dot{m}_{out} \, i_{out} = 0 \tag{28}$$

Where, q is the heat rate (J/s) added to the system, w is the work rate (J/s) done by the system, $\dot{m}$ is the mass flow rate into or out of the control volume (kg/s), and i is the specific enthalpy at the inlet or outlet of the control volume (J/kg). Normalizing each term of Equation (28) yield Equations (29) through (32).

$$q^+ = \frac{q}{q^o} \tag{29}$$

$$w^+ = \frac{w}{w^o} \tag{30}$$

$$i_{in}{}^+ = \frac{i_{in}}{i_{in}{}^o} \tag{31}$$

$$i_{out}{}^{+} = \frac{i_{out}}{i_{out}{}^{o}} \tag{32}$$

Substituting Equations (29) through (32) into Equation (28) yields Equation (33).

$$q^{+}\, q^{o} - w^{+}\, w^{o} + \sum \dot{m}_{in}^{+}\, \dot{m}_{in}^{o}\, i_{in}^{+}\, i_{in}^{o} - \sum \dot{m}_{out}^{+}\, \dot{m}_{out}^{o}\, i_{out}^{+}\, i_{out}^{o} = 0 \tag{33}$$

Dividing Equation (33) by q^{o} yields Equation (60).

$$q^{+} - w^{+}\left(\frac{w^{o}}{q^{o}}\right) + \frac{\sum \dot{m}_{in}^{+}\, \dot{m}_{in}^{o}\, i_{in}^{+}\, i_{in}^{o}}{q^{o}} - \frac{\sum \dot{m}_{out}^{+}\, \dot{m}_{out}^{o}\, i_{out}^{+}\, i_{out}^{o}}{q^{o}} = 0 \tag{34}$$

From Equation (34) two additional unit-less characteristic time ratios ($\prod_{IV}$ & $\prod_{V}$) were derived. Those are a potential time ratios that would be used to estimate the scaling Similarity Level values for the turbine control volume as shown in Equations (35) and (36)

$$\prod_{IV} = \frac{w^{o}}{q^{o}} \tag{35}$$

$$\prod_{V} = \frac{\dot{m}^{o}\, i^{o}}{q^{o}} \tag{36}$$

The unsteady state (transient) energy conservation equation is shown in Equation (37) considering the time dependent flow volume, where mass and energy flow can change. Normalizing process yields an additional unit-less time ratio to the ones at Equations (35) and (36) as can be seen at Equation (38). The mass of the system volume has internal energy (E) at a pressure *P* and temperature T.

$$\frac{dE}{dt} + p\frac{\mathrm{dV}}{\mathrm{dt}} = q - w + \sum \dot{m}_{in}\, i_{in} - \sum \dot{m}_{out}\, i_{out} \tag{37}$$

$$\prod_{VI} = \frac{E^o}{q^o\, t^o} \tag{38}$$

Solving for the system internal energy reference scaling time (τ_{VI}) under the unsteady state condition for a full similarity condition ($\prod_{VI} = 1$) yields Equation (39).

$$\tau_{VI} = \frac{E^o}{q^o} \tag{39}$$

6.2 RCIC System Suppression Pool Governing Equations and Analysis

6.2.1 RCIC system pool thermal stratification governing equations

Thermal stratification in the Suppression Pool increases the water surface temperature which in turn affects the containment pressure. Also, increasing the suction point temperature could cause cavitation in the pump due to a decreased Net Positive Suction Head available (NPSHa) to the RCIC pump, and this threatens the availability of the RCIC system. The pump is located at an elevation lower than both suction sources to ensure that sufficient NPSH is available. Existence of NPSH allows the pump to operate without cavitation. If the pressure at the pump inlet drops below the local saturation pressure, cavitation could occur at the pump inlet, creating bubbles that can collapse inside the pump and lead to eventual destruction to the pump. Pump failure would terminate RCIC system operation. The NPSHa to the RCIC pump is represented by Equation (40) (Zhao, Zou, & Zhang, 2012).

$$NSPHa = \frac{P_{nc} + P_v\left(T_{surface}\right) - P_v\left(T_{suction}\right)}{\rho g} + \Delta H - H_{loss} \tag{40}$$

Where P_{nc} is the non-condensable gas pressure, P_v ($T_{surface}$) is the vapor pressure by the surface temperature, P_v ($T_{suction}$) is the vapor pressure by the suction point temperature, ΔH is the distance between the suction point and surface point, and H_{loss} *is* the pressure loss on the suction side.

To have some insight investigations about the thermal stratification and the pool long-term operation as a part of the RCIC system, tests were conducted at the NHTS facility tank with varied parameters such as the steam flow rate, the steam quality, and the pressure conditions. It was found that the tank with dependency on the testing conditions, can experience thermal stratification after the operation of the RCIC system. This would accelerate the rate of containment pressurization (Solom, 2016).

Stratification in large complex enclosures can be modeled using 1-D differential equations, since (Peterson, 1994) has shown that the fluid between the control volume boundary and the jet flows organizes into homogeneously mixed conditions or vertically stratified conditions. This finding is adopted in the scaling model development for the NHTS Suppression Pool, where the analysis considers 1-D governing equations in the Z-direction. For a macroscopic size geometry, the details of the shape become unimportant once applying the 1-D assumption. So, the small distortion in shape can be neglected between the two Suppression chambers for control volume scaling Similarity Level purposes.

In addition, experimental results of thermal stratification for BWR Suppression Pool can be estimated using numerical solutions of equations that describes the vertical temperature distribution of buoyant jets. Efforts were made to study the transport of flow

by free jets and plumes and it was found that strong stratification is common in ecological systems (Peterson, 1994). Peterson (Peterson, 1994) derived the governing equations for stratified fluids in large enclosures and used the Hierarchal Two-tiered Scaling analysis (HTTS) (Zuber , 1991) method for scaling. In this dissertation, the control volume for scaling Similarity Level analysis has been chosen as a hypothetical cube for the two scaled systems. Moreover, the mass, energy, and momentum transport equations have been used as the basics for scaling analysis to estimate the Similarity Level between the scaled systems.

In stratified mixing volumes, the heat source causes the rise of a thermal plume up to the top of the enclosure. The stratification driving forces could be: the heat source, wall jet, and ambient fluid motion. In large volumes, buoyant jets are expected to be turbulent (Peterson, 1994). The equations covered the motion of the flow under stratified condition can be useful to estimate some input parameters for scaling. For buoyant plumes, mainly it caused by injection of buoyant fluid into lighter or heavier fluid. In addition to that, momentum jets, steam jets, and natural convection flows are considered mixing forces that cause stratification. The buoyancy flux B (m^4/s^3), which is related to fluid density and a flow rate is given by Equation (41) (Peterson, 1994).

$$\mathrm{B} = g\,\frac{\rho_a - \rho_o}{\rho_a}\;\mathrm{Q}_o \tag{41}$$

Where g is the gravitational acceleration (m/s^2), ρ_a is the density of the ambient fluid (kg/m^3), ρ_o is the injected fluid density (kg/m^3), and Q_o is the jet volume flow rate (m^3/s).

While for a plume generated by a heat source, the buoyancy flux is given by Equation (42) (Peterson, 1994).

$$\mathrm{B} = \frac{g\,\beta\,q}{\rho_a\,C_P} \tag{42}$$

Where q is the heat rate (W), β is the constant of thermal expansion (k^{-1}) and C_P is specific heat at constant pressure (J/kg-k). These equations control the fluid motion in the 1-D flow path inside a specific control volume. For this study and to serve scaling analysis, the control volume that governs the Suppression Chambers in both NHTS facility and any full-size facility such as Monticello facility is a cubic control volume almost half filled with water as shown in Figure 31 and represent the development of stratified environment showing the motion direction in the plume. The 1-D differential equations analysis is applied on the Z-direction starting from steam (flow) injection from a Sparger submerged in the pool toward the pool bottom. H^o in the figure represents the distance between the Sparger exit and the pool bottom, which can be measured for any pool design.

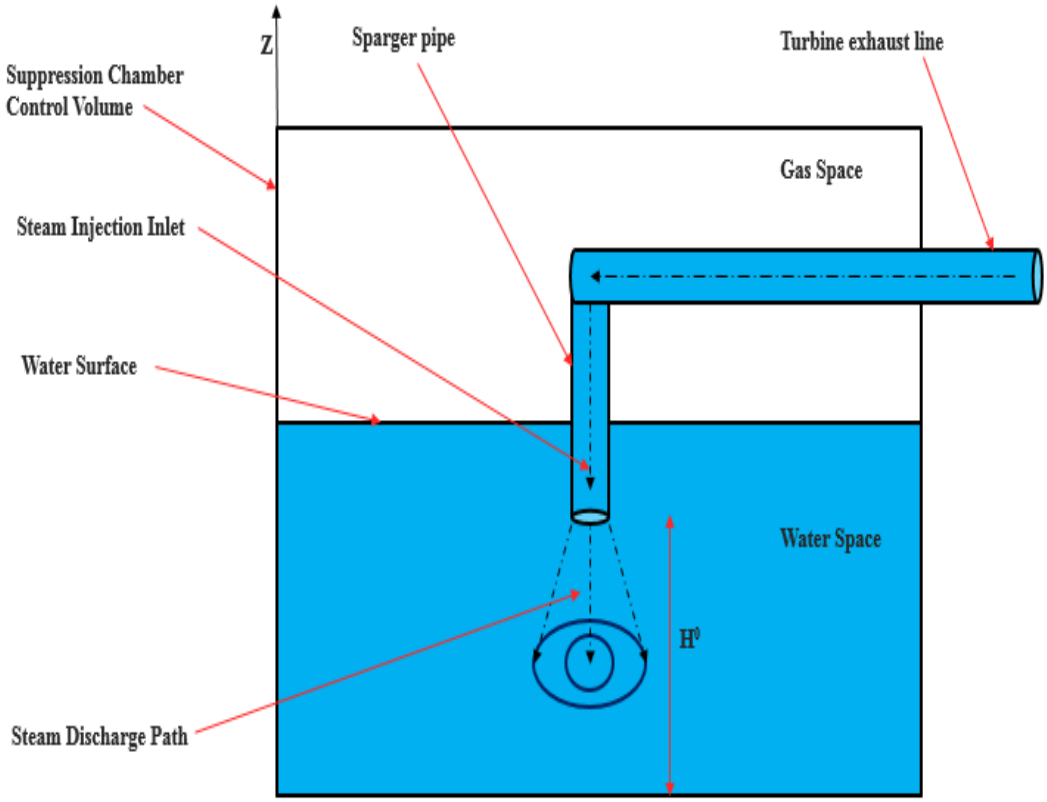

Figure 31 RCIC system suppression chamber control volume

6.2.2 RCIC system pool conservation equations and dimensionless analysis

The conservation equations to perform scaling Similarity Level for a large volume enclosure such as the Suppression Pool are the equations of mass, momentum, and energy. Those equations are used as the basic equations for non-dimensionalization. However, not all of the equations produce unit-less time ratios. When one or more of the conservation equation results in a unit-less time ratios, certain control volume properties can be considered for scaling Similarity Level estimation with an associated value between the scaled model and the prototype. The unit-less time ratios can also be used for system design optimization. For example: if the resulted Similarity Level value is too low or too

high, the system can be solved for full Similarity Level condition (unity) and estimates the system design or characteristic parameters that satisfy it.

The pre-described Suppression Chamber control volume is used with the 1-D differential equation application assumption to apply scaling for Similarity Level value estimation in the pool volume. The governing equations are applied to describe the control volume transient process under operation. For a cubic large enclosure control volume with the vertical flow in 1-D (z-direction), the conservation of mass is defined as:

$$\frac{\partial \rho}{\partial t} = -\nabla \left(\rho \, V_z \right) \tag{43}$$

Where, V_z is the injected flow velocity on the z-direction, the left term of the equation represents the time rate of system mass per unit volume, and the right term represents the net rate that mass enters through the control volume surfaces per unit volume. Normalizing Equation (43) parameters as a direct step of the scaling Similarity Level process result in reformulating the equation itself. Normalization can be done by dividing each term by its nominal quasi-steady value, denoted by the superscript "o". This is shown in the normalized parameters in Equations (44)-(47).

$$\rho^{+} = \frac{\rho}{\rho_a} \tag{44}$$

$$t^{+} = \frac{t \, V_z^o}{H^o} \tag{45}$$

$$\nabla^{+} = H^o \, \nabla \tag{46}$$

$$V_Z^{+} = \frac{V_Z}{V_Z^o} \tag{47}$$

Substituting Equations (44) through (47) into Equation (43) yields Equation (48) as follows.

$$\frac{\partial \rho^{+} \rho_{a}}{\partial (\frac{\mathrm{H}^{o}\, \mathrm{t}^{+}}{\mathrm{V}_{z}^{o}})} + \frac{\nabla^{+}}{H^{o}} \quad (\rho^{+} \rho_{a} \mathrm{V}_{Z}^{+} \mathrm{V}_{z}^{o}) = 0 \tag{48}$$

Equation (48) after simplification and terms rearranging yields Equation (49).

$$\frac{\partial}{\partial \mathrm{t}^{+}} \rho^{+} + \nabla^{+} (\rho^{+} \mathrm{V}_{Z}^{+}) = 0 \tag{49}$$

From Equation (49), there are no quasi-steady state parameters left to form a unit-less time ratios. This makes the mass equation inapplicable for unit-less time ratios. Next, the momentum equation is considered for the Suppression Pool control volume. Important unit-less time ratios can be derived from the momentum equation and used for scaling Similarity Level estimation. The momentum equation of the flow particles in the Z-direction is expressed by Equation (50).

$$\frac{\partial}{\partial \mathrm{t}} \rho \mathrm{V}_{\mathrm{Z}} = -(\frac{\partial}{\partial x} \phi_{xz} + \frac{\partial}{\partial y} \phi_{yz} + \frac{\partial}{\partial \mathrm{z}} \phi_{zz}) + \rho\, \mathrm{g}_{\mathrm{Z}} \tag{50}$$

Where the ϕ_{ij} is the total momentum flux inside the control volume in the j-direction passing through the surface perpendicular to i-direction. The left term of Equation (50) represents the net rate of increase of the momentum per unit volume (N/m^3). The first term of the right side is the net rate of total momentum entering through control volume boundaries per unit volume, and the last term is representing the external body force per unit volume. Substituting the flux convection and diffusive terms for Newtonian fluids in

the Z-direction and assuming a constant ambient density, Equation (50) reduces to Equation (51).

$$\rho_a \left(\frac{\partial}{\partial t} V_Z + \nabla V_Z^2\right) = -\nabla P + \mu \nabla^2 V_Z + \rho\, g_Z \tag{51}$$

Where P is the pressure (Pa), μ is the fluid viscosity (Pa. s). For direct normalizing of Equation (51) terms, two more normalized values yielded and shown in Equations (52) and (53) for the pressure and viscosity respectively.

$$P^+ = \frac{P}{P^o} \tag{52}$$

$$\mu^+ = \frac{\mu}{\mu^o} \tag{53}$$

Substituting Equations (44) through (47) and Equations (52) and (53) into Equation (51) and rearranging yields Equation (54).

$$\begin{aligned}&\left(\rho_a \frac{V_Z^{o2}}{H^o}\right)\left(\frac{\partial}{\partial t^+} V_z^+ + \nabla^+ V_z^{+2}\right) = -\left(\frac{P^o}{H^o}\right)\nabla^+ P^+ + \\ &\left(\frac{\mu^o V_Z^o}{H^{o2}}\right)\mu^+ V_z^+ \nabla^{+2} + \rho_a\, \rho^+ g^o g^+\end{aligned} \tag{54}$$

Dividing both sides of Equation (54) by $\left(\rho_a \frac{V_Z^{o2}}{H^o}\right)$ yields Equation (55).

$$\begin{aligned}&\left(\frac{\partial}{\partial t^+} V_z^+ + \nabla^+ V_z^{+2}\right) = -\left(\frac{P^o}{\rho_a V_Z^{o2}}\right)\nabla^+ P^+ \\ &+\left(\frac{\mu^o}{\rho_a V_Z^o H^o}\right)\mu^+ V_z^+ \nabla^{+2} + \left(\frac{g^o H^o}{V_Z^{o2}}\right)\rho^+ g^+\end{aligned} \tag{55}$$

Equation (55) yields two unit-less time ratios which are the inverse of the Richardson and Reynold numbers as appear in Equations (56) and (57) respectively. For simplicity, the author called the two time ratios as the Richardson and Reynolds time ratios ($\prod_{Ri} \& \prod_{\mathrm{Re}}$) since they have similar parameters. These yielded unit-less time ratios in conjunction with other derived time ratios are tested (as shown in the results section) to estimate the scaling Similarity Level value between the NHTS facility Suppression Pool and any other facility Suppression Pool such as the Monticello reactor Suppression Pool. The scaling Similarity Level value can be found by dividing the unit-less time ratios of the (*M*) over the prototype (*P*) one, as shown in Equation (3).

$$\prod_{Ri} = \frac{\mathrm{P}^{o}}{\rho_a \ \mathrm{V}_z^{o2}} \tag{56}$$

$$\prod_{\mathrm{Re}} = \frac{\mu^{o}}{\rho_a \ \mathrm{V}_z^{o} \ \mathrm{H}^{o}} \tag{57}$$

Finally, energy conservation is considered by considering the forces in the z-direction for the Suppression Pool with a Sparger exist - pool bottom distance (H). Also, applying the 1-D principle over the fluid velocity to just consider the z-direction. The equation's variables are on the macro scale level to estimate the parameters that conserve the transient properties properly. In addition, neglecting the external and body forces on infinitesimal flow particles in the control volume is shown in Equation (22).

$$\frac{\partial}{\partial \mathrm{t}}(\rho(\mathrm{h}+\frac{\mathrm{V}_z^2}{2})) + \nabla(\rho(\mathrm{h}+\frac{\mathrm{V}_z^2}{2})\mathrm{V}_z) = \rho q^{\cdot} + \frac{\partial}{\partial z}(\mathrm{k}\frac{\partial \mathrm{T}}{\partial z}) - \frac{\partial}{\partial z}(\mathrm{V}_z \mathrm{P}) + \frac{\partial}{\partial z}(\mathrm{V}_z \tau_{zz}) \tag{58}$$

Where, $q^{\cdot}$ is the heat rate per unit mass (W/kg) added to the system, $(h+\frac{V_z^2}{2})$ is the total energy of the fluid E_T with *h* as the enthalpy per unit mass representing the fluid internal energy (J/kg), T is the fluid temperature (K), and the τ_{zz} is the shear stress on the z-direction through a surface perpendicular to the z-direction (N/m^2). Expressing Equation (58) in terms of the total energy E_T yields Equation (59).

$$\frac{\partial}{\partial t}(\rho\, E_T)+\nabla(\rho\, E_T\, V_z)=\rho\, q^{\cdot}+ \\ \frac{\partial}{\partial z}(k\frac{\partial T}{\partial z})-\frac{\partial}{\partial z}(V_z\, P)+\frac{\partial}{\partial z}(V_z\, \tau_{zz}) \tag{59}$$

Normalizing each term of Equation (59) yields the Equations (60) through (65)in addition to the previous normalized terms.

$$q^{\cdot +}=\frac{q^{\cdot}}{q^{\cdot o}} \tag{60}$$

$$E_T^{\ +}=\frac{E_T}{E_T^{\ o}} \tag{61}$$

$$\tau^{+}=\frac{\tau}{\tau^{o}} \tag{62}$$

$$T^{+}=\frac{T}{T^{o}} \tag{63}$$

$$Z^{+}=\frac{Z}{H^{o}} \tag{64}$$

$$K^{+}=\frac{K}{K^{o}} \tag{65}$$

Substituting the Equations (60) through (65)in addition to previous defined normalized values into Equation (59) yields Equation (66).

$$
\begin{aligned}
&(\frac{\rho_a V_z^o E_T^o}{H^o})\frac{\partial}{\partial t^+}(\rho^+ E_T^+)+(\frac{\rho_a V_z^o E_T^o}{H^o})(\rho^+ E_T^+ \nabla^+ V_z^+)=(\rho_a \dot{q}^o)(\dot{q}^+ \rho^+) \\
&+(\frac{T^o K^o}{H^{o2}})\frac{\partial}{\partial t^+}(K^+ \frac{\partial T^+}{\partial z^+})-(\frac{V_z^o P^o}{H^o})\frac{\partial}{\partial z^+}(V_z^+ P^+)+(\frac{V_z^o \tau_{zz}^o}{H^o})\frac{\partial}{\partial z^+}(V_z^+ \tau_{zz}^+)
\end{aligned}
\tag{66}
$$

Dividing both sides of Equation (66) by $(\rho_a \dot{q}^o)$ yields Equation (67).

$$
\begin{aligned}
&(\frac{V_z^o E_T^o}{\dot{q}^o H^o})\frac{\partial}{\partial t^+}(\rho^+ E_T^+)+(\frac{V_z^o E_T^o}{\dot{q}^o H^o})(\rho^+ E_T^+ \nabla^+ V_z^+)=(\dot{q}^+ \rho^+) \\
&+(\frac{T^o K^o}{H^{o2}\rho_a \dot{q}^o})\frac{\partial}{\partial t^+}(K^+ \frac{\partial T^+}{\partial z^+})-(\frac{V_z^o P^o}{\rho_a \dot{q}^o H^o})\frac{\partial}{\partial z^+}(V_z^+ P^+) \\
&+(\frac{V_z^o \tau_{zz}^o}{\rho_a \dot{q}^o H^o})\frac{\partial}{\partial z^+}(V_z^+ \tau_{zz}^+)
\end{aligned}
\tag{67}
$$

From Equation (67), two unit-less time ratios can be extracted and used to test for estimating the scaling Similarity Level value between the NHTS facility Suppression Pool and a full-scale Pool such as the Monticello reactor Suppression Pool. These unit-less time ratios are represented by Equations ((68) and (69)) and are given numbers VII and VIII to easy identify them.

$$\Pi_{VII} = \frac{V_z^o E_T^o}{H^o \dot{q}^o} \tag{68}$$

$$\Pi_{VIII} = \frac{T^o K^o}{H^{o2}\rho_a \dot{q}^o} \tag{69}$$

7. RESULTS AND DISCUSSION

7.1 RCIC Turbomachinery Scaling Results and Discussion

7.1.1 RCIC system pump scaling similarity level estimation

Input parameters are applied to the unit-less characteristic time ratios to estimate the expected low Similarity Level value between the prototype and test facility RCIC pumps based on Equation (3) to support the distortion finding based on Reynolds number. Since the input parameters for Equation (11) are available or capable of being estimated, the pump specific speed can be calculated for both the Peach Bottom RCIC System pump and the NHTS RCIC System pump.

As in (Ross , et al., 2015), the RCIC System pump specific speed input parameters can be considered the same as the standard RCIC System pump parameters. Accordingly, the Peach Bottom RCIC System pump rotational speed, *N*, is 4500 rpm, *Q* is 425 gpm (96.5 m^3/h), and H is 508 ft. (155 m). Applying these parameters to Equation (11) yields a RCIC System specific pump speed number of 867.

The NHTS RCIC System pump rotational speed, *N*, is 3450 rpm, and at the pump design conditions, the volumetric flow rate is estimated at 12 gpm (the highest pump efficiency) with a pressure of 6.0 atm (88 psig) (see Figure 11), and H of 203 ft. (6193 m). Then, the specific pump speed number for NHTS pump is 222 using Equation (11).

Applying the specific pump speed numbers (222 and 867) in Equation (3) yields a Similarity Level of 0.25 between the NHTS and Peach Bottom RCIC pumps based on the pumps specific speed number. The Similarity Level value is much less than 1.0, which

indicates that the transported momentum and energy are not conserved to a large extent between the pumps based on pump specific speed. The pumps specific speed input parameters and calculation are summarized in Table 1, where the $(SL)_{Ns}$ is the Similarity Level value based on the pumps specific speed calculation.

Table 1 NHTS and full scale system pumps specific speed number input parameters.

Parameter	**NHTS RCIC Pump**	**Peach Bottom Pump**
Rotational speed (RPM)	3450	4500
H (ft.)	203	508
Q (gpm)	12	425
Ns	222	867
$(SL)_{Ns}$	0.25	

The low level of Similarity Level between the prototype and model pumps is an important finding of this scaling Similarity Level analysis. Complete Similarity Level can be achieved by matching the unit-less numbers such as Reynolds, Nusselt, and pump specific speed between the prototype and model pumps to produce a Similarity Level of 1.0 using Equation (3). Solving for Similarity Level value of 1.0 may produce changes to the model pump design characteristics. Adjustments can be accomplished such as: reduce the Q value (removal of one of the pump stages may achieve this reduction in Q) for the NHTS facility; to adjust the H value; or, to have the pump run at a different rotational speed than the turbine. Mechanically linking the pump to the turbine with gears in order for the pump speed to be modified without changing the turbine speed is another possible

equipment modification. These changes would work in the direction of increasing the resulting Similarity Level.

7.1.2 RCIC system turbine similarity level estimation

In order to calculate the torque for the turbopump, the input parameters of Equation (10) need to be determined. The RCIC turbine wheel diameter is 0.61m, which determines *r* for Equation (10). The mass flow rate into the pump is 26.8 kg/s (425 gpm), where the turbine flow rate at actual operating conditions is almost 1/10 of the pump flow (2.68 kg/s is assumed). For the Peach Bottom RCIC System pump, the input parameters of the CAD model (Ross , et al., 2015) are used. The correlation in Equation (70) calculates the average velocity of the outlet nozzle at the bucket inlet area as a function of the nozzle pressure ratio that was derived based on FLUENT CFD calculations (Ross , et al., 2015). In this dissertation, the average velocity of the nozzle outlet in the bucket inlet area is considered as the jet velocity of the nozzle (V_j). The jet velocity is calculated to be 758 m/s (2758 ft/s) using Equation (70) for an operation nozzle pressure ratio (750/43.5) for the full scale RCIC system turbine nozzle (Ross , et al., 2015).

$$V_j = 244.08\, ln(\frac{P_{in}}{P_{out}}) + 54.98 \tag{70}$$

The turbine speed, ω, is 471.24 rad/s and β is 0.79 rad (45^0 degree). Applying these input parameters into Equation (10) yields the Peach Bottom pump torque (T_{pump}) of 614 N.m (569.4 lb.ft).

The input parameters were collected for the NHTS RCIC turbopump torque calculation. The turbine wheel diameter is 0.4572 m (1.5 ft.) and the steam inlet mass flow

rate for one of the NHTS tests was 0.03 kg/s (0.48 gpm). At a turbine inlet pressure of 3.2 atm (46.6 psig) and outlet pressure of 1 atm (15 psig), the nozzle jet velocity is calculated to be 326 m/s (1070 ft./s) using Equation (70) since the nozzle design is the same for the two turbines. Turbine speed was recorded at 314.15 rad/s (3000 rpm) during an NHTS experiment under the given steam inlet mass flow rate and inlet and outlet pressures, and the β was measured as 0.52 rad (30^0 degree). Inserting these parameters into Equation (10) yields a pump torque (T_{pump}) of 3 N.m (2.21 lb.ft).

Since the parameters of the unit-less time ratio ($\prod$) in Equations (21) and (22) are now available, the $\prod_I$, $\prod_{II}$, and Similarity Level can be calculated. The turbine input parameters and Similarity Level calculation results are summarized in Table 2. Where the $(SL)_I$ and $(SL)_{II}$ represent the Similarity Level values for the $\prod_I$ and $\prod_{II}$ using Equation (3).

Table 2 NHTS and prototype RCIC system turbine parameters.

Parameter	**NHTS RCIC Turbine**	**Peach Bottom RCIC Turbine**	
$\dot{m}$ (kg/s)	0.03	26.8	
V_j (m/s)	326	758	
r (m)	0.46	0.61	
β (rad)	0.52	0.79	
ω (rad/s)	314.15	471.24	
T (N.m)	3.00	772	
$\prod_I$	1.53	1.51	$(SL)_I = 1.01$
$\prod_{II}$	0.47	0.49	$(SL)_{II} = 0.96$

The RCIC turbines Similarity Level is estimated using the two derived unit-less ($\prod_I$ and $\prod_{II}$) time ratios for the quasi-steady state operation condition since they have many parameters that govern the control volume characteristics. The $(SL)_I$ is 1.01, which indicates high similarity being close to 1.0. To achieve full similarity (SL=1), input parameters of the NHTS $\prod_I$ equation such as the nozzle jet velocity could be adjusted. On the other hand, The $(SL)_{II}$ calculation is close to the full similarity condition with a value of 0.96. Both derived unit-less equations indicated a high Similarity Level value between the NHTS and Peach Bottom RCIC turbines.

To test the RCIC turbine Similarity Level sensitivity, range of tests with variable input parameters (related to $\prod_I$ and $\prod_{II}$) controlled by the steam mass flow rate were conducted at the NHTS RCIC turbine and compared to the operating conditions and parameters of the Peach Bottom RCIC system. The steam mass flow rate was chosen as the main variable since it is easy to control and affect the rest of the parameters in the ($\prod_I$ and $\prod_{II}$) equations such as the torque and jet velocity. Table 3 summarizes turbine Similarity Level's sensitivity to the test input parameters characteristic time ratios.

The steam inlet flow was delivered from the NHTS steam generator and the steam and water were discharged to a water-filled tank at atmospheric pressure. The turbine load was a water-brake dynamometer. The inlet and outlet pressures are the measured pressures across the turbine, while the jet velocity is the average calculated velocity of the steam in the bucket. Figure 32 shows the RCIC turbine Similarity Level sensitivity based on the ($\prod_I$ and $\prod_{II}$) calculations.

Table 3 RCIC system turbine Similarity Level sensitivity at the NHTS facility.

$\dot{m}$ (kg/s)	P_{In} (atm)	P_{out} (atm)	V_j (m/s)	T (N.m)	Π_I	Π_{II}	$(SL)_I$	$(SL)_{II}$
0.030	3.17	1.04	326.80	3.00	1.52	0.47	1.01	0.96
0.035	3.26	1.05	331.90	3.50	1.53	0.47	1.01	0.96
0.040	3.33	1.05	337.50	4.00	1.54	0.46	1.01	0.94
0.045	3.43	1.05	344.40	4.80	1.55	0.45	1.03	0.92
0.050	3.72	1.07	359.20	5.60	1.57	0.43	1.04	0.88

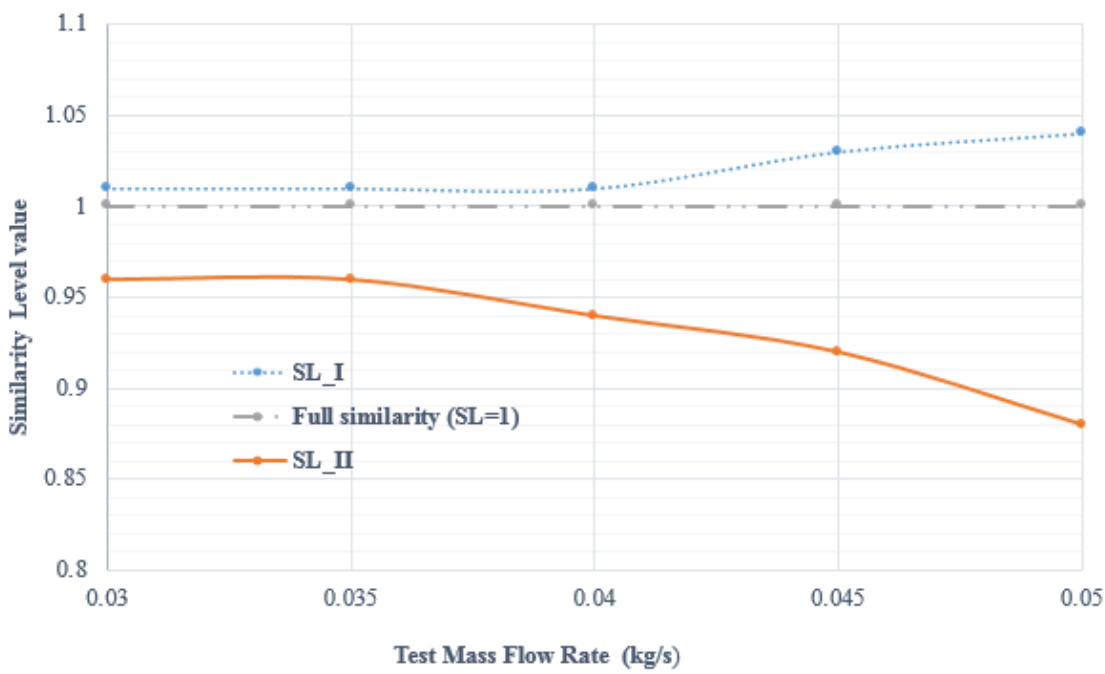

Figure 32 RCIC system turbine Similarity Level sensitivity.

Based on the Similarity Level sensitivity calculations, the $(SL)_I$ and $(SL)_{II}$ vary between 1.01 – 1.04 and 0.88-0.96 respectively. This indicates low sensitivity on the turbine Similarity Level as the flow rate increase (for the NHTS capability) using the

turbine control volume derived $\prod_I$ and $\prod_{II}$ (up to 4% and up to 12% respectively) calculations, which lowers the Similarity Level to a value of 88% (resulting from $(SL)_{II}$ calculations). Error propagation of the calculated Similarity Levels indicates that the uncertainty is within the range of 10%, which makes the lowest achieved turbine Similarity Level to be 78% based on the $(SL)_{II}$. The uncertainty comes from the parameters used in the Similarity Level calculations, such as the test mass flow rate, flow jet velocity, and torque. ***The Similarity Level analysis and test results indicate that the NHTS RCIC turbine simulates well the processes in the full size turbine and can be used to study the prototype model over design basis operating conditions. Also, the results indicate that for higher Similarity Level with regards to the Peach Bottom system turbine requires operating conditions at the NHTS facility that have a lower flow rate values.*** Another benefit of the Similarity Level is that it tells the best operating conditions that yield high Similarity Level with respect to the full size system.

If considering the unsteady state turbomachinery system operation, the input parameters for $\prod_{III}$ were collected from the earlier NHTS testing to check the ability to estimate the Similarity Level using the $\prod_{III}$ for the unsteady state condition. As an example: For the test of a 0.055 kg/s mass flow rate, the registered enthalpy was 2750 kJ/kg with a calculated work value of 23.5 kJ/s and heat rate of 182 kJ/s. Calculation of ($\prod_{III}$) resulted in a value of 0.13, which is <<1 and eliminates its use for Similarity Level estimation as explained before in section 4. On the other hand, using the mentioned input parameters for ($\prod_{IV}$) resulted in a value of 0.83 which is <1 but still can be used for

Similarity Level estimation. However, the enthalpy and heat rate values are not available for the Peach Bottom system and that makes estimating the Similarity Level using ($\prod_{IV}$) unavailable for the time being.

7.2 RCIC System Suppression Pool Scaling Results and Discussion

In this dissertation, the unique derived unit-less characteristic time ratios (Equations (56), (57), (68), and (69)) are the basis for NHTS Suppression Pool Similarity Level model since the tests performed with the NHTS pool provide the necessary input data. So, to use the developed similarity model, the input parameters of the unit-less time ratios for both scaled facility systems need to be collected or calculated such as: the flow velocity, flow total energy, distance between the Sparger exit and bottom of the pool, heat rate per mass, thermal conductivity of the flow, and pool ambient fluid density. Unfortunately, those input parameters are not available for the Monticello Suppression Pool. For this reason, simulations can be a source of input data that compensate the lack of available information about a full size system in the future. Simply, by adjusting the developed CFD model to match the geometrical and operating conditions of the Monticello Suppression Pool upon availability. On the other hand, there are a wide range of testing data available for the NHTS facility Suppression Pool for the purpose of studying the pool thermal stratification. These data collected from (Solom, 2016) and analyzed to provide the correct input parameters in order to develop a similarity model.

The similarity model, is the time ratio values of the NHTS Suppression Pool system without dividing over the time ratio values for the full scale system. Upon availability of the full scale system pool data, the scaling Similarity Level values can be

estimated with respect to the NHTS one. In fact, this developed similarity model can be applied to estimate the Similarity Level for any test facility pool with reference to any full size pool system since the conservation equations that would be applied are the same. In another words, if the unit-less time ratios input data would be available for any full size facility Suppression Pool, then the Similarity Level can be calculated with respect to the NHTS Suppression Pool using Equation (3). The Similarity Level estimates how applicable using the test facility to draw a conclusion about the full size system performance.

To provide a reference data for the NHTS pool similarity model, dry steam flow was injected into the NHTS pool for a range of tests mentioned in Table 4 and Table 5 regarding calculating of the unit-less time ratios. Average quasi- steady state NHTS pool characteristic time ratios input parameters collected for the NHTS pool during the performed tests. The steam parameters collected inside the Sparger at a constant mass flow rate condition (mass flow rate is different for each test) such as: the steam quasi-steady state thermal conductivity, density, temperature, and enthalpy. Similar parameter were collected for the liquid fluid at the pool. Time ratios calculation of Equations (57) and (69) resulted in values much less than unity, which eliminate the important of the values for Similarity Level estimation. While the time ratios of Equations (56) and (68) yields values close or greater than unity and remain of importance for Similarity Level estimation, which herein reported in this research as the basic NHTS pool similarity model values.

The tests were governed by the steam mass flow rate as the main variable because it is easy to control and affect the Similarity Level model parameters, which provide a

range of testing conditions. Importantly, the thermal hydraulics conditions changes between scaled systems at normal and transient (might match at some conditions and geometries), which required similarity evaluation at each application. In all steam injection tests the steam quality was 1 as measured in the Sparger. The NHTS facility Suppression Pool Sparger diameter is 0.041 m and has a cross sectional area of 0.001313 m^2. The Distance between the Sparger pipe exits to the bottom of the pool H^o is 0.381 m. Table 4 has important NHTS pool data of a single phase flow tests required to calculate other input parameters of the unit-less characteristic time ratios, which were collected from (Solom, Experimental Study on Suppression Chamber Thermal-Hydraulic Behavior for Long-Term Reactor Core Isolation Cooling System Operation, 2016). The uncertainty of the steam flow rate parameters comes from the instruments used for measurements as well analytical uncertainty.

Table 4 Single phase tests data for the NHTS suppression pool.

Test #	**Steam Flow Rate (g/s)**	**SP time averaged Pressure (Pa)**	**Injection steam enthalpy (kJ/kg)**	**Duration of test (s)**
1	23.5 ± 0.5	(1.43 ±0.32) E5	2720 ± 1.32	12878
2	65.8 ± 0.5	(1.88 ± 0.80) E5	2745 ± 1.57	6678
3	45.3 ± 0.5	(1.77 ± 0.68) E5	2737 ± 0.9	8917
4	45.0 ± 0.5	(1.05 ± 0.0073) E5	2730 ± 0.65	6466
5	66.8 ± 0.5	(1.06± 0.014) E5	2741 ± 0.48	4542
6	23.7 ± 0.5	(2.09 ± 0.58) E5	2720 ± 1.04	16245
7	44.8 ± 0.5	(2.01 ± 0.48) E5	2733 ± 0.92	8209
8	45.6 ± 0.5	(1.34 ± 0.40) E5	2734 ± 1.32	8602
9	44.6 ± 0.5	(2.09 ± 0.01) E5	2734 ± 1.32	10221
10	44.7 ± 0.5	(1.84 ± 0.70) E5	2734 ± 0.84	9675

At the single phase injection into the pool, temperature of the pool were measured by having thermocouples distributed at different locations. The hydrostatic average temperature of the pool liquid was averaged based on analyzing the registered test temperature data during the test period from thermocouples at:

- The outlet of the pool.
- Lower part of the pool.
- Middle part of the pool.
- Upper part of the pool.

More and detailed information about the tests and the registered temperature values can be found at (Solom, 2016). The ambient density of the fluid in the pool was estimated for each test based on the Suppression Pool averaged temperature and quality values. The quality of steam in the pool is zero for long term mixing condition in the pool since condensation at the inlet is happened very rapidly under the Direct Contact Condensation (DCC) phenomena. Table 5 presents the processed data for NHTS Suppression Pool testing, which is used to calculate the similarity model unit-less time ratios. The uncertainties are calculated using error propagation rules. Substituting these values into Equations (56) and (68) resulted in unit-less time ratios values for the range of tests performed. Table 6 summarizes the values of the unit-less time ratios values for the developed similarity model with the related uncertainties. The (Π_{Ri} is close to unity this means the specific process would be of importance in the transient process of the system.

The $\Pi_{VII} \geq 1$, which means the energy transient transfer process is of importance and would be used to estimate the similarity between the scaled systems.

Table 5 Processed data for single phase tests at the NHTS suppression tank

Test #	**Sparger steam time averaged Temperature (C°)**	**SP time averaged Temperature (C°)**	**Sparger flow total energy E_T (kJ/kg)**	**Heat rate per mass $\dot{q}$ (kW/kg)**	**Injection flow velocity (m/s)**	**SP time average fluid density (kg/m^3)**
1	110	60.16	2720.13 ± 63.91	0.21 ± 0.01	16 ± 4	983
2	118	77.95	2745.42 ± 157.32	0.41 ± 0.02	29 ± 5	973
3	116	71.02	2737.47 ± 171.02	0.31 ± 0.02	31 ± 6	977
4	101	62.63	2730.25 ± 105.02	0.42 ± 0.02	22 ± 5	982
5	101	74.64	2741.52 ± 182.77	0.6 ± 0.03	32 ± 6	975
6	122	84.02	2720.19 ± 84.71	0.17 ± 0.01	19 ± 4	969
7	120	54.80	2733.46 ± 168.2	0.33 ± 0.02	30 ± 6	986
8	108	74.17	2734.38 ± 144.75	0.32 ± 0.02	28 ± 5	975
9	122	61.93	2734.2 ± 87.8	0.27 ± 0.01	20 ± 4	982
10	118	62.82	2734.26 ± 108.16	0.28 ± 0.01	23 ± 5	982

Testing was performed at the NHTS Suppression Pool for wide range of testing conditions. To provide a better view of the testing results and time ratio values, Figure 33 shows the log scale of the Π_{VII} unit-less time ratio versus the heat rate addition per unit mass ($\dot{q}$) to the pool as a reference model for scaling. The ($\dot{q}$) Was chosen to represent the model graph since it is common between the time ratios and can be controlled during testing, which specifies the operating conditions. This reference model provides processed data related to the NHTS Pool, which can be used to estimate the scaling Similarity Level

value if compared to any full-scale system pool. If the Similarity Level value is close to unity, that means the scaled systems are similar enough and this validates using the NHTS Suppression Pool for testing to predict a full scale Suppression Pool behavior.

Table 6 NHTS Suppression Pool unit-less time ratio values of the performed tests.

Test #	Π_{VII}	Π_{Ri}
1	540262.5 ± 139713	0.57 ± 0.004
2	510854.5 ± 102011	0.23 ± 0.001
3	721207.8 ± 142127	0.19 ± 0.001
4	377792.3 ± 84343	0.22 ± 0.001
5	384003.2 ± 75631	0.11 ± 0.0003
6	822447.3 ± 193605	0.60 ± 0.004
7	656614.1 ± 130209	0.23 ± 0.001
8	622501.3 ± 127005	0.170 ± 0.001
9	529928.1 ± 122975	0.530 ± 0.003
10	576493.4 ± 126211	0.350 ± 0.002

To use the model correctly, data has to be collected for the full size facility and used with Equations (56) and (68) to estimate the scaling Similarity Level using Equation (3) Basically, the scaling Similarity Level estimates the level of confidence about using the NHTS facility for testing and drawing a conclusion about specific full scale system performance.

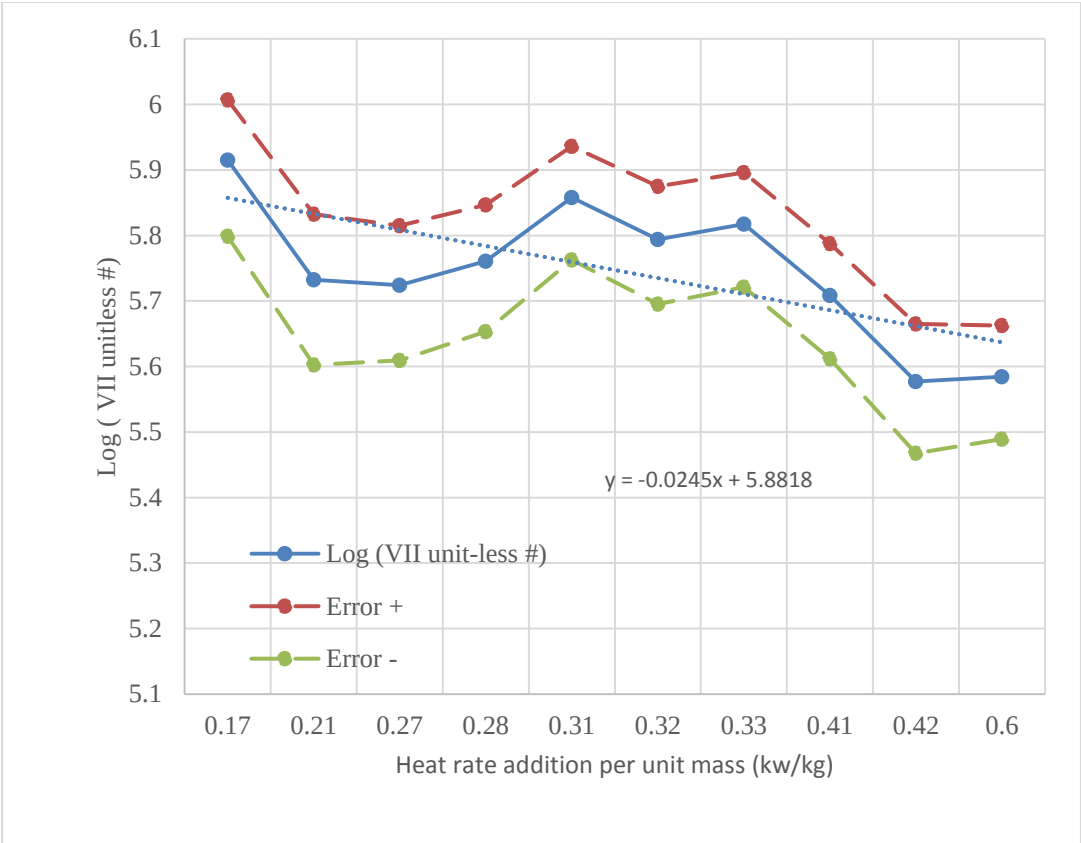

Figure 33 NHTS facility Suppression Pool Log (Π_{VII}) versus heat rate addition to the pool per unit mass.

Based on the trend line of the test data time ratio in Figure 33, the following correlation yields and is expressed in Equation (71). The correlation allows to predict the Π_{VII} with regards to the heat rate addition per unit mass to the pool system and that represent the NHTS pool data side with 1% error value. Similar analysis can be applied with regards to Π_{Ri} to provide a correlation to predict its value.

$$Log_{10}\ (\Pi_{VII}) = -0.0245\ q^{\cdot} + 5.8818 \tag{71}$$

7.3 STAR-CCM+ Scaling Results

7.3.1 RCIC system GS-1 turbine model simulation

The purpose of the STAR-CCM+ simulations were to provide input data for the derived unit-less time ratios to estimate the scaling Similarity Level values. Additionally, to provide a reference model for future comparison with other RCIC systems. Simulations were prepared and run for the GS-1 Terry turbine model with the previous mentioned operating conditions at subsection 5.2.1. Table 7 summarizes the selected physical models, meshing properties, and simulation conditions that were applied to the GS-1 turbine model simulation. Running a simulation after the mentioned setup, Figure 34 shows a section plane that represents the steam velocity distribution at the turbine interior wheel and exterior body, where the section plane cut is at the mid thickness of the geometry.

Table 7 GS-1 turbine CAD model simulation setup parameters and conditions.

GS-1 model simulation setup	Property
Physical models	Coupled flow and energy
	Ideal gas (compressible)
	RANS
	Three dimensional
	Steady state
	K-epsilon turbulence model (turbulence density 1%)
	Reference frame
	Two- Layer All y+ Wall Treatment
Mesh	Polyhedral meshing
	Prism-layer mesher (5 layers)
	Base size : 0.001 m
	# of cells: 12 million
	# of optimization cycles: 8
	Quality threshold: 1
	Maximum skewness angle: 75 degree
Boundary conditions	Inlet pressure: 750 psi
	Outlet pressure: 29 psi
	Static temperature: 538 K
	Rotation rate: 4500 rpm

Based on the simulation results, the velocity magnitude outside the nozzle is maximum at the bucket entrance where the steam hits first, where the average steady velocity (jet velocity) is 711m/s inside the bucket as measured by STAR-CCM+ code. This average velocity is lower than the value resulted from FLUENT model Equation (70) of 758 m/s, which predicts the jet velocity for an inlet/outlet pressure ratio. The rotation rate relative to the reference frame is 4500 rpm. The velocity distribution outside the

nozzle as a function of the bucket depth is represented by Figure 35 as appear in the STAR-CCM+ code. The total distance investigated inside the bucket is 0.5 cm. The X-axis starts with the value 0.1845 m, which represent the location of the bucket entrance on the Cartesian coordinate system. The flow velocity decreased almost linearly while traveling inside the bucket as a function of depth.

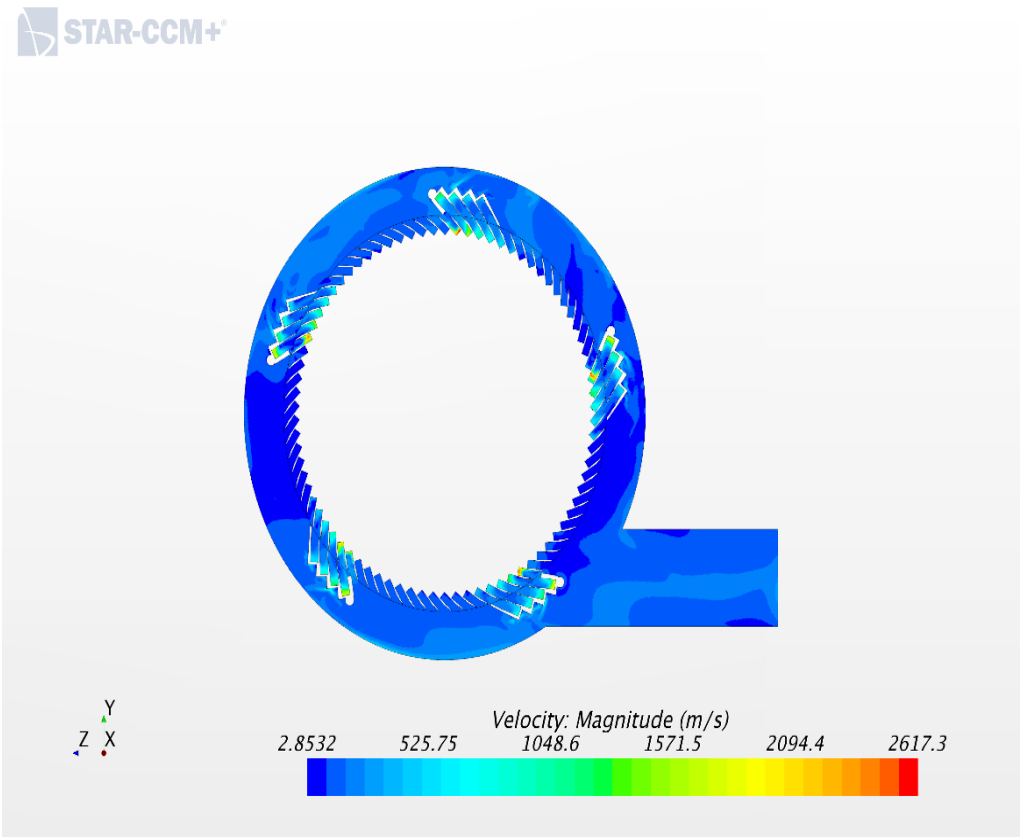

Figure 34 Velocity distribution over GS-1 geometry scalar section plane.

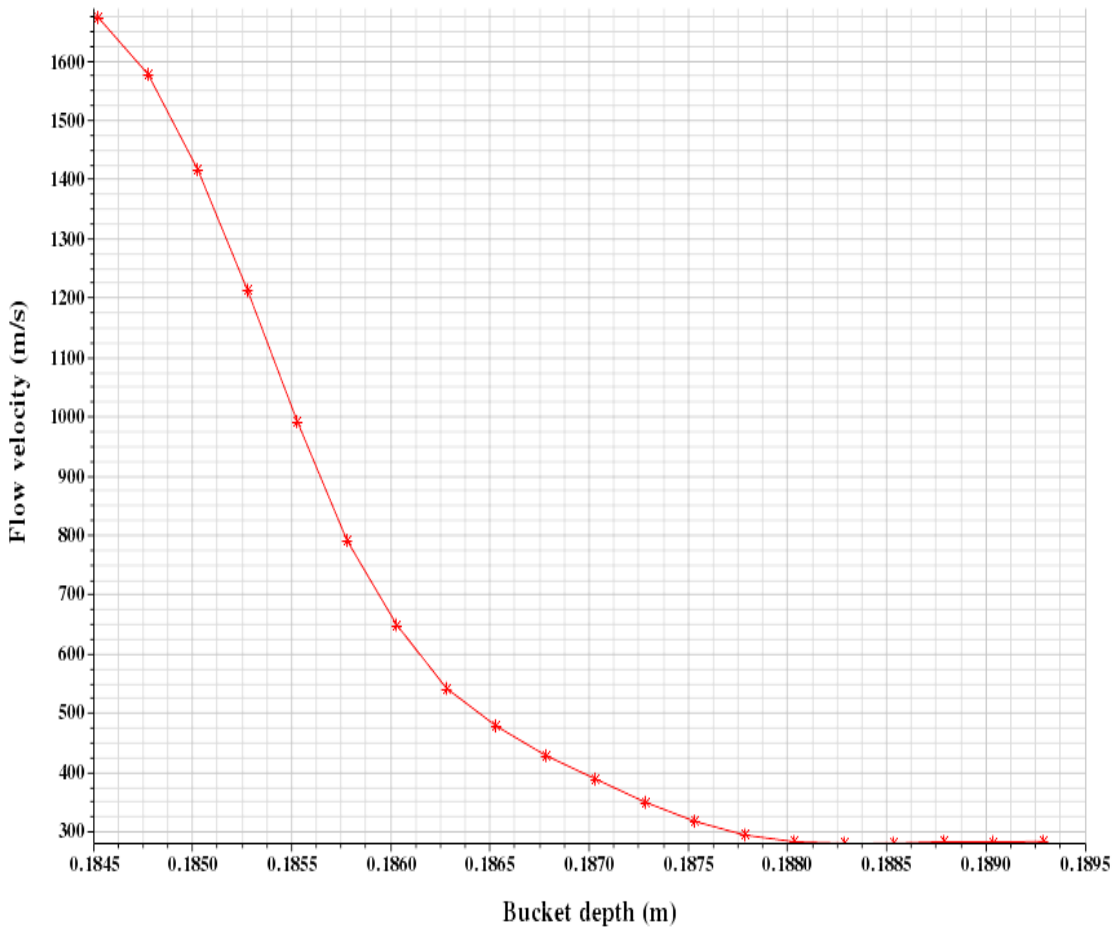

Figure 35 Velocity distribution inside GS-1 turbine bucket.

The pressure distribution in the nozzle was investigated near the nozzle exit after the steam passed through the nozzle throat to make sure the simulation results are accurate and worthy. The pressure decreased as expected by passing through the nozzle throat increasing the flow velocity. The flow pressure at the nozzle exit was measured at the simulation and its value is 29 psi, which represents the pressure at the rest of the flow at the rest of the turbine body. Figure 36 shows the linear decrease of the flow pressure as it

pass through the nozzle throat. The X-axis ended near the value of 0.1824 on the Cartesian coordinate system, which is located before the turbine bucket entrance location of 0.1845 as appears on the X-axis starting of Figure 36. The distance between the nozzle exit and the bucket entrance in the turbine geometry model is 2 mm, which is the distance the flow passes before hitting the bucket. The value of the jet velocity resulted from the GS-1 simulation is an example of an input parameter for Equations (21) and (22), which lead to the calculation of the Similarity Level of scaling.

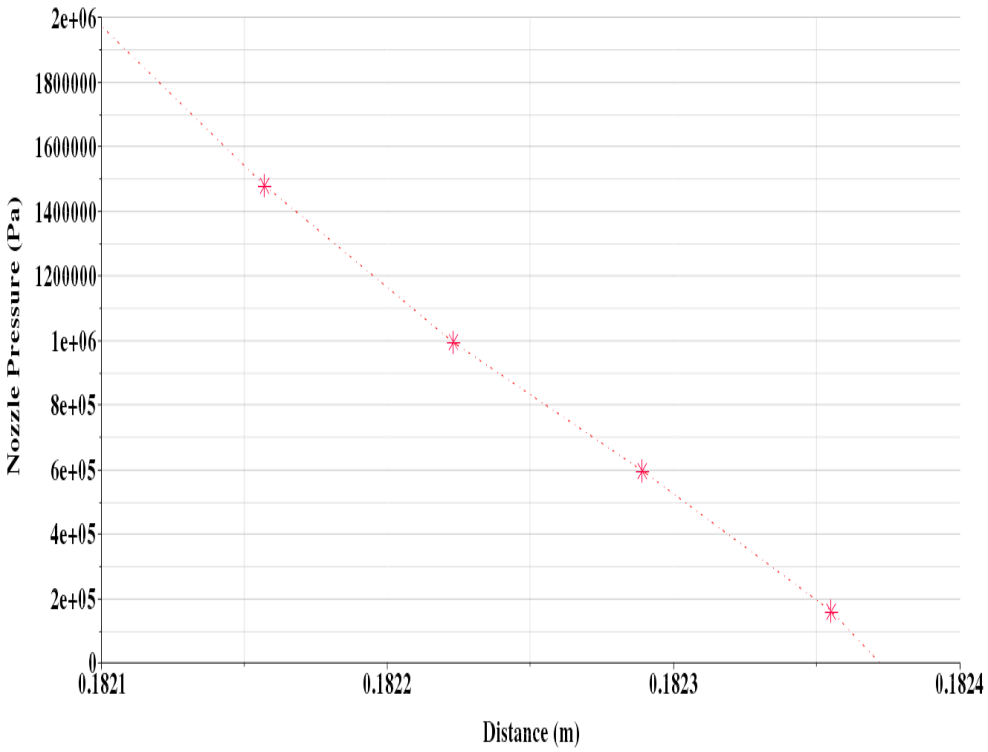

Figure 36 Pressure distribution through the nozzle throat.

7.3.2 NHTS RCIC system ZS-1 turbine CAD model simulation

Similar to the GS-1 CAD model, simulations are prepared using the ZS-1 CAD model to measure the nozzle jet velocity hitting the buckets at the NHTS RCIC system operating conditions with a polyhedral mesh. Steam injected into the turbine wheel through one inlet nozzle at a pressure of 55 psi (Operating pressure of most of the tests that were done at the NHTS facility) and exiting at a pressure of 15 psi of the turbine exit pipe. Table 8 summarizes the ZS-1 turbine model simulation setup. The Mesher properties are similar to the ones at Table 7 as well except that the number of cells for the ZS-1 model was 7 million cell and the skewness angle was 79°. Besides the pressure conditions values, the static temperature value used at the simulation was 415 K with a rotation rate relative to the outside turbine body of a 3000 rpm.

Table 8 ZS-1 turbine CAD model simulation setup parameters and conditions.

ZS-1 model simulation setup	Property
Physical models	Coupled flow and energy
	Ideal gas (compressible)
	RANS
	Three dimensional
	Steady state
	K-epsilon turbulence model (turbulence density 1%)
	Reference frame
	Two- Layer All y+ Wall Treatment
Mesh	Polyhedral meshing
	Prism-layer mesher (5 layers)
	Base size : 0.0005 m
	# of cells: 7 million
	# of optimization cycles: 8
	Quality threshold: 1
	Maximum skewness angle: 79 degree
Boundary conditions	Inlet pressure: 55 psi
	Outlet pressure: 15 psi
	Static temperature: 415 K
	Rotation rate: 3000 rpm

Mesh sensitivity analysis was applied with wake mesh refinement, 8 optimization cycles, and 79° best achieved skewness angle. Also, simulations were applied with range of mesh base sizes to make sure the results are accurate and independent on the mesh size. Table 9 summarizes the average jet velocity calculated by STAR-CCM+ code as a function of mesh base size for both turbine models (GS-1 and ZS-1). As the mesh base size gets finer more accurate and steady jet velocity resulted as shown in Figure 37. Based on the results, the average velocity values for the GS-1 turbine model is in the 700m/s range (for 750 psi inlet and 29 psi outlet), while the ZS-1 one is in the ranges of 300m/s.

Table 9 GS-1 and ZS-1 models simulations sensitivity analysis data.

Mesh Size (m)	Flow Jet Velocity (m/s)	
	GS-1 Turbine Model	ZS-1 Turbine model
0.015	628	236
0.013	641	248
0.011	655	267
0.009	686	278
0.007	683	286
0.005	707	291
0.003	709	293
0.001	710	294

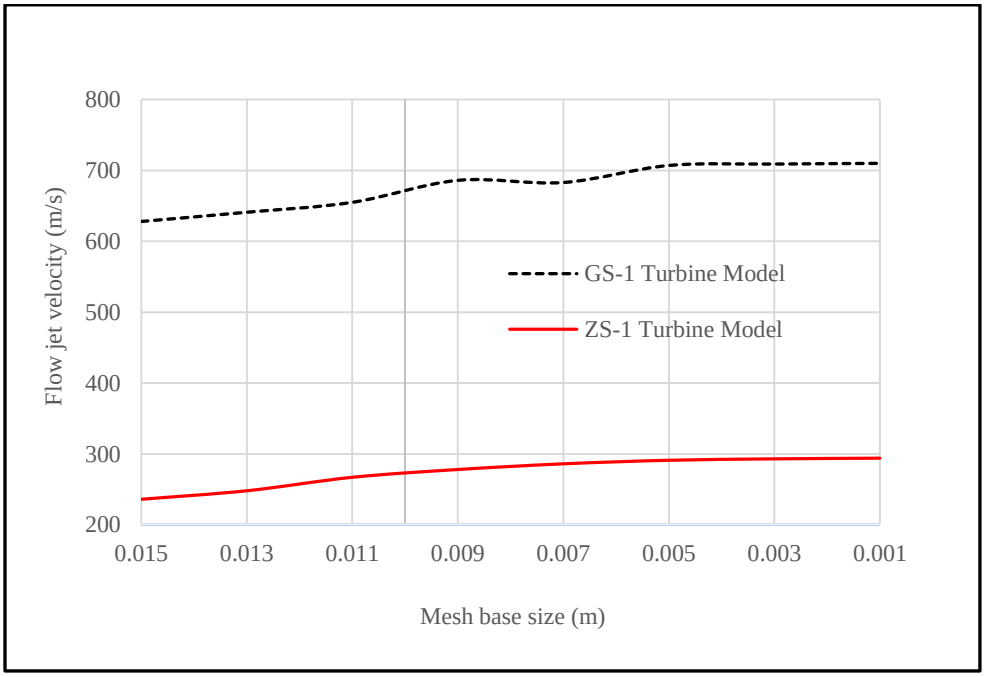

Figure 37 Flow jet velocity as a function of the mesh base size.

A section plane represents the Y-Z of the turbine body shows the velocity distribution of the steam inside the turbine as shown in Figure 38. As expected, the steam velocity hitting the wheel is maximum at the bucket entrance after exiting the nozzle

outlet. The STAR-CCM+ calculates the average steady velocity of the bucket as 294m/s with a velocity spike at the bucket entrance of around a 560m/s.

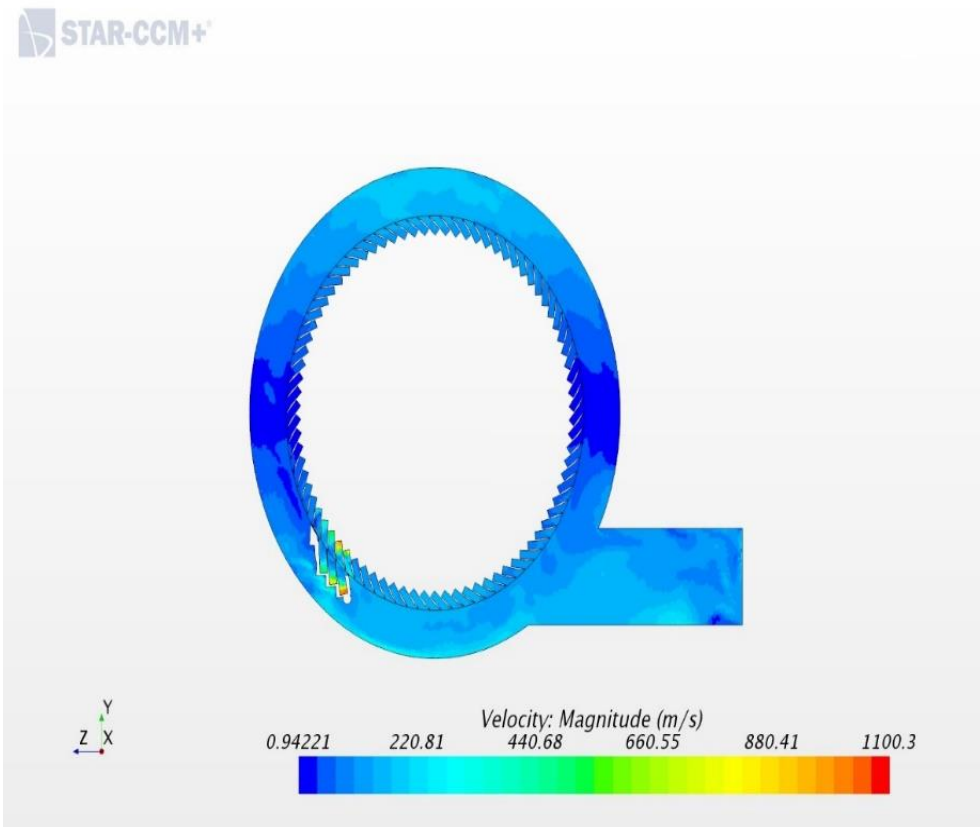

Figure 38 Velocity distribution over the ZS-1 geometry scalar section plane.

Similar to the GS-1 turbine model simulation, the ZS-1 turbine model simulation investigated the velocity distribution inside the bucket as function of the bucket depth. The total depth investigated is 0.5 cm, while ***the purpose of the velocity investigation is to estimate the steady jet velocity in the bucket that is used in the torque value estimation***. Figure 39 shows the flow velocity distribution inside the bucket as a function of the depth. The velocity distribution of the ZS-1 model is similar to GS-1 one. The difference is in

the velocity values level, which is higher for the GS-1 because it operates at higher pressure values. In Figure 39 below the bucket depth starts at 0.188 m, which is representing the location of the bucket entrance with regards to the Cartesian coordinate system.

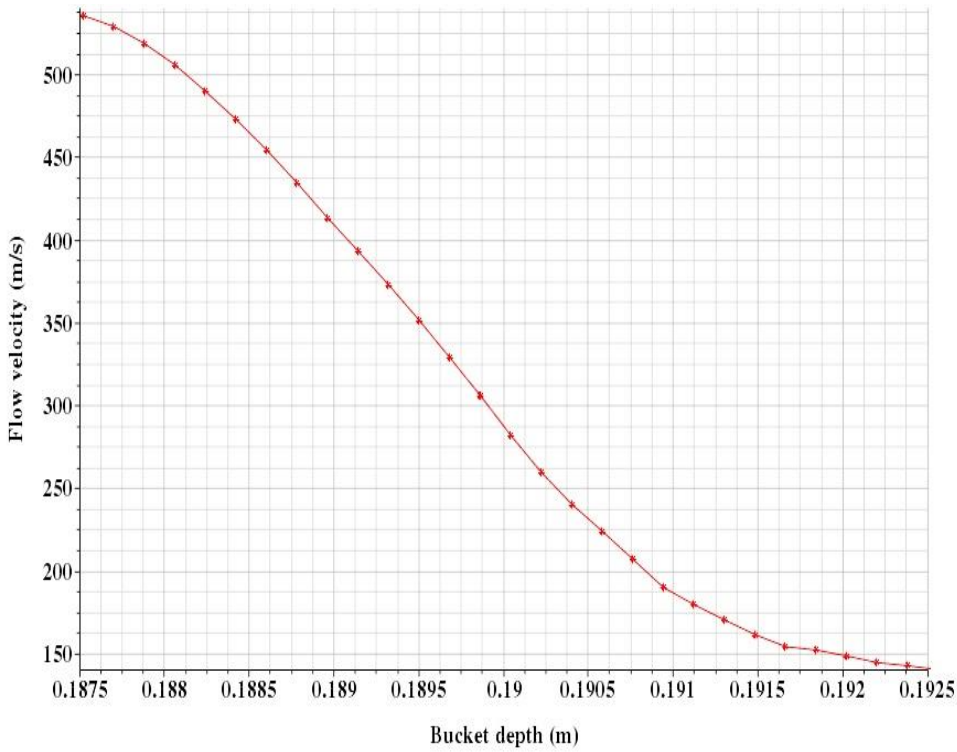

Figure 39 Velocity distribution at the ZS-1 turbine model bucket.

7.3.3 NHTS ZS-1 turbine model validation

To validate the NHTS RCIC system turbine model simulation results and to enable using the model to represent the full size system turbine, the STARCCM+ torque results is compared to the experimental torque results that were conducted at the NHTS RCIC system turbine for testing a dry steam (Luthman, 2017). The testing conditions were

matched with the experimental ones at the NHTS facility (3000 rpm rotational speed, inlet pressure of 55 psi, outlet pressure of 15 psi, and the flow is very dry steam). The experimental torque values are adopted from (Luthman, 2017) tests, where the uncertainty of the values is including the random errors and operator adjustment during data collection in the range of ±1 N.m as estimated from the author (Luthman, 2017) for the selected tests. Table 10 shows the testing torque results at the NHTS RCIC system versus the estimated torque results using STARCCM+ simulations. The error propagation of the simulated torque results is in the range of ± (0.5-1) N.m. Tests at the NHTS facility were controlled by the steam mass flow rate, in which changing the flow rate values changed the resulted torque values. Several tests conducted to test the sensitivity of the torque values as the flow rate changes. Similarity, simulations were run with range of flow rate values to compare to the NHTS testing conditions. The torque values versus the dry steam flow rate for both experimental and simulation is represented in Figure 40. The simulations of the NHTS RCIC turbine resulted in a close values to the experimental ones with difference in the values ranging between 0.1 to 4 N.m. The resulted similarity of values between the experimental and simulations gives a confident in the use of the developed model to represent the system turbine.

Table 10 ZS-1 dry steam tests torque values versus simulated ones.

Dry steam mass flow rate (kg/s)	**Experimental torque estimation (N.m)**	**STARCCM+ torque estimation (N.m)**
0.030	3.4	3.3
0.045	6.2	5
0.060	11.8	9.2

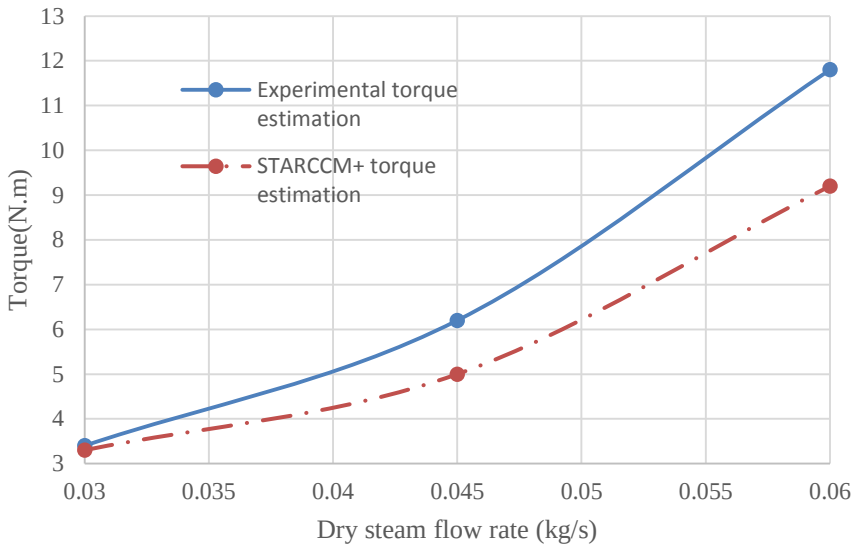

Figure 40 Experimental versus simulation torque results for dry steam testing.

7.3.4 RCIC system turbine nozzle model simulation

The nozzle model was tested on FLUENT code with an inlet pressure of 750 psi of the nozzle and 43.5 psi outlet pressure, the average inlet bucket velocity calculated to be 758.26 m/s (Ross , et al., 2015). A simulation with similar conditions was run on the nozzle model using STAR-CCM+ yielded average velocity of 711m/s, the following Figure 41 through Figure 46 represent the simulation results. The physical modules used for the simulations were:

- Coupled flow and energy
- Exact wall distance
- Ideal gas (compressible)
- K-Epsilon turbulence

- 3D and steady state
- RANS

The simulation results showed a reasonable pressure, velocity and temperature distributions as solved numerically. Figure 41 and Figure 42 presents a section plane 2D and full 3D view of the flow pressure distribution inside the nozzle using STAR-CCM+. Figure 43 shows a closer 3D view of the pressure distribution at the nozzle throat and to the exit way, which clearly indicated the huge difference in the pressure distribution as the flow transfer through the nozzle. The 2D and 3D view sections of the simulations show the velocity and pressure distribution for the nozzle part, which seems as a defined boundary condition at the inlet. However, the outlet pressure and velocity values are simulated by STAR-CCM+ and are not a predefined values.

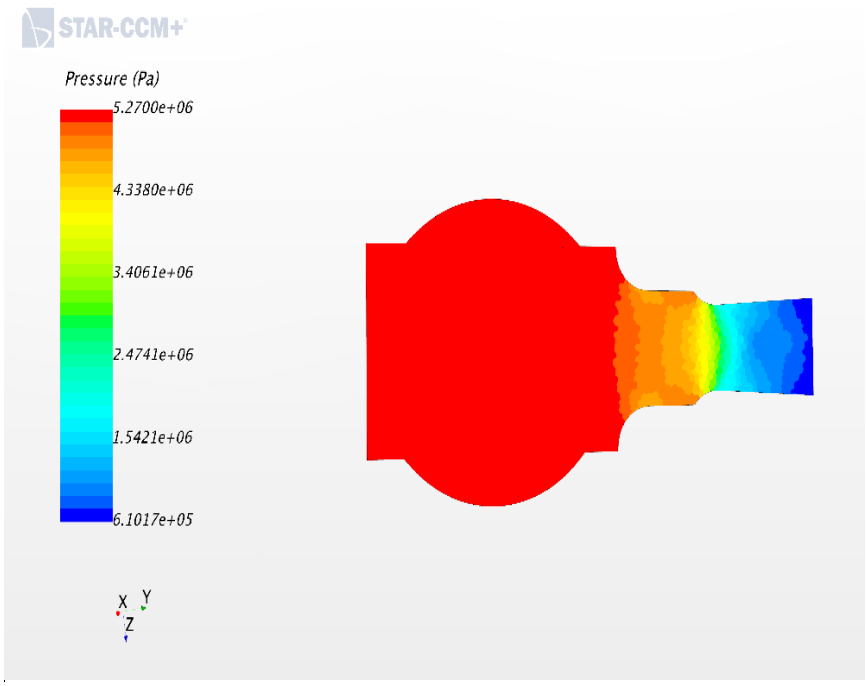

Figure 41 Bottom 2D view of flow pressure distribution inside the nozzle.

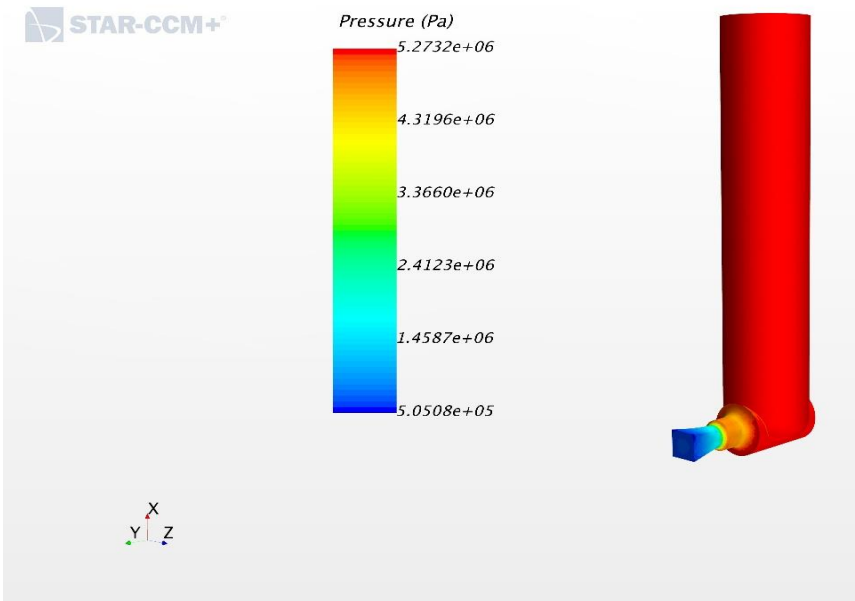

Figure 42 Full 3D view of flow pressure distribution inside the nozzle.

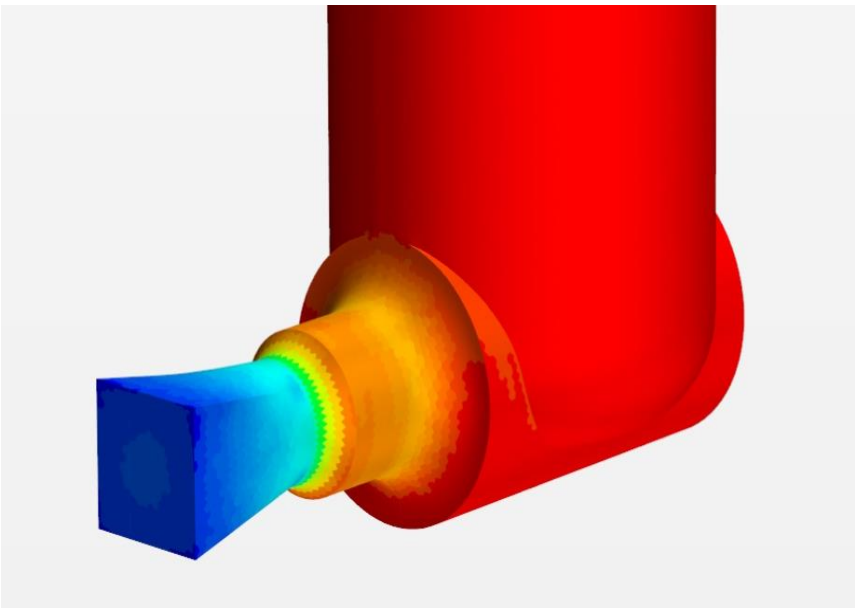
Figure 43 Closer 3D view of the pressure distribution at the nozzle throat and exit.

The parameter of interest for the scaling analysis is the jet velocity value, for this regards a view of the velocity distribution inside the nozzle is helpful to check the numerical calculations of the STAR-CCM+ nozzle model. Figure 44 shows a 2D distribution of the velocity inside the nozzle for the realistic flow conditions from the RPV. The velocity of the flow at the inlet is around 1m/s and increases up to 890 m/s is it comes to through the nozzle through to the exit way. Figure 45 and Figure 46 show full 3D and 2D section plane of the temperature distributions of the steam as it goes through the nozzle. Based on the simulation results, the temperature of the steam dropped down to 53 C^{o} near at the exit of the turbine.

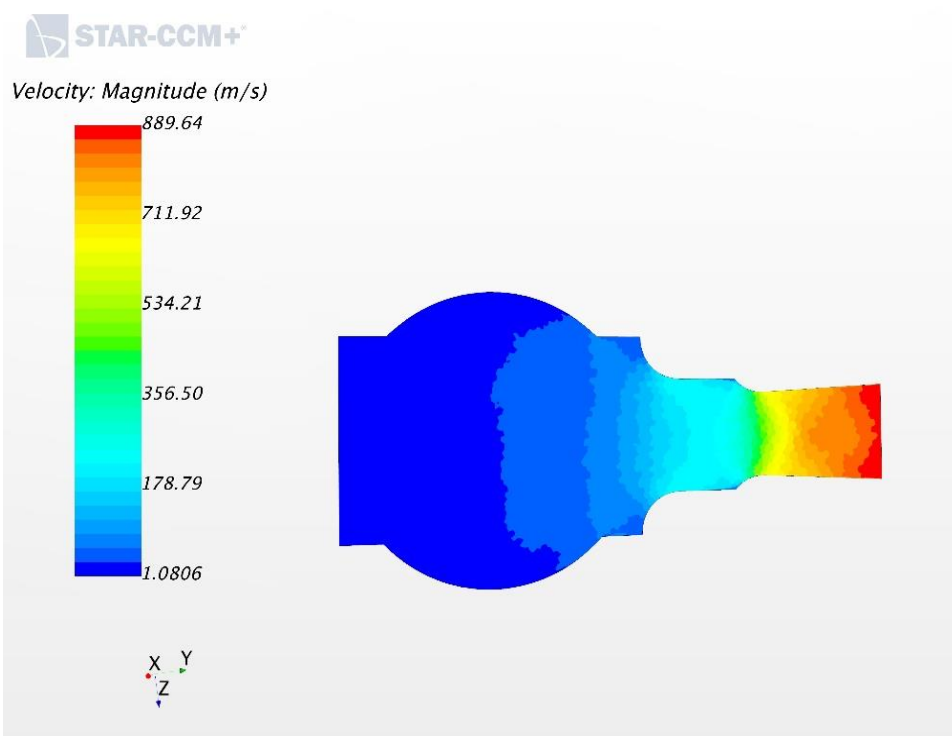

Figure 44 Bottom 2D view of flow velocity distribution inside the nozzle.

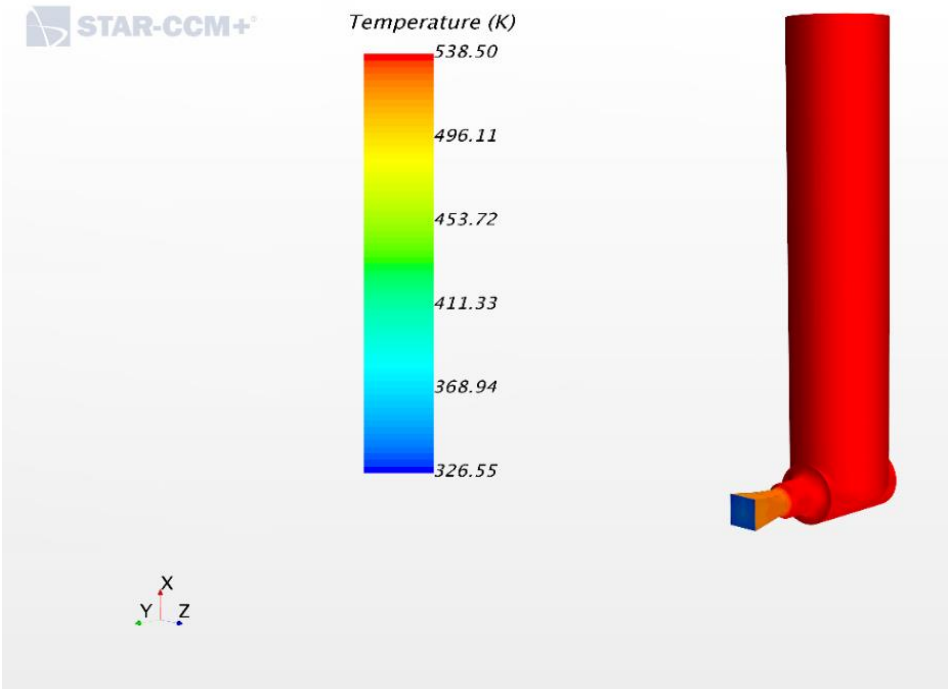

Figure 45 Full 3D view of flow temperature distribution inside the nozzle.

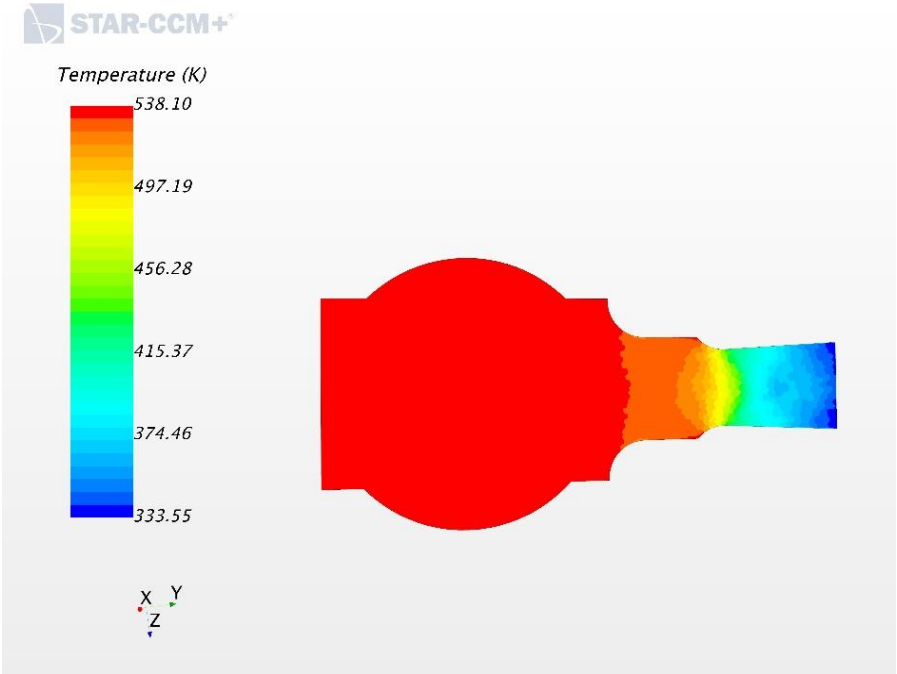

Figure 46 Bottom 2D view of flow temperature distribution inside the nozzle.

Many time ratio input parameters can be estimated by doing simulation for a beyond design basis conditions. Since the jet velocity is used in the scaling ratio estimation, an effort is made to estimate a correlation to calculate the jet velocity using the STAR-CCM+ simulation results. The velocity distribution simulated at the bucket inlet (jet velocity) at range of pressures. The pressure ranges between 250-900 psi for the inlet with pressure increment of 50 psi. Table 11 summarizes the results of the model jet velocity testing at range of nozzle inlet pressures based on STAR-CCM+ calculations. As seen in Table 11, larger pressure drop ratio yields higher jet velocity at the bucket. The velocity increase is dominated by increasing the nozzle inlet pressure, which in turn increases the enthalpy of the inlet flow. Figure 47 shows the relation between the pressure drop ratio and the average velocity results, where STAR-CCM+ results are covered by a linear correlation as shown in Equation (72) that calculates the jet velocity based on a pressure ratio value.

Table 11 Nozzle jet velocity as a function of nozzle inlet/outlet pressure.

Inlet pressure (psi)	Outlet pressure (psi)	Pressure drop ratio (psi)	Jet velocity value (m/s)
250	15	16.70	499
300	15	20	541
350	15	23.30	574
400	15	26.70	604
450	15	30	633
500	15	33.30	661
550	15	36.70	686
600	15	40	719
650	15	43.30	739
700	15	46.70	759
750	15	50	787
800	15	53.30	808
850	15	56.7	827
900	15	60	858

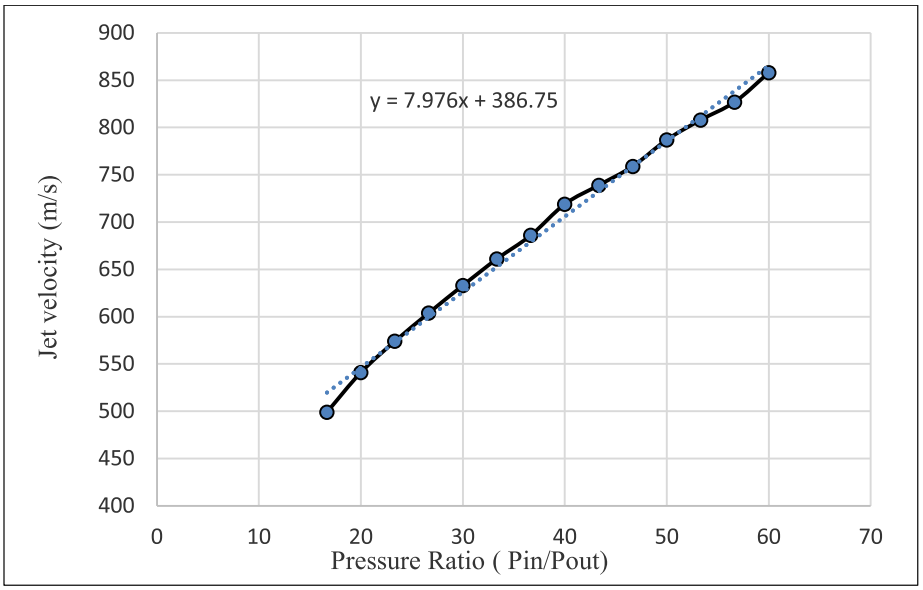

Figure 47 Flow jet velocity distribution as a function of the nozzle pressure ratio.

$$V_j = 7.97\left(\frac{P_{in}}{P_{out}}\right) + 386.75 \tag{72}$$

Equation (72) predicted by STAR-CCM+ model calculates jet velocity values lower than the Equation (70) by FLUENT model of SNL team work, which might be related to the physical models and conditions used as well as meshing quality. For a reasonable result, Equation (72) is applicable for a minimum pressure ratio of 15.

7.4 Scaling Similarity Level Informed by CFD

Similarity Level analysis is to be applied between the NHTS and Peach Bottom RCIC systems turbo-pump. Calculating the unit-less time ratios ($\prod$) is the first step to estimate the scaling Similarity Level value. The input parameters for the time ratios need to be collected from experimental as well as the GS-1 and ZS-1 turbine models as well as available experimental data. The GS-1 RCIC Terry turbine wheel is 0.61m in diameter and the mass flow rate into the pump is 26.8 kg/s, with an actual turbine flow rate of 2.68kg/s. The turbine speed is 471.24 rad/s and β is 45^0 as collected from (Ross , et al., 2015).While, the jet velocity (average bucket velocity) was estimated in both FLEUNT and STARCCM+ for the inlet/outlet nozzle pressure of (750/43.5) psi as 758m/s, 711m/s respectively. The resulted pump torque (T_{pump}) using Equation (3) for parameters from the two CFD codes are 614±61 N.m for FLUENT code and 667±64 for STAR-CCM+ code. The general error propagation principle is used for the calculation of the uncertainties in the torque and similarity time ratios calculations. Using the pump torque values and other input parameters to calculate its ($\prod$). The ($\prod_I$) for the GS-1 model (FLUENT), (STAR-

CCM+) parameters are 1.51±0.16 and 1.54±0.16 respectively. The ($\prod_{II}$) for the GS-1 model (FLUENT), (STAR-CCM+) parameters are 0.49±0.05 and 0.46±0.05 respectively.

Calculating the unit-less time ratios for the NHTS RCIC systems requires collecting related input parameters. The turbine wheel diameter is 0.46 m and the steam inlet mass flow rate is 0.03 kg/s. The turbine inlet pressure was 55 psi and outlet pressure was 15 psi, the nozzle jet velocity is estimated to be 305 m/s using STAR-CCM+ code. Turbine speed was recorded at 314rad/s during an NHTS experiment under the given steam inlet mass flow rate and inlet and outlet pressures, and the β was measured as 30^0. Inserting these parameters into Equation (3) yields a pump torque (T_{pump}) of 2.7±0.35 N.m, $\prod_{I}$ of 1.50±0.20, and $\prod_{II}$ of 0.50±0.06. Similarity Level can be found using Equation (3), where the previous simulations used to help providing data to calculate input parameters for the unit-less time ratios. The yields of unit-less time ratios and Similarity Level values between the NHTS RCIC turbo-pump and the full size RCIC turbo-pump are summarized in Table 12 and Table 13.

Table 12 Turbine unit-less time ratios calculation through CFD simulations.

Unit-less Number/ Facility	**NHTS turbine**	**Full size RCIC turbine**	
		FLUENT parameters	**STAR-CCM_ parameters**
$\prod_{I}$	1.50±0.20	1.51±0.16	1.54±0.16
$\prod_{II}$	0.50±0.06	0.49±0.05	0.46±0.05

Table 13 RCIC turbine Similarity Level values using CFD codes.

Similarity Level $(\Pi)_R$	**FLUENT code**	**STAR-CCM+ code**
$(SL)_I$	0.99±0.17	0.97±0.16
$(SL)_{II}$	1.02±0.16	1.08±0.17

As seen from Table 13, the minimum of similarity can be estimated through calculating the difference from unity (Full similarity condition) by measuring difference using the uncertainty from right and left of unity. As an example, the STAR-CCM+ IV minimum scaling Similarity Level $(SL)_{II}$ can be calculated as: (1.08-0.17, 1.08+17) = (0.91, 1.25), where the difference from unity (right or left sides) is 0.09 from the left and 0.25 from the right side. The highest difference is 0.25, subtracting the difference from the unity gives a minimum conservation of 75%. The 75% represent the amount of transferred properties conserved between the two systems. Applying the same calculations on the other Similarity Level calculations at Table 13 gives a Similarity Level using the FLUENT code parameters closest to unity with a minimum value of 82% for $(SL)_I$ and $(SL)_{II}$. While the STAR-CCM+ $(SL)_I$ is calculation is 81%. The minimum Similarity Level values between the NHTS and prototype turbo-pump component are summarized in Table 14.

Table 14 minimum Similarity Level values for the RCIC system turbine.

Minimum similarity level	**FLUENT code**	**STAR-CCM+ code**
$(SL)_I$	82%	81%
$(SL)_{II}$	82%	75%

7.5 Summary of the RCIC System Developed Characteristic Time Ratios.

This section provides the reader with a summary of the derived RCIC system characteristic time ratios. Table 15 has the derived time ratios, related RCIC subsystem, and other information about the time ratios. It is also considered as an overview of the whole RCIC system scaling Similarity Level analysis and application.

Table 15 Summary of the RCIC system scaling Similarity Level time ratios.

($\prod$)	**Equation #**	**RCIC subsystem**	**Operation status**	**NHTS Value**	**Full–scale subsystem data available**
$\prod_{Ns}$	(11)	Pump	Steady state	> 1	Yes
$\prod_{I}$	(21)	Turbine	Quasi- steady	> 1	Yes
$\prod_{II}$	(22)	Turbine	Quasi- steady	<< 1	Yes
$\prod_{III}$	(26)	Turbine	Transient	< 1	No
$\prod_{IV}$	(35)	Turbine	Steady state	< 1	No
$\prod_{V}$	(36)	Turbine	Steady state	< 1	No
$\prod_{VI}$	(38)	Turbine	Transient	-	No
$\prod_{Ri}$	(56)	Suppression Pool	Transient	< 1	No
$\prod_{\mathrm{Re}}$	(57)	Suppression Pool	Transient	<< 1	No
$\prod_{VII}$	(68)	Suppression Pool	Transient	> 1	No
$\prod_{VIII}$	(69)	Suppression Pool	Transient	<< 1	No

8. CONCLUSIONS AND RECOMMENDATIONS

A test facility is being modified at Texas A&M University for investigating the BWR RCIC System performance under Extended Loss of AC Power conditions. A scaling Similarity Level methodology has been developed and applied herein for the NHTS RCIC system. The scaling steps were applied over the various components of the RCIC system (turbopump, and Suppression Pool) to derive unique scaling time ratios that describe the system's control volume properties.

RCIC System geometrical configurations of the integral system, turbine, pump, and pool were described. The governing equations of the RCIC System were determined for this study, namely, the momentum, mass, and energy equations. Unique unit-less characteristic time ratios were derived from the governing equations. These time ratios are used for estimation of the Similarity Level between the NHTS RCIC turbopump and a prototype turbopump such as the Peach Bottom RCIC system turbine.

The RCIC system's turbine Similarity Level estimation showed a high similarity between the NHTS RCIC turbine and the Peach Bottom turbine, which enables the use of the current NHTS turbine to test over normal operating and design basis accident conditions. Sensitivity of the Similarity Level of the NHTS RCIC turbine has been examined by varying operating conditions of the NHTS RCIC turbine over the ranges of the NHTS facility testing capabilities. The variation of operating conditions has low sensitivity on the turbine Similarity Level, where the scaling Similarity Level values can aid in choosing the best operating conditions at the NHTS facility for future testing. The

scaling similarity analysis and previous test results indicate that the NHTS RCIC turbine control volume is appropriate for representing the full-size turbomachinery and can be used to study the prototype turbomachinery's behavior under normal operation and design basis accident conditions.

The similarity criteria level based on the specific pump speed number is a low value of 0.25 between the two facilities' pumps, which indicates that there is not good similarity between the two pumps. This result supports the low similarity between the pumps based on the flow characteristics described by dimensionless numbers, such as Reynolds number. Modifications to the NHTS pump that can be applied to achieve closer similarity have been suggested.

Models for the geometrical configuration and Similarity Level have been developed for the NHTS RCIC system Suppression Pool experimental facility at Texas A&M University to cover the transient operation as an emergency cooling system. The model was used to assess the Similarity Level between the NHTS and a prototype facility Suppression Pools. The characteristic time ratio input parameters for the NHTS facility system Suppression Pool control volume were collected and used to estimate the unitless time ratios values.

The resulting $\prod_{\mathrm{Re}}$ and $\prod_{VIII}$ values for the NHTS pool were much less than unity and were found to describe phenomena not important to the scaling of the pool. Conversely, the $\prod_{VII}$ and $\prod_{Ri}$ values were found important to the scaling evaluation and easily adoptable into scaling analyses, rendering these parameters the most impactful time

ratios for future evaluations of Similarity Level. Based on the calculation of the $\prod_{VII}$, a curve was developed as a function of variable operating conditions in the NHTS Suppression Pool system. This curve provides an operation correlation that predicts the NHTS Suppression Pool time ratio values for specific operating conditions that would be seen in actual Suppression Pool during operation. For future tests at the NHTS Suppression Pool, related to a specific prototype facility, input parameters of the prototype system need to be collected and the dimensionless time ratios ($\prod$) should be calculated to estimate the Similarity Level between scaled systems.

Due to insufficient available data for full-scale RCIC systems, it is recommended as a future work to develop and use a CFD approach similar to the turbine CFD model approach to describe the RCIC system long term operation and Suppression Pool mixing during emergency conditions. Also, the implementation of the boundary conditions in the turbine CFD model can be further investigated. Specifically, the addition of a piping section upstream of the calculation region of interest would assure that the expected flow patterns into the turbine are captured numerically. The future CFD model should provide the required characteristic time ratios input parameters that describes the pool operation.

In this dissertation, CFD simulation was a main pillar in providing a source of data for characteristic time ratio input parameters. The data provided an insight about what the Similarity Level values would be with respect to a full-scale system component. Two CFD models that represent the GS-1 and ZS-1 turbines have been developed, partially validated, and tested to provide data that serves as input for Similarity Level estimation. In addition, calculations with the GS-1 model with STAR-CCM+ at Texas A&M

University were benchmarked against GS-1 calculations performed with FLUENT at Sandia National Laboratories and shown to produce similar results. The NHTS ZS-1 turbine model was validated by comparing with experimental test data that had been obtained by running steam through the ZS-1 turbine in the NHTS Laboratory.

The jet velocity and other input parameters from the CFD analyses were used to calculate the unit-less time ratios and Similarity Levels. The resulting Similarity Levels were close to unity. The high Similarity Levels are a partial validation that the NHTS ZS-1 Terry Turbine may be used as a component in the experimental facility for full-size RCIC system testing.

Furthermore, a CFD model for the turbine steam inlet nozzle was developed and simulated with STAR-CCM+ code to provide a simple yet accurate analytical formulation of the steam inlet velocity as a function of the inlet-to-outlet pressure ratio. The model represents the standard geometry of the RCIC turbine steam inlet nozzle. Nozzle simulations were performed over a range of steam pressures to calculate the jet velocity at the nozzle outlet. As a use of the models in future, the turbine CAD models is recommended to be adjusted to match any full-scale turbine geometry (upon availability of information) that is of interest.

A byproduct of this research is an experimentally-validated CFD benchmark of the steady-state Terry turbine thermal hydraulics. Finally, scaling will justify the use of the NHTS facility with the current configuration or with modifications to understand the full-scale system behavior and to investigate ways to expand operation for longer time, which is of great interest for the U.S nuclear industry.

REFERENCES

Asai, R., Benes, L., Brodrick, R., Buzek, E., Byron, J., Fawal, O., Wheaton, J. (1979). *Mark I Containment Program, Final Report, Monticello T-Quencher Test.* San Jose, California : General Electric.

Bestion, D., D'Auria, F., Lien, P., & Nakamura, H. (2016). *A state of the art report on scaling in system thermal hydraulics applications to nuclear reactor safety and design.* Retrieved from oecd-new.org: https://www.oecd-nea.org/nsd/docs/2016/csni-r2016-14.pdf

Buckingham, E. (1914). On Physically Similar Systems: Illustration of the Use of Dimentional Equations. In *Physics Review (4)* (pp. 345-376).

CD-ADAPCO. (2018). *STAR-CCM+ User Guide.*

Cudnik, R., & Carbiener, W. (1969). Similitude Considerations for Modeling Nuclear Reactor Blowdowns . *American Nuclear Society* , (p. 361).

Dayton Pump Manual. (n.d.). *Dayton Horizantal Multistage Pressure Booster Pumps.* Retrieved from Operating Manual Instructions & Parts Manual: https://www.grainer.com/ec/pdf/Dayton-Horz-Multistage-Booster-Pump-OIPM.pdf

Electric Power Research Institute. (2002). *Terry Turbine Maintenance Guide, RCIC Application: Replaces TR-105874 and TR-016909-RI.* Palo Alto, CA. 1007460: EPRI.

Gamble, R., Nguyen, T., Shiralkar, B., Peterson, P., Greif , R., & Tabata, H. (2001). Pressure Suppression Pool Mixing in Passive Advanced BWR Plants . *Nulcear Engineering and Desgin* , 321-336.

General Electric. (2018, June 19). *General Electric Systems Technology Manual, Chapter 6, BWR Differences.*

General Electric. (2011). *GE BWR_4 Technology, General Electric Systems Technology Manual, Chapter 2.7, Reactor Core Isolation Cooling Systems* .

Houghton, J., & Hamzehee, H. (2000). *Component Performance Study- Turbine-Driven Pumps, 1987-1998.* USNRC (NUREG-1715), Volume.1.

Institute of Nuclear Power Operators . (2011). *Special Report on the Nuclear Accident at the Fukushima Daiichi Power Plant.* INPO 11-005.

Ishii, M. (1975). *Thermo-Fluid Dynamic Theory of Two Phase Flow.* Paris: Eyerolles.

Ishii, M., & Kataoka, I. (1983). *Similarity Analysis and Scaling Criteria for LWR's under Single-Phase and Two Phase Natural Circulation.* NUREG/CR-3267 ANL-83-32.

Kirkland, K. (2018). Private Communications .

Krantz, W. (2007). *Scaling Analysis in Modeling Transport and Reaction Processes.* Wiley Interscience.

Leland, W. (1917). *Steam Turbines.* Chicago, IL: American Technical Society.

Li, H., & Kudinov, P. (2009). GOTHIC code simulation of thermal stratification in POOLEX facility. *Royal Institute of Technology (KTH), NKS-196*.

Lobanoff, V., & Ross, R. (2013). *Centrifugal Pumps: Design and Application* (2nd ed.). Gulf Professional Publishing.

Lochbaum, D. (2016, May 3). *Nuclear Plant Containment Failure: Overpressure*. Retrieved from All Things Nuclear : https://allthingsnuclear.org/dlochbaum/nuclear-plant-containment-failure-overpressure

Luthman, N. (2017). *Evaluation of Impulse Turbine Performance under Wet Steam Conditions.* College Station, Texas : TAMU- NUEN- Master thesis.

Moyer, J. A. (1917). *Steam Turbines: A Practical and Theoretical Treatise for Engineers and Students.* New York: John Wiley & Sons.

Nahavandi, A., Castellana, F., & Moradkhanian, E. N. (1979). Scaling Laws for Modeling Nuclear Reactor Systems . *Nuclear Science and Engineering, 72:1,* 75-83.

Patterson, B. (1979). *Mark I Containment Program, Monticello T-quencher Thermal Mixing Test, Final Report* . NEDO-24542,79NED101.

Peterson, P. (1994). Scaling and analysis of mixing in large stratified volumes . *International Journal of Heat and Mass Transfer, 37,* 97-106.

Reyes, J. (2001). *Scaling Analysis for the OSU APEX-CE Integral System Test Facility* . Washington DC: USNRC.

Ross , K., Cardoni , J., Wilson, C., Morrow, C., Osborn, D., & Gauntt, R. (2015). *Modeling of the Reactor Core Isolation Cooling Response to Beyond Desgin Basis Operations- Phase 1.* Albuquerque: Sandia National Laboratories .

Sandia National Laboratory. (2017). *Terry Turbopump Expanded Operating Band Full-Scale Component and Basic Science Detailed Test Plan- Final.* New Mexico: SNL.

Solom, M., & Kirkland, K. (2016). Experimental investigation of BWR Suppression Pool stratification during RCIC system operation. *Nuclear Engineering and Desgin* , 564-569.

Solom, M. (2016). *Experimental Study on Suppression Chamber Thermal-Hydraulic Behavior for Long-Term Reactor Core Isolation Cooling System Operation.* College Station: Texas A&M University (Doctoral Dissertation).

Terry Steam Turbine Company. (1953). *Terry Instruction Manual Type Z-1 and ZS-1* . Connecticut: Hartford.

USNRC. (1994). Analysis of Long-Term Station Blackout without Automatic Depressurization at Peach Bottom using MELCOR. *NUREG/CR-5850, version 1.8*.

USNRC. (2012, October 8th). *Reactor Concept Manual, Boiling Water Reactor (BWR) Systems.* Retrieved October 8th, 2018, from NRC: https://www.nrc.gov/docs/ML1209/ML120970422.pdf

Woods, B., Jackson, R., & Nelson, B. (2009). *Scaling Analysis for the very High Temperature Reactor Test Facility at Oregon State University* . USNRC.

Yun, B., Cho, H., Euh, D., Song , C., & Park , G. (2004). Scaling for the ECC bypass Phenomena during the LBLOCA reflood Phase. *Nuclear Engineering and Design 231,* 315-325.

Zhao, H., Zou, L., & Zhang, H. (2012). *An Efficient Modeling Method for Thermal Stratification Simulation in a BWR Suppression Pool.* Idaho Falls: Idaho National Laboratory.

Zhao, H., Zou, L., Zhang, H., & Edward, J. (2016). *Development and Implementation of Mechanistic Terry Turbine Models in RELAP-7 to Simulate RCIC Normal Operation Conditions.* Idaho Falls : Idaho National Laboratory.

Zuber, N. (1991). *An Integrated Structure and Scaling Methodology for Severe Accident Technical Issue Resolution* . Washington DC : USNRC .